Triangulating Cappell-Shaneson homotopy 4-spheres

Ahmad Issa

ORCID Identifier: 0000-0003-2444-6552

Submitted in total fulfillment of the requirements of
the degree of Master of Philosophy

August 2017

School of Mathematics and Statistics
The University of Melbourne

Declaration

This is to certify that:

(i) the thesis comprises only my original work towards the MPhil except where indicated in the Preface,

(ii) due acknowledgement has been made in the text to all other material used,

(iii) the thesis is fewer than 50,000 words in length, exclusive of tables, maps, bibliographies and appendices.

Signed:

Ahmad

Ahmad Issa

Preface

My original work towards the MPhil is contained in Chapter 5, Sections 6.2-6.3, Chapter 7, as well as Proposition 3.7. All other sections, in particular Chapters 1, 2, 4 and most of Chapter 3 contain no original results.

The material in Chapter 4 was primarily taken from my MSc thesis [Iss12, Section 1.7]. Chapter 4 contains no original results and serves only as relevant background material.

Acknowledgements

First, I would like to thank my supervisor Craig Hodgson for all his guidance, encouragement and patience throughout my MPhil. Thank you for all the wonderful maths discussions, for keeping me on track administratively, and for all the detailed feedback on an earlier draft of this thesis. More broadly, Craig has had a huge positive influence on my mathematical development from my early days, some 9 or so years ago, as a first year undergraduate when he posed extra challenge problems on assignments, through supervising me as an MSc student, and now to the completion of this MPhil thesis. For all of this I'm very grateful.

Next, I'd like to thank Hyam Rubinstein. It was during a random conversation in the tearoom when I asked him "what's the deal with 4-manifold triangulations?" that he told me about the fascinating triangulation of Budney-Burton-Hillman, which kickstarted this whole project. Thank you also for the useful conversations and the encouragement.

Much of this thesis was completed during my spare time in the summer and winter breaks while undertaking a PhD at UT Austin, with most of the mathematical ideas worked out in 2013-14 and the writing slowly completed over the last few years. I would like to thank my advisory committee Craig, Hyam and Lawrence Reeves for patiently helping me jump through all the administrative hoops to make this possible, and for having the confidence that I'd complete, which helped make it happen.

I'd like to thank Henry Segerman for helping me visualise the bundle triangulations, Neil Hoffman for his interest in my work and for explaining inflations to me, Jonathan Spreer for useful references, Nadim Rustom for help with SageMath and Bob Gompf for a helpful conversation. I'd like to thank Kyle Larson and Max Stolarski for listening to me rant about some of this work, and Xikai Zhao for keeping me sane throughout the writeup. Lastly, I'd like to thank my parents for encouraging me to follow my heart and pursue maths, and all my friends at both Melbourne Uni and UT Austin for making it such an enjoyable experience.

Contents

List of Figures

List of Tables

Abstract

The smooth 4-dimensional Poincaré conjecture states that if a smooth 4-manifold is homeomorphic to the 4-sphere then it is diffeomorphic to the standard 4-sphere S^4. Historically, one of the most promising families of potential counterexamples to this conjecture is the family of Cappell-Shaneson homotopy 4-spheres. Over time, with difficult Kirby calculus computations, an infinite subfamily of Cappell-Shaneson homotopy 4-spheres was shown to be standard, that is, diffeomorphic to the 4-sphere and hence are not counterexamples. More recently, Gompf showed that a strictly larger subfamily is standard using the fishtail surgery trick.

In another direction, Budney-Burton-Hillman discovered a fascinating ideal triangulation of a smooth 4-manifold which they show is homeomorphic to a certain Cappell-Shaneson 2-knot complement X^4. They pose as a problem to show that it is in fact diffeomorphic to X. We solve this problem by directly triangulating X and observing that the triangulation we obtain is combinatorially isomorphic to theirs. In fact, we show that this triangulation is a layered triangulation. We then generalise our construction to show how to construct layered triangulations of once-punctured 3-torus bundles, generalising the well-known Floyd-Hatcher triangulations of once-punctured torus bundles.

Next, we describe how we can use these triangulations of once-punctured 3-torus bundles to construct triangulations of Cappell-Shaneson homotopy 4-spheres. This involves understanding the Gluck twisting operation via triangulations. For some particular examples, we simplify the triangulations using Pachner moves to a standard triangulation of the 4-sphere. For these examples, this provides a new computational proof that the corresponding Cappell-Shaneson homotopy 4-spheres are diffeomorphic to the 4-sphere.

Structure of this thesis

In **Chapter 1**, we discuss the smooth 4-dimensional Poincaré conjecture and describe the construction of Cappell-Shaneson homotopy 4-spheres, the main object of study in this thesis. We survey the literature describing work done towards showing that Cappell-Shaneson spheres are standard. Finally, we give an overview of our work done on triangulating Cappell-Shaneson spheres and using triangulations to give an alternative proof that certain examples of Cappell-Shaneson spheres are standard.

In **Chapter 2**, we provide some background material on various types of triangulations, in particular piecewise linear triangulations and their relation to smooth manifolds. We also briefly describe some key notions related to 4-manifolds, including the intersection form which plays an important role when we perform Gluck twisting via triangulations. We give an exposition of one of the simplest constructions of an exotic $\mathbb{R}^4$. Note that, in contrast, the smooth 4-dimensional Poincaré conjecture is equivalent to the non-existence of an exotic S^4.

In **Chapter 3**, we discuss how conjugacy classes of Cappell-Shaneson matrices may be understood via ideal classes of an appropriate ring, and describe how SageMath [Dev17] can be used in many cases to enumerate representatives of conjugacy classes of a given trace (this is used in Chapter 7). Note that Cappell-Shaneson matrices which are conjugate give rise to diffeomorphic Cappell-Shaneson spheres. Finally, we briefly discuss Gompf's work on fishtail neighbourhoods and how it can often be used to show Cappell-Shaneson homotopy 4-spheres coming from distinct monodromy matrix conjugacy classes are diffeomorphic.

In **Chapter 4**, we provide an exposition of the monodromy or Floyd-Hatcher triangulations of once-punctured 2-torus bundles over the circle. In the next chapter we generalise this construction to triangulate once-punctured 3-torus bundles. For this reason, this chapter serves as an easier to visualise and understand case to help understand the next chapter.

In **Chapter 5**, we show that the triangulation of Budney-Burton-Hillman may be viewed as a layered triangulation. We then generalise this to show how one can obtain a PL triangulation of any given once-punctured 3-torus bundle over the circle given its monodromy matrix. This generalises the construction of the previous chapter to 4-dimensions. Triangulating these bundles is an important step towards building triangulations of Cappell-Shaneson homotopy 4-spheres.

In **Chapter 6**, we explain how to go from a triangulation of a once-punctured 3-torus bundle with monodromy a Cappell-Shaneson matrix to a pair of triangulations corresponding to the two associated Cappell-Shaneson homotopy 4-spheres. This involves understand the Gluck twisting operation via triangulations.

In **Chapter 7**, we give an overview of some computational results obtained by a computer program we wrote to build and simplify triangulations of Cappell-Shaneson homotopy 4-spheres. We also provide some data, see for example Tables 7.1 and 7.2. Finally, we discuss possible further work.

In **Appendix A**, we provide pseudocode illustrating the algorithm we used to try to simplify some of the triangulations of Cappell-Shaneson homotopy 4-spheres discussed in Chapter 7.

Chapter 1

Introduction

Perhaps the most famous unsolved problem in 4-dimensional topology is the smooth 4-dimensional Poincaré conjecture:

Conjecture 1.1. If a smooth 4-manifold has the homotopy type of the 4-sphere, then it is diffeomorphic to S^4.

Freedman [Fre82], as part of his Fields medal winning work, proved that the homeomorphism type of a simply-connected topological 4-manifold is determined by two invariants, the intersection form and a $\mathbb{Z}_2$-valued invariant called the Kirby-Siebenmann invariant. These invariants depend only on the homotopy type of the 4-manifold, which implies that a 4-manifold which is a homotopy 4-sphere is necessarily homeomorphic to the 4-sphere. Hence, the smooth 4-dimensional Poincaré conjecture may also be stated as follows.

Conjecture 1.2. If a smooth 4-manifold is homeomorphic to the 4-sphere, then it is diffeomorphic to S^4.

Hence, a counterexample to the smooth 4-dimensional Poincaré conjecture would be a smooth 4-manifold homeomorphic to the 4-sphere, but not diffeomorphic to the 4-sphere (with its standard smooth structure). If such a manifold exists then it would be called an "exotic" 4-sphere.

1.1 Exotic manifolds

Two smooth manifolds M and N are called an *exotic pair* if they are homeomorphic but not diffeomorphic. In this case we often say that M is an *exotic* N, especially when the smooth structure of N is commonly thought of as the "standard" smooth structure on the underlying topological manifold. For example, an exotic $\mathbb{R}^n$ is a smooth manifold homeomorphic but not diffeomorphic to $\mathbb{R}^n$ (equipped with its standard smooth structure). We might expect there not to exist an exotic $\mathbb{R}^n$, and indeed this is true for $n \neq 4$, but surprisingly, there are uncountably many distinct exotic $\mathbb{R}^4$'s [Tau87]. In fact, some of these exotic $\mathbb{R}^4$'s can even be viewed as open subsets of the standard $\mathbb{R}^4$ with the induced smooth structure. Some other exotic

$\mathbb{R}^4$'s have the strange property that they contain a compact set which cannot be enclosed by a smoothly embedded 3-sphere.

An exotic pair of smooth manifolds can be thought of as putting different (up to diffeomorphism) smooth structures on the underlying topological manifold. Consider a closed topological n-manifold M. If $n > 4$ then it is known that there are finitely many (possibly zero) smooth structures on M. If $n < 4$ then there is exactly one way to smooth M. The case $n = 4$ is less well understood. There exist topological 4-manifolds, such as the E_8 manifold, which cannot be smoothed. However, it seems that whenever the gauge theoretic machinery works to prove that a topological 4-manifold admits multiple distinct smooth structures, then it is eventually shown that in fact it admits infinitely many smooth structures. Whether this is true in general remains open. One of the major goals in 4-manifold topology is to understand this exotic behaviour.

The number of exotic n-spheres for $n \neq 4$ is well understand. For a fixed $n \neq 4$, the set of smooth manifolds homeomorphic to the n-sphere forms a finite abelian group under the operation of connect sum with the standard n-sphere playing the role of the identity element [KM63]. The table below shows the order of such groups for $n \leq 18$ ($n \neq 4$).

n	1	2	3	4	5	6	7	8	9	10	11	12	13	14	15	16	17	18
	1	1	1	?	1	1	28	2	8	6	992	1	3	2	16256	2	16	16

Table 1.1: The second row is the number of smooth structures on S^n (Kervaire & Milnor 1963 [KM63]).

The resolution of the smooth 4-dimensional Poincaré conjecture is equivalent to filling in the question mark in the table above.

1.2 Cappell-Shaneson homotopy 4-spheres

Many potential exotic 4-spheres have been constructed. Historically, one of the most promising families is the family of Cappell-Shaneson homotopy 4-spheres, first constructed in the 1970's. One reason why they appeared promising is that two Cappell-Shaneson homotopy 4-spheres are known to double cover exotic $\mathbb{RP}^4$'s [CS76a].

It is interesting to note that Cappell and Shaneson's original interest in these homotopy 4-spheres was because they were interested in the question: does the complement of a 2-knot (i.e. smoothly embedded S^2 in S^4) determine the 2-knot [CS76b]? The analogous question in dimension 3 is known to be true [GL89]. However, there exist pairs of distinct 2-knots with diffeomorphic complements. Some Cappell-Shaneson knot complements provide an example of this.

Cappell-Shaneson homotopy 4-spheres are constructed as follows. Choose a *Cappell-Shaneson matrix*, i.e. $A \in \mathrm{SL}_3(\mathbb{Z})$ such that $\det(A - I) = \pm 1$. Let $T = \mathbb{R}^3/\mathbb{Z}^3$ denote the 3-torus. Let $E = T \times [0,1]/(x,0) \sim (Ax,1)$ be the 3-torus bundle over S^1 with monodromy A. Let $s = \{0\} \times S^1 \subset E$ be the zero section of the bundle. Let $E^\circ = E - \mathring{\nu}(s)$, i.e. the manifold given by removing an open tubular neighbourhood of the zero section. Hence the boundary of E° is diffeomorphic to $S^2 \times S^1$. In fact, up to isotopy there are eight distinct ways to make this identification of the boundary with $S^2 \times S^1$ (see Section 6.1). However there is a canonical choice that can be made and we use this identification (see Remark 1.3 below). The Cappell-Shaneson homotopy 4-sphere corresponding to (A, φ) is the smooth 4-manifold

$$C = E^\circ \cup_\varphi (S^2 \times D^2),$$

where $\varphi : S^2 \times S^1 \to S^2 \times S^1$ is a diffeomorphism. See Proposition 3.1 for a proof that C is a homotopy sphere. The diffeomorphism type of C is determined by A and a $\mathbb{Z}_2$ choice of "framing" φ. Hence, up to isotopy we may assume that φ is either the identity or a *Gluck twist* given by,

$$\varphi(x, \theta) = (\mathrm{rot}_\theta(x), \theta) \quad \text{for } x \in S^2 \text{ and } \theta \in S^1,$$

where $\mathrm{rot}_\theta(x)$ is rotation of $S^2 \subset \mathbb{R}^3$ by an angle of θ about the z-axis.

Remark 1.3. Starting with any Cappell-Shaneson monodromy matrix, Aitchison-Rubinstein define a canonical way to isotope it to the identity in a neighbourhood of the fixed point $(0, 0, 0) \in \mathbb{R}^3$, which is moreover independent of the conjugacy class (see Lemma 3.2 [AR84]). This gives a canonical identification of ∂E° with $S^2 \times S^1$ in the construction above.

In this thesis we are primarily interested in the unordered pair of Cappell-Shaneson homotopy 4-spheres that arise from the above construction. That is, we are not concerned with being able to distinguish between the Cappell-Shaneson homotopy 4-sphere with trivial and non-trivial framings and hence we will have no need to explicitly use the canonical identification.

1.3 History of Cappell-Shaneson 4-spheres

Supposing a Cappell-Shaneson homotopy 4-sphere were exotic, how can we check that it is? Thus far, the only known way to verify an exotic manifold is indeed exotic comes from gauge theory and related invariants. Unfortunately, at present these invariants are unable to directly give information in the case that the 4-manifold has trivial second homology. Due to this, much of the work done on Cappell-Shaneson homotopy 4-spheres has been in attempting to show that they are standard, i.e. not exotic. This can be done in some cases using Kirby calculus.

A closed smooth 4-manifold M can be represented by a diagram called a *Kirby diagram*. A Kirby diagram gives instructions for building M out of k-handles ($D^k \times D^{4-k}$ for $k = 0, 1, 2, 3, 4$) in a fashion somewhat analogous to a CW complex. Two manifolds are diffeomorphic if and only if two Kirby diagrams representing them are related by Kirby moves (handle cancellation/creation and handle slides). Thus, in order to show that a Cappell-Shaneson homotopy 4-sphere is diffeomorphic to S^4, it suffices to represent it as a Kirby diagram, then show using Kirby moves that this diagram is the same as one for S^4, e.g. one with no 1-handles, 2-handles or 3-handles.

Most research focused on the infinite subfamily of Cappell-Shaneson homotopy

4-spheres where the 3-torus bundle in the construction has monodromy given by

$$A_m = \begin{pmatrix} 0 & 1 & 0 \\ 0 & 1 & 1 \\ 1 & 0 & m+1 \end{pmatrix}, \quad m \in \mathbb{Z}.$$

All possible values of the trace are represented in this subfamily. It is known that for a fixed value of the trace, there are only finitely many conjugacy classes of Cappell-Shaneson matrices (see Chapter 3 for further discussion). This subfamily includes two double covers of exotic $\mathbb{RP}^4$'s corresponding to $m = 0$ and $m = 4$, and so it was thought that perhaps this meant that this subfamily might contain an exotic 4-sphere.

Recall that for a given A_m, there is a $\mathbb{Z}_2$ choice of framing in the construction of Cappell-Shaneson homotopy 4-spheres. There seemed to be one "easy" framing corresponding to φ equal the identity in our description of the construction in Section 1.2, and one "hard" framing to deal with corresponding to a Gluck twist. Here is a chronological list of the main results towards showing these Cappell-Shaneson homotopy 4-spheres are standard using Kirby calculus.

- In 1979, Akbulut and Kirby [AK79] showed using Kirby calculus that the Cappell-Shaneson homotopy 4-sphere with $m = 0$ and easy framing is diffeomorphic to S^4.

- In 1984, Aitchison and Rubinstein [AR84] generalised this for all $m \in \mathbb{Z}$ with easy framing.

- Akbulut and Kirby worked for 6 years to obtain a nice Kirby diagram (no 3-handles) of $m = 0$ with the hard framing [AK85].

- In 1991, Gompf [Gom91] then showed that this $m = 0$ case with hard framing was standard. He then obtained Kirby diagrams with no 3-handles for all $m \in \mathbb{Z}$ with the hard framing.

- Using this, in 2009, almost 20 years later, Akbulut [Akb10] then showed that the Cappell-Shaneson homotopy 4-spheres are standard for all $m \in \mathbb{Z}$ with the hard framing. More precisely, he showed that the Kirby diagrams can be changed via Kirby moves to the Kirby diagram corresponding to the $m = 0$ case, which was previously shown to be standard.

Soon after Akbulut's work in 2009, Gompf showed using the "fishtail surgery trick" that a strictly larger class of Cappell-Shaneson homotopy 4-spheres are standard [Gom10]. He introduces a trace changing operation one can perform on certain Cappell-Shaneson matrices, and shows that Cappell-Shaneson homotopy spheres of a fixed framing which are related by this operation are diffeomorphic. Furthermore he conjectures that all Cappell-Shaneson homotopy spheres (of a fixed framing) are related by conjugacy and this operation. Proving this would show that all Cappell-Shaneson homotopy spheres are standard. This is further discussed in Section 3.5.

1.4 Triangulations

In dimension 4 the category of piecewise linear (PL) manifolds is equivalent to the category of smooth manifolds [HM74]. This implies that a triangulation of a 4-manifold can be smoothed to a uniquely determined smooth 4-manifold. A smooth manifold also determines a class of triangulations, any two triangulations of which are related by Pachner moves. This is somewhat analogous to the situation with Kirby diagrams and Kirby moves. Hence, if we can triangulate a Cappell-Shaneson homotopy 4-sphere then use Pachner moves to simplify the triangulation to a triangulation of S^4, then we have computationally proved that the Cappell-Shaneson homotopy 4-sphere is standard.

In this thesis, we describe how to algorithmically triangulate Cappell-Shaneson homotopy 4-spheres. For some examples of Cappell-Shaneson homotopy 4-spheres we simplify these triangulations using Pachner moves to a triangulation of the standard 4-sphere, hence showing that they are standard. The starting point of this work is a fascinating example discovered by Budney-Burton-Hillman [BBH12], which we now describe.

Given a Cappell-Shaneson matrix $A \in \mathrm{SL}_3(\mathbb{Z})$, let E denote the 3-torus bundle over S^1 with monodromy A. An associated Cappell-Shaneson homotopy 4-sphere C is obtained by surgering E along the zero section, cutting out $B^3 \times S^1$ and gluing in $S^2 \times D^2$. The image of $S^2 \times \{0\} \subset S^2 \times D^2$ in C is a 2-knot, i.e. embedded S^2. The complement of this 2-knot in C is $E \backslash$(zero section) which is diffeomorphic to the punctured 3-torus bundle with monodromy A.

In 2011, Budney, Burton and Hillman [BBH12] found, by enumerating 4-dimensional triangulations, a triangulation consisting of two 4-simplices with their vertices removed (such triangulations are called *ideal*), homeomorphic to the Cappell-Shaneson knot complement with monodromy

$$A = \begin{pmatrix} 0 & 0 & 1 \\ 1 & 0 & 0 \\ 0 & 1 & -1 \end{pmatrix}.$$

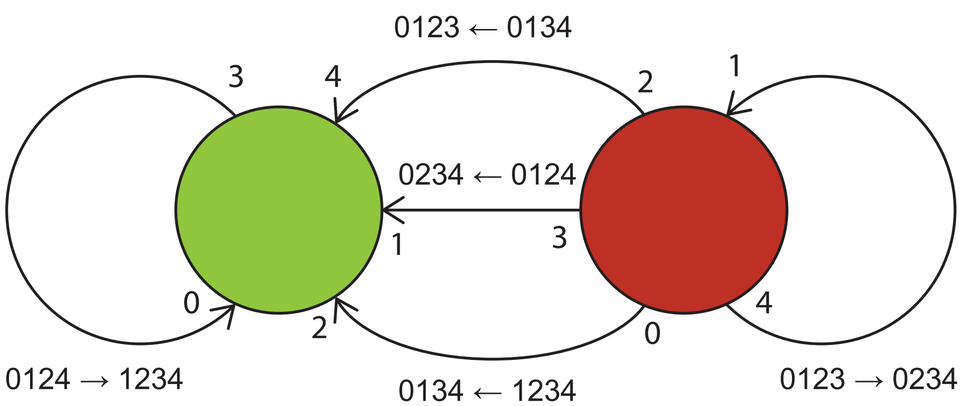

Figure 1.1: Triangulation of Cappell-Shaneson knot complement by Budney, Burton and Hillman, based on Figure 1 of [BBH12].

The triangulation may be described as follows. In Figure 1.1, the green and red disks correspond to the two ideal 4-simplices. The five (ideal) vertices of each 4-simplex are numbered from 0 to 4. The directed arrow, say, from 3 of the red disk to 1 of the green disk means that the tetrahedral facet opposite vertex 3 is glued to the facet opposite vertex 1 of the other 4-simplex, and the gluing is done by an affine map in such a way that the vertices of the facets are mapped by $(0,1,2,4) \mapsto (0,2,3,4)$.

One fascinating aspect of this four-dimensional triangulation is its similarity with the famous two ideal tetrahedron triangulation of the figure-eight knot complement. They are both ideal triangulations of a knot complement in a sphere (of the appropriate dimension). They are both extremely simple triangulations with only two top dimensional simplices. They are both punctured n-torus bundles over S^1. In fact, in Section 5.1, we show that this triangulation is a layered triangulation. Hence, both triangulations are layered.

We point out that Budney-Burton-Hillman only prove that the triangulated manifold is *homeomorphic* to the Cappell-Shaneson knot complement. They conjecture that the two manifolds are in fact diffeomorphic. In this thesis we triangulate the Cappell-Shaneson knot complement directly, and we show that the triangulation we obtain is the same triangulation that they found. This proves their conjecture positively. Our triangulation of the knot complement is an example of a layered triangulation and is somewhat analogous to the well known Floyd-Hatcher triangulations of once-punctured torus bundles [Lac03].

Moreover, we generalise this method allowing us to triangulate any given once punctured 3-torus bundle. A detailed discussion of this is given in Chapter 5. In brief, given a monodromy matrix A we factorise it into a product of simple matrices. For an appropriately selected triangulation $\mathcal{T}$ of the once-punctured 3-torus, the factorisation gives rise to a sequence of triangulations starting with $\mathcal{T}$ and ending with $A(\mathcal{T})$. We show that we can interpolate between any two triangulations in this sequence by layering four (ideal) 4-simplices. This allows us to construct a layered triangulation of the bundle. In fact, we can use this general method to construct a triangulation of the bundle of Budney-Burton-Hillman then use Pachner moves to obtain their triangulation.

We can use such a triangulation $\mathcal{T}$ of a Cappell-Shaneson knot complement to obtain a triangulation of a corresponding Cappell-Shaneson homotopy 4-sphere. In order to do this we need to perform the surgery combinatorially. We describe a strategy for doing this:

1. Triangulate $S^2 \times D^2$.

2. We would like to remove a regular neighbourhood of the ideal vertex of $\mathcal{T}$. This can be achieved by subdividing the triangulation $\mathcal{T}$, then removing all 4-simplices containing the ideal vertex.

3. We would like to glue the new triangulation and $S^2 \times D^2$ along their triangulated boundaries. However, this requires that the boundary triangulations of $S^2 \times S^1$ are combinatorially isomorphic. We can achieve this by performing elementary shellings, that is, layering 4-simplices along the boundary, which effectively changes the boundary triangulations by Pachner moves. In particular, this allows us to simplify the boundary triangulations to the unique minimal two tetrahedron triangulation of $S^2 \times S^1$.

4. Glue the two triangulated manifolds by a combinatorial isomorphism of their boundaries to obtain a triangulated Cappell-Shaneson homotopy 4-sphere.

When we carry out this procedure we do not know which $\mathbb{Z}_2$ choice of framing the resulting Cappell-Shaneson homotopy 4-sphere corresponds to. However, we triangulate $S^2 \times D^2$ in two different ways, such that the two triangulations have combinatorially isomorphic boundaries (minimal two tetrahedron triangulations), with the property that when we perform the gluing using each of these triangulations we obtain two Cappell-Shaneson homotopy 4-spheres, one of each framing. The details of this are described in Section 6.3.1.

We wrote Python code to triangulate once-punctured 3-torus bundles, build the corresponding pair of Cappell-Shaneson homotopy 4-spheres and simplify triangulations. Using this, we constructed Cappell-Shaneson homotopy 4-spheres for all conjugacy classes of Cappell-Shaneson matrices with trace between 0 and 20 (inclusive). For those Cappell-Shaneson homotopy 4-spheres corresponding to bundles with trace betweeen 0 and 5, we attempted to simplify the triangulations using Pachner moves. In all cases we simplified the triangulations to have at most 18 4-simplices. In a number of cases, including triangulations for both framings in the trace 0 and trace 1 cases, we simplified the triangulation to a two 4-simplex triangulation of S^4, providing an alternative computational proof that they are standard. This is discussed in further detail in Chapter 7. Our computer code and data are available from the author upon request[1].

1.5 Akbulut-Kirby spheres and triangulations

The Akbulut-Kirby spheres [AK85] provide another interesting family of homotopy 4-spheres. The work done in showing that these homotopy 4-spheres are standard is related to the Cappell-Shaneson homotopy spheres case. Since, moreover, there has been work on triangulating Akbulut-Kirby spheres we briefly describe these developments.

Let H be a contractible compact 4-manifold with a handle decomposition given by a single 0-handle, k 1-handles and k 2-handles. The double of H is the closed 4-manifold given taking two copies of H, where for one copy we reverse its orientation, and gluing them along their common boundary by the identity map. Since H is contractible, its double is a homotopy 4-sphere. However, it is difficult in general to decide whether the double is diffeomorphic to S^4. This gives another source of potentially exotic 4-spheres.

The double of H may also be thought of as the boundary of $H \times [0, 1]$, where we smooth the corners of $H \times [0, 1]$ here and throughout. The handle decomposition of H gives a corresponding handle decomposition of $H \times [0, 1]$ obtained by thickening each of the handles. Consider the 5-dimensional handle moves on $H \times [0, 1]$ only involving 1- and 2-handles, that is, we can perform handle slides, as well as add or remove cancelling 1-handle/2-handle pairs. These moves change the presentation of the fundamental group of $H \times [0, 1]$ coming from the handle decomposition by

[1]Send an email to ahmadissa@gmail.com.

what are called Andrews-Curtis moves on the presentation. Note that Andrews-Curtis moves can be described as moves on the presentation without reference to the handle decomposition.

Since we know that $\pi_1(H\times[0,1]) = 1$, we can attempt to simplify the presentation by Andrews-Curtis moves to the trivial presentation. If we can do this, then we can perform handle moves to obtain a handle decomposition of $H \times [0,1]$ with only a 0-handle, and hence its boundary, which is the double of H, is diffeomorphic to S^4.

It is unknown whether every presentation of the trivial with k generators and k relators is Andrews-Curtis trivial, i.e. there is a sequence of Andrews-Curtis moves to the trivial presentation. For example, the presentations

$$P_n = \langle x, y \mid yxy = xyx, x^{n+1} = y^n \rangle,$$

of the trivial group are not known to be Andrews-Curtis trivial for $n \geq 3$, and expected by many experts to not be Andrews-Curtis trivialisable. A sufficient, but not necessary, condition to show that the double of H is diffeomorphic to S^4 is to show that the handlebody presentation of $H \times [0,1]$ is Andrews-Curtis trivial.

Consider the Cappell-Shaneson homotopy 4-sphere corresponding to $m = 0$ and twisted framing. Let H denote the contractible 4-manifold obtained by lifting off the 4-handle (removing a ball). Akbulut and Kirby [AK85] produce a handle decomposition of H with no 3-handles, two 1-handles and two 2-handles such that the corresponding presentation of $\pi_1(H)$ is Andrews-Curtis equivalent to P_4 (this latter part is due to a calculation of Casson). If, as many experts suspect, P_4 were not Andrews-Curtis trivialisable then $H \times [0,1]$ (and therefore H) would not be trivialisable by moves only involving 1- and 2-handles.

However, by cleverly introducing a cancelling 2-handle/3-handle pair, Gompf [Gom91] later showed that H is diffeomorphic to the standard B^4. Hence, both the corresponding Cappell-Shaneson homotopy 4-sphere and the double of H are diffeomorphic to S^4. In fact, Gompf does this for a more general family of such H with handle decompositions representing all the presentations P_n, $n \geq 3$.

An Akbulut-Kirby sphere AK_n is the homotopy 4-sphere given as the boundary of the 5-manifold constructed by taking a 5-ball and attaching two 1-handles and two 2-handles so that the induced presentation on the fundamental group is P_n (AK_n is completely determined by the presentation). Using precisely this description of AK_n, Tsuruga and Lutz [TL13], [Tsu15] a construct triangulation of AK_n, for each $n \geq 2$ with $5592 + 1856n$ 4-simplices.

For $n = 2$, they are able to simplify the triangulation of the Akbulut-Kirby sphere using Pachner moves which shows that AK_2 is diffeomorphic to the 4-sphere. Note that Gompf [Gom91] shows that all Akbulut-Kirby spheres are standard.

Chapter 2

Background

2.1 Simplicial complexes

An *n-simplex* σ in $\mathbb{R}^d$ is the convex hull of $n+1$ points $p_0, \ldots, p_n \in \mathbb{R}^d$ which are in *general position*, i.e. where no subset of points spans a hyperplane of the same dimension. The k-simplex given by the span of any subset of $k+1$ elements of $p_0, \ldots, p_n$ is a *(k-)subsimplex* or *face* of σ. The 0-subsimplices of σ are called *vertices*, the 1-subsimplices are called *edges*, the 2-subsimplices are called *faces* and the $(n-1)$-subsimplices are called *facets*.

A *simplicial complex* is a collection K of simplices in $\mathbb{R}^d$ satisfying the conditions:

(i) The collection K is locally finite, meaning that every point in $\mathbb{R}^n$ has a neighbourhood intersecting only finitely many simplices in K.

(ii) If σ is a simplex in K then all subsimplices of σ are in K.

(iii) The intersection of two simplices in K is either empty or a face of both simplices.

The *polyhedron* $|K|$ of a simplicial complex K is the topological space given by the union of the simplices of K. A *simplicial triangulation* of a topological space X is a simplicial complex K together with a homeomorphism $\phi : |K| \to X$. The homeomorphism can be used to transfer notions about K to those on X, e.g. a vertex, face or simplex in X.

Remark 2.1. Although not technically correct, it is common in the literature to use the term *simplicial complex* when what is meant is more correctly a *polyhedron* or a *simplicial triangulation*. We also use this abuse of terminology.

Since we are mostly interested in simplicial triangulations of manifolds. There are two natural question one can ask about simplicial complexes:

(1) When is a simplicial complex a topological manifold?

(2) Does every topological manifold admit a simplicial triangulation?

The first question is answered by Theorem 2.2 below. In order to state it, we first need the concept of a link. Let K be a simplicial complex. Let σ be a simplex in K, and let $\tau_1, \ldots, \tau_k$ be the simplices of K containing σ as a subsimplex. Each simplex τ_i has a subsimplex $\sigma_i^\perp$ opposite to σ, which is the unique subsimplex spanned by the vertices of τ_i which are not vertices of σ. The *link* of σ is the simplicial complex consisting of $\sigma_1^\perp, \ldots, \sigma_k^\perp$. The union of the interiors of the τ_i is called the *star* of σ.

Theorem 2.2. Let K be a simplicial complex. Then $|K|$ is a topological n-manifold if and only if the following conditions hold:

(i) Every simplex in K is a subsimplex of an n-simplex in K.

(ii) If σ is a k-simplex of K then the link of σ is a homology S^{n-k-1}, i.e. has the same $\mathbb{Z}$-homology as S^{n-k-1} in all dimensions.

(iii) If $n \neq 2$ and v is a vertex in K, then the link of v is simply connected.

Theorem 2.2 is mentioned in Section 3.2 of [Thu97] (just before Proposition 3.2.7). One way to see Theorem 2.2 is that it follows by combining [GS78, Theorem 1] with the double suspension theorem [Can79], and noting that a homotopy 3-sphere is necessarily S^3 by the Poincaré conjecture.

Note that if p is a point in the interior of a k-simplex σ in a simplicial complex K, then p has a neighbourhood homeomorphic to $D^k \times C(\mathrm{link}(\sigma))$ where $C(\mathrm{link}(\sigma))$ denotes the cone of the link of σ in K. Hence, the simplicial complex is homeomorphic to a manifold if and only if all such neighbourhoods are topological manifolds. It is tempting to guess that a necessary condition for this is that $C(\mathrm{link}(\sigma))$ is a $(n-k-1)$-sphere, but this surprisingly turns out to be incorrect. We have the following example:

Example 2.3 (Double suspension)**.** Let M^3 be a homology 3-sphere with non-trivial fundamental group, for example the Poincaré homology sphere. Fix a triangulation of M. Recall that the suspension of a space X is the quotient space $\Sigma(X) = X \times [0,1]/\sim$ with $X \times \{0\}$ and $X \times \{1\}$ each identified to a point, called the suspension points. The suspension of a triangulated space X has an induced triangulation such that the link of a suspension point is X.

Cannon [Can79], building on work of Edwards [Edw06], showed that the double suspension $\Sigma^2(M) = \Sigma(\Sigma(M))$ is homeomorphic to S^5. Hence, a suspension point of $\Sigma^2(M)$ has link $\Sigma(M)$ which is not even a manifold, in particular, it is not S^4 as we might expect.

In order to see that $\Sigma(M)$ is not a manifold, note that the link of a suspension point p of $\Sigma(M)$ is homeomorphic to M which is not simply-connected. Then $\Sigma(M)$ is not locally simply-connected at p (whereas n-manifolds, $n > 2$, are locally simply connected), i.e. there does not exist a neighbourhood of V of p such that $V \backslash \{p\}$ is simply-connected. If such a V did exist then $V \backslash \{p\}$ has the same fundamental group as V minus a neighbourhood of p homeomorphic to the cone of M, which we denote by U. Then we have inclusions $M \hookrightarrow U \hookrightarrow M \times [0,1]$ where the composition is the identity map on the level of fundamental groups. In particular, U is not simply-connected, which is a contradiction.

The second question is related to a famous conjecture called *the triangulation conjecture*, which states that every topological n-manifold, $n > 4$, is homeomorphic to a simplicial complex. Note that the triangulation conjecture is true for $n < 4$. For $n = 1$ the only closed topological manifold is the circle, which admits a triangulation. For $n = 2$, this was shown by Radó [Rad25], and for $n = 3$ by Moise [Moi52]. When $n = 4$ there are topological manifolds which are not homeomorphic to a simplicial complex, e.g. the E_8 manifold (see Example 2.18). However, dimension 4 is pathological in many ways, so it was thought that the triangulation conjecture may hold in other dimensions.

The triangulation conjecture has only relatively recently been resolved (negatively) by Manolescu [Man16]. Thus, there exist topological manifolds of dimension greater than 4 which cannot be triangulated. Manolescu's disproof builds on work by Galewski and Stern [GS80] and independently by Matumoto [Mat78]. They prove the following surprising result:

Theorem 2.4 ([GS80], [Mat78])**.** The triangulation conjecture is true (i.e. every topological n-manifold, $n > 4$, is homeomorphic to a simplicial complex) if and only if there exists a homology 3-sphere Σ^3 with Rokhlin invariant equal to 1 such that $\Sigma \# \Sigma$ is the boundary of a smooth homology 4-ball, that is, the boundary of a smooth 4-manifold with the same integral homology as B^4.

Manolescu constructed a homology cobordism invariant β coming from Pin(2)-equivariant Seiberg-Witten theory which is a $\mathbb{Z}$-lift of the Rokhlin invariant. The β invariant has the property that $\beta(-\Sigma) = -\beta(\Sigma)$. Suppose Σ is an integral homology 3-sphere such that $\Sigma \# \Sigma$ is null homology cobordant. Then Σ and $-\Sigma$ are homology cobordant, and so $\beta(\Sigma) = \beta(-\Sigma) = -\beta(\Sigma)$ which implies that $\beta(\Sigma) = 0$, and thus the Rokhlin invariant must also be 0. This shows that the triangulation conjecture is false since such a homology sphere as in Theorem 2.4 cannot exist.

2.2 Piecewise linear (PL) manifolds

We saw in Example 2.3 that there are simplicial triangulations of topological manifolds where the link of a vertex may not be a sphere of the appropriate dimension. In this section we describe piecewise linear (PL) manifolds, which can be thought of as a topological manifold with the additional structure of a triangulation satisfying the additional property that the links of cells are standard piecewise linear spheres. In this sense they have nicely behaved triangulations which avoid the pathologies of Example 2.3.

The topological manifold in Example 2.3 is homeomorphic to S^5 but the simplicial triangulation is not piecewise linear, see Proposition 2.5. Note however that S^5 admits a PL structure, indeed even a smooth structure. If X^5 is the manifold in the example, then the simplices of X are not smoothly embedded with respect to any smooth structure on X, rather they have "wild" topological embeddings.

In fact, the additional structure of a PL manifold will imply that not all topological manifolds are PL manifolds. In 4-dimensions PL manifolds are in one-to-one correspondence with smooth 4-manifolds. However, the upside to this is that one is able to prove theorem about the smooth category of 4-manifolds by proving them for PL 4-manifolds (and vice versa).

Let K be a simplicial complex in $\mathbb{R}^n$. A map $f : |K| \to \mathbb{R}^m$ is *linear* if it the restriction of a linear map from $\mathbb{R}^n$ to $\mathbb{R}^m$. It is *piecewise linear* if the restriction $f|\sigma$ to each simplex σ of K is linear. A map $f : |K_1| \to |K_2|$ between two simplicial complexes is *piecewise linear* (PL) if the underlying map $f : K_1 \to \mathbb{R}^m$ is piecewise linear, where K_2 lives in $\mathbb{R}^m$. A homeomorphism between subsets of $\mathbb{R}^n$ is piecewise linear if the domain and codomain have simplicial triangulations so that the homeomorphism is piecewise linear.

A *piecewise linear n-manifold* is a manifold with an atlas such that the transition maps are piecewise linear homeomorphisms between open subsets of $\mathbb{R}^n$. A map $f : |K| \to X$, between a simplicial complex and a PL manifold is a *piecewise linear map* if the compositions of f with PL charts of X are piecewise linear. If K is a simplicial complex and M is a piecewise linear manifold, then a map $f : |K| \to M$ is a *piecewise linear triangulation* if f is a piecewise linear homeomorphism. If K is a simplicial complex and there exists a piecewise linear triangulation $f : |K| \to X$, where X is some piecewise linear manifold, then we say that K has a *piecewise linear structure*, or is a *piecewise linear manifold*. The simplicial complexes which are piecewise linear manifolds have a simple characterisation:

Proposition 2.5 (Proposition 3.9.6 of [Thu97])**.** A simplicial complex K is a piecewise linear manifold if and only if the link of each simplex of K is a piecewise linear manifold equivalent to the standard piecewise linear sphere. By standard piecewise linear structure of S^k we mean the piecewise structure induced by the triangulation of S^k as the boundary of a $(k+1)$-simplex.

Remark 2.6. In fact, if the link of every vertex of a simplicial complex is PL equivalent to the standard PL sphere then the simplicial complex is a piecewise linear manifold. To see this note that if the links of vertices are standard PL spheres then the stars of the vertices are standard PL balls, and they form a PL atlas.

2.3 Comparing PL and smooth manifolds

The book [HM74] by Hirsch and Mazur provides a good reference for the material in this section.

Let $f : M \to X$ be a homeomorphism from a PL manifold to a smooth manifold. We call f a *piecewise differentable (PD) homeomorphism* if M has a piecewise linear triangulation such that the restriction of f to each simplex is a smooth map with injective differential at each point. If such a PD homeomorphism exists, then X is a *smoothing* of M.

We have the following theorem due to Whitehead:

Theorem 2.7 ([Whi40])**.** Let X be a smooth manifold. Then there exists a piecewise linear manifold M and a piecewise differentiable homeomorphism $f : M \to X$. Moreover, any two such PL manifolds are PL homeomorphic.

We can think of this result as saying that a smooth manifold is the smoothing of some PL manifold, and that PL manifold is unique up to PL homeomorphism. It is natural to ask if every PL manifold has a smoothing, and if so, is that smoothing unique up to diffeomorphism. It turns out that both of these questions have a negative answer, that is, there are PL manifolds which do not admit a smoothing [Ker60], and there are PL manifolds which admit multiple non-diffeomorphic smoothings. For example, Kervaire and Milnor [KM63] building on work of Milnor [Mil56] proved there are 28 oriented-diffeomorphism types of manifolds homeomorphic to S^7, yet by the generalised Poincaré conjecture for PL n-manifolds, $n > 4$, there is only a single PL 7-sphere. Thus, all 28 smooth 7-spheres are smoothings of a single PL manifold.

However we have the following result.

Theorem 2.8. A piecewise linear manifold of dimension $n \leq 7$ admits a smoothing. Furthermore, if $n \leq 6$ then the smoothing is unique up to diffeomorphism.

For an exposition of this result see [HM74], or Lecture 23 of [Lur09] which reduces the problem to understanding the homotopy groups of a certain space and [Rud98] IV. 4.27 (iv) for references to proofs of the computations of the necessary homotopy groups.

Remark 2.9. Thus, combining Theorems 2.8 and 2.7, for $n \leq 6$, there is a one-to-one correspondence between smooth n-manifolds up to diffeomorphism and PL n-manifolds up to PL homeomorphism.

Finally, we mention that a topological n-manifold M, $n > 4$, is homeomorphic to a PL manifold if and only if an obstruction known as the Kirby-Siebenmann class $\kappa(M) \in H^4(M; \mathbb{Z}_2)$ vanishes [KS77]. If $n = 4$, then further obstructions may exist.

2.4 Triangulations

We have encountered simplicial triangulations which have the property that each simplex is embedded and is determined by its vertices so that no two distinct simplices share the same vertices. Low dimensional topologists most often deal with a more general, flexible type of triangulation.

An n-dimensional *pseudo-triangulation*, *semi-simplicial triangulation* or simply a *triangulation* consists of a finite collection of n-simplices and a choice of pairs of simplex facets such that each facet appears in exactly one of the pairs, and an affine identification map between the facets of each pair, see Definition 3.2.1 of [Thu97]. This type of triangulation is the most commonly used in this thesis, and thus, when we refer to a *triangulation*, unless qualified e.g. *simplicial* triangulation, we usually mean a pseudo-triangulation. We think of the triangulation as a triangulation of an associated quotient space which is the union of the simplices with the facets glued by affine maps according to the pairings.

As an example of a triangulation which is not a simplicial triangulation, consider a square $[0,1] \times [0,1]$ divided into two triangles by a diagonal $\{(x,x) : x \in [0,1]\}$, then glue opposite edges together in the usual way to get a torus. This gives a triangulation of the torus into two triangles. In the glued manifold all vertices are identified to a single point, so this is not a simplicial triangulation. The most efficient simplicial triangulation of a torus in fact has 14 triangles. This highlights one of the main advantages of using pseudo-triangulations, they can triangulate spaces using far fewer simplices.

The *barycentric subdivision* of an n-simplex σ is a subdivision into $(n+1)!$ simplices as follows. Let $p_0, p_1, \ldots, p_n$ be some permutation of the vertices of σ. Then there is an associated simplex in the subdivision with vertices $v_0, \ldots, v_n$, where each v_i is the barycentre (average) of $p_0, \ldots, p_i$. The barycentric subdivision of a triangulation is the triangulation obtained by taking the barycentric subdivision of each simplex.

A triangulation can be turned into a simplicial complex by first taking its barycentric subdivision then embedding it into Euclidean space. In order to see that such an embedding is possible, first note that in the barycentric subdivision every simplex is determined uniquely by its vertices. Let $v_1, \ldots, v_n$ be the collection of vertices in the barycentric subdivision. Then we can embed the barycentric subdivision in $\mathbb{R}^n$ as a simplicial complex where each vertex v_i is sent to the unit coordinate $e_i = (0, \ldots, 0, 1, 0, \ldots, 0)$ with a 1 in the ith slot.

Since a triangulation has a naturally associated simplicial complex, provided the link of vertices are PL spheres as in Proposition 2.5, the triangulation can also be thought of as having a naturally associated PL manifold structure.

2.4.1 Isomorphism signatures

The isomorphism signature of a triangulation is a string which efficiently encodes the combinatorial data of the triangulation. Moreover, it has the important property that two triangulations are combinatorially isomorphic if and only if their isomorphism signatures are identical. Isomorphism signatures are described in [Bur11] and are used in the computer software Regina [BBP+14].

For a fixed dimension n, the isomorphism signature of a triangulation with k n-simplices has length of size $O(k \log k)$ and can be computed in $O(k^2 \log k)$ time. Hence isomorphism signatures provide an efficient way to check that two triangulations are combinatorially isomorphic. We describe triangulations using isomorphism signatures in a number of places throughout this thesis. These can be copied and imported into the computer software Regina. As an example, the isomorphism signature of the two 4-simplex triangulation of Burton-Budney-Hillman [BBH12] is given by `cMkabbb+aAa3blb`.

Remark 2.10. Some of the triangulations of Cappell-Shaneson homotopy 4-spheres that we produce in Chapter 7 have thousands of 4-simplices. For such large triangulations the isomorphism signature becomes rather slow to compute. Moreover, we have no need to compare the combinatorial isomorphism type of these triangulations. Hence, we store these in a custom file format which is a simple generalisation of the SnapPy [CDGW] 3-manifold triangulations file format.

2.5 Pachner moves

If we have two triangulations of a fixed piecewise linear manifold we may wonder how the triangulations are related. Pachner [Pac91] showed that there is a small set of moves, called *bistellar flips* or *Pachner moves*, which we can use to modify a PL triangulation (we allow pseudo-triangulations) in such a way that the PL type is unchanged and any two triangulations of a fixed PL manifold are related by a finite sequence of such moves. A nice exposition of Pachner's result, including the proof, is given in [Lic99].

Before describing the moves in full generality, we illustrate them in lower dimensions. In 2-dimensions, there are two types of Pachner moves, as shown in Figure 2.1. First, there is a Pachner move which we can perform on any triangle in the triangulation which replaces it by three triangles given by coning off from the centre of the original triangle. This move is called a 1-3 move, since 1 triangle is replaced by 3 triangles. The inverse of this move is also a Pachner move called a 3-1 move.

There is also a 2-2 move which replaces two distinct triangles glued along a common edge. The two triangles glued along the common edge form a quadrilateral, and a 2-2 replaces one diagonal edge of this quadrilateral by the other, as shown in Figure 2.1. For this reason, a 2-2 move is also commonly called a *diagonal exchange*. Note that the quadrilateral could have other edges being identified (and we could perform Pachner moves exchanging them, too). The Pachner move depends not only on the pair of triangles, but also the common edge which is chosen to be exchanged.

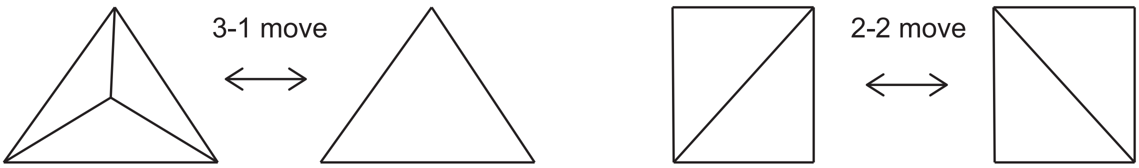

Figure 2.1: Pachner moves in 2-dimensions.

Consider the 1-3 move, where we replace a single triangle by three triangles. If we glue a single triangle to the three triangles along their boundary (three distinct edges) we obtain a 2-dim triangulation which is precisely the boundary of a 3-simplex. Similarly, with a 2-2 move if we glue the two triangles before and afterwards along their common boundary, we obtain a triangulation equivalent to the boundary of a 3-simplex. This is the key property which defines a Pachner move.

In 3-dimensions there are also two types of Pachner moves, a 1-4 move and a 2-3 move (and their inverses, 4-1 and 3-2 moves). A 1-4 move is analogous to the 2-dimensional case, a single tetrahedron is replaced by four tetrahedra given by introducing a vertex (cone point) in the centre of the original tetrahedra and coning off the four faces from this vertex. A Pachner 2-3 move, shown in Figure 2.3, is the move which replaces two tetrahedra glued at a common face by three tetrahedra obtained by removing the common face and inserting a dual edge so that there are three tetrahedra containing this edge.

Let M be a piecewise linear n-manifold with a fixed piecewise linear simplicial triangulation. Let Δ_{n+1} denote a $(n+1)$-simplex, and $\partial\Delta_{n+1}$ its boundary which is a triangulation of S^n. Let $C \subset M$ be a codimension-0 subcomplex given as the

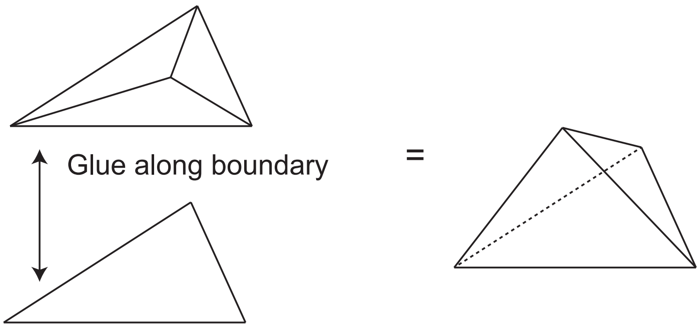

Figure 2.2: Gluing the triangles before and after in a 1-3 (or 3-1) move gives a triangulation of a tetrahedron (minus its interior).

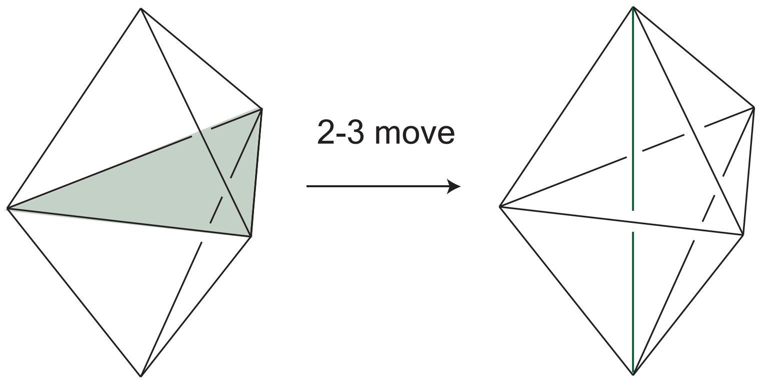

Figure 2.3: A 3-dimensional 2-3 Pachner move. The common face shown in green is removed and the green dual edge is inserted.

union of $k > 0$ n-simplices and all their faces. Suppose that $\phi : C \to C' \subset \partial\Delta_{n+1}$ is a simplicial isomorphism of C with a proper subcomplex C' of the boundary of an $(n+1)$-simplex. The *Pachner move, or Bistellar flip, on the triangulation of M associated with ϕ* is the triangulated manifold $(M\backslash C) \cup_\phi (\partial\Delta_{n+1}\backslash C')$. We also call this operation a (k)–$(n-k+2)$ (e.g. 2-3) n-dimensional Pachner move as k n-simplices are replaced by $(n-k+2)$ n-simplices.

A Pachner move on a piecewise linear pseudo-triangulation of a manifold is defined similarly. Briefly, it can thought of as follows. Let $\mathcal{T}$ be the collection of n-simplices defining the triangulation. Suppose that there is an identification ϕ of the simplices of $C' \subset \partial\Delta_{n+1}$ with those in $C \subset \mathcal{T}$ which respects the gluings in C'. That is, if two simplices are glued in C' along some facet then they are also glued in C in precisely the same way. Note that the simplices in C may have additional facet pairings, which we allow. Then the Pachner move on $\mathcal{T}$ replaces the simplices in C with the n-simplices in $\partial\Delta_{n+1}\backslash C'$.

Theorem 2.11 ([Pac91])**.** Suppose $\mathcal{T}_1$ and $\mathcal{T}_2$ are triangulations with piecewise linear structures. Then $\mathcal{T}_1$ and $\mathcal{T}_2$ are related by a finite sequence of Pachner moves if and only if they define PL homeomorphic piecewise linear manifolds.

2.6 4-manifolds

In this section we briefly discuss some basic notions related to 4-manifolds, in particular, the intersection form of a 4-manifold and exotic smooth structures. We shall only summarise the most pertinant facts for our needs, for proofs consult the excellent sources [GS99] and [Sco05].

Let X^4 be a compact, oriented, topological 4-manifold. The *intersection form*, or *intersection pairing* on X is the symmetric bilinear form

$$Q_X : H^2(X, \partial X; \mathbb{Z}) \times H^2(X, \partial X; \mathbb{Z}) \to \mathbb{Z}$$

given by $Q_X(a, b) = \langle a \cup b, [X] \rangle$, where $[X] \in H_4(X, \partial X; \mathbb{Z})$ is the fundamental class. By Poincaré duality, $H^2(X, \partial X; \mathbb{Z}) \cong H_2(X; \mathbb{Z})$, thus we can think of Q_X as defined on $H_2(X; \mathbb{Z}) \times H_2(X; \mathbb{Z})$. If X is a smooth 4-manifold then the intersection form can also be computed as follows. If $a, b \in H_2(X; \mathbb{Z})$, then a, b can be represented by smoothly embedded surfaces in X which intersect transversely. Then $Q_X(a, b)$ is given by the signed intersection number of the two surfaces. This is where the name *intersection* form comes from, and the way we shall think of it most of the time.

Remark 2.12. Since the intersection form is bilinear, we see that for any torsion element $a \in H_2(X; \mathbb{Z})$, $Q_X(a, \cdot\,) = Q_X(\,\cdot\,, a) = 0$. Thus, the intersection form descends to a pairing

$$Q_X : H_2(X; \mathbb{Z})/\text{tors} \times H_2(X; \mathbb{Z})/\text{tors} \to \mathbb{Z}.$$

Since $H_2(X)/\text{tors} \cong \mathbb{Z}^k$ for some k, we can choose a $\mathbb{Z}$-basis for $\alpha_1, \ldots, \alpha_k$. Since Q_X is bilinear it is determined by the matrix $A_{i,j} = Q_X(\alpha_i, \alpha_j)$, $1 \leq i, j \leq k$. We call k the *rank* of Q_X, which is equal to the second Betti number $b_2 = b_2(X)$.

Two intersection forms are *equivalent* or *isomorphic* if with respect to some choice of bases their matrices are equal. Thus, if $A, B \in \mathrm{M}_n(\mathbb{Z})$ are matrices representing intersection forms with respect to some bases, then the intersection forms are equivalent if and only if there exists a matrix $P \in \mathrm{GL}_n(\mathbb{Z})$ such that $A = P^t B P$.

Suppose X is a 4-manifold with intersection form Q_X. Choose any matrix representing Q_X. Since this matrix is symmetric it has only real eigenvalues. Let b_2^+ (resp. b_2^-) be the number of positive (resp. negative) eigenvalues of this matrix. The *signature* of X is $\sigma(X) = b_2^+ - b_2^-$. The intersection form Q_X is *positive definite* if $b_2^+ = b_2$, and *negative definite* if $b_2^- = b_2$. It is *definite* if it is either positive or negative definite, otherwise it is called *indefinite*. The intersection form is *even* if $Q_X(x, x)$ is *even* for all $x \in H_2(X; \mathbb{Z})$, otherwise it is called *odd*. If Q_X is represented by a matrix then Q_X is even if and only if the matrix has all diagonal entries even numbers.

If we have a Kirby diagram of a 4-manifold without 1- or 3-handles then the following is often very useful for computing the intersection form:

Proposition 2.13 (Prop 4.5.11 of [GS99])**.** Let X be a 4-manifold given by a Kirby diagram with single a 0-handle, a collection of 2-handles and (possibly) a 4-handle. Suppose the 2-handles are attached along a framed link L with components $K_1, \ldots, K_k$. We fix some choice of orientation on the components of L. We have that $H_2(X) \cong \mathbb{Z}^k$ has a basis $\alpha_1, \dots, \alpha_k$, where α_i is represented by the surface given by gluing a Seifert surface for K_i and the core disk of the 2-handle attached to K_i. The surfaces are oriented so that the Seifert surfaces' boundary orientations match the orientation of the components of L.

Then, with respect to the basis $\alpha_1, \dots, \alpha_k$ the intersection form Q_X is represented by the linking matrix of the framed link L. Equivalently, $Q_X(\alpha_i, \alpha_i)$ is given by the framing of K_i, and $Q_X(\alpha_i, \alpha_j)$, $i \neq j$ is given by the linking number of K_i and K_j in S^3.

Proposition 2.14 (Corollary 5.3.12 [GS99])**.** *If X^4 is built from a 0-handle and a collection of 2-handles then $H_1(\partial X; \mathbb{Z})$ is presented by any matrix representing the intersection form of X.*

The intersection form of a 4-manifold is one of the most important invariants of a 4-manifold. In the early 1980's, two very significant advances occurred in 4-manifold topology. The first is a result of Freedman which implies that one of the key tools in high-dimensional topology, the h-cobordism theorem, can be extended to *topological* 4-manifolds. The second is a theorem of Donaldson which places restrictions on the types of intersection forms which can arise as the intersection form of a *smooth* 4-manifold. In 1986 both Freedman and Donaldson received Fields medals for their work.

Theorem 2.15 (Freedman's theorem [Fre82], [FQ90])**.** *If X_1 and X_2 are smooth, closed, connected, simply-connected 4-manifolds with isomorphic intersection forms then X_1 and X_2 are homeomorphic.*

Freedman in fact proved a more general theorem stating that simply connected topological 4-manifolds are determined up to homeomorphism by their intersection form and an invariant called the Kirby-Siebenmann invariant. In fact, he showed that every combination of unimodular intersection form and Kirby-Siebenmann invariant can be realised with the caveat that if the intersection form is even then the Kirby-Siebenmann invariant must be given by $\frac{\sigma}{8} \pmod 2$, where σ is the signature. A noteworthy corollary of this is the following:

Theorem 2.16 (4-dimensional topological Poincaré conjecture)**.** *If X is a topological 4-manifold homotopy equivalent to the 4-sphere then X is homeomorphic to the 4-sphere.*

Theorem 2.17 (Donaldson's theorem [Don83])**.** *If the intersection form of a smooth, closed 4-manifold is definite, then it is diagonalisable, i.e. there exists a $\mathbb{Z}$-basis for which the intersection form matrix is diagonal.*

Note that it follows from Poincaré duality that the intersection form of a closed, oriented 4-manifold is *unimodular*, that is, when represented as a matrix its determinant is ± 1. Thus in Donaldson's theorem, the diagonal matrix will consist of 1's (resp. -1's) on the diagonal if the intersection form is positive (resp. negative) definite.

Freedman and Donaldson's results complement each other in the following sense. Freedman's work implies that there is an abundance of topological 4-manifolds, whereas Donaldson's work places restrictions on which topological 4-manifolds admit smooth structures.

Two smooth manifolds M and N are called an *exotic pair* if they are homeomorphic but not diffeomorphic. In this case we often say that M is an *exotic* N, especially when the smooth structure of N is commonly thought of as the "standard" smooth structure on the underlying topological manifold. For example, an exotic $\mathbb{R}^n$ is a smooth manifold homeomorphic but not diffeomorphic to $\mathbb{R}^n$ (equipped with its standard smooth structure).

We might expect that there does not exist an exotic $\mathbb{R}^n$, and indeed this is true for $n \neq 4$, but intriguingly, there are uncountably many distinct exotic $\mathbb{R}^4$'s. Some of these exotic $\mathbb{R}^4$'s can be viewed as open subsets of the standard $\mathbb{R}^4$ with the induced smooth structure. While some others have the property that they contain a compact set which cannot be enclosed by a smoothly embedded 3-sphere. Notice that any such compact set is contained in a sufficiently large closed ball centred at the origin in $\mathbb{R}^4$, however, for some exotic smooth structures the boundary 3-sphere is not smoothly embedded.

An exotic pair of smooth manifolds can be thought of as putting different (up to diffeomorphism) smooth structures on the underlying topological manifold. Consider a closed topological n-manifold. If $n > 4$ then it is known that there are finitely many (possibly zero) smooth structures on M. If $n < 4$ then there is exactly one way to smooth M. The case $n = 4$ is less well understood. There exist topological 4-manifolds, such as the E_8 manifold, which cannot be smoothed. However, for many examples it is known that if a topological 4-manifold admits a smooth structure, then it admits infinitely many distinct smooth structures. Whether this is true in general remains open. One of the major goals in 4-manifold topology is to understand exotic behaviour.

Example 2.18. The E_8 manifold is a simply connected, closed, topological 4-manifold with intersection form given by the so called E_8 matrix, which we will describe. The E_8 manifold does not admit a smooth structure, as we shall see. Consider the compact 4-manifold X^4 represented by the Kirby diagram shown in Figure 2.4.

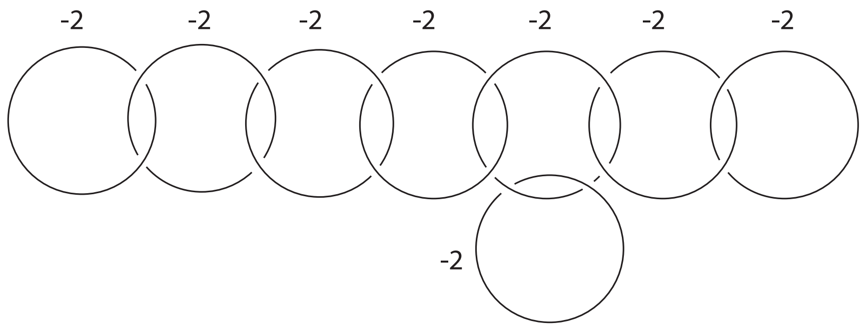

Figure 2.4: The E_8 2-handlebody.

By Proposition 2.13, with respect to some choice of orientation on the link, it has intersection form Q_X represented by

$$E_8 = \begin{pmatrix} -2 & 1 & 0 & 0 & 0 & 0 & 0 & 0 \\ 1 & -2 & 1 & 0 & 0 & 0 & 0 & 0 \\ 0 & 1 & -2 & 1 & 0 & 0 & 0 & 0 \\ 0 & 0 & 1 & -2 & 1 & 0 & 0 & 0 \\ 0 & 0 & 0 & 1 & -2 & 1 & 0 & 1 \\ 0 & 0 & 0 & 0 & 1 & -2 & 1 & 0 \\ 0 & 0 & 0 & 0 & 0 & 1 & -2 & 0 \\ 0 & 0 & 0 & 0 & 1 & 0 & 0 & -2 \end{pmatrix}.$$

The boundary of X is the Poincaré homology 3-sphere. It follows from Freedman's work [Fre82, Theorem 1.4] that any integral homology sphere bounds a contractible topological 4-manifold. In particular, we can glue such a piece to X to obtain a closed topological 4-manifold called the E_8-manifold. The intersection form of the E_8-manifold is still given by the E_8 matrix as gluing a contractible piece does not change the intersection from.

Suppose that the E_8-manifold is smoothable, i.e. it admits a smooth structure. We denote the smooth manifold by Y^4. By computing the eigenvalues and seeing that they are all negative, the E_8 intersection form is negative definite. The intersection form is even since all its diagonal entries are even. By Donaldson's theorem (Theorem 2.17), Y must have diagonalisable (and hence odd) intersection form, which is a contradiction. Hence, the E_8 manifold is not smoothable.

2.6.1 An exotic $\mathbb{R}^4$

We now explain how the existence of topologically slice but not smoothly slice knots implies the existence of an exotic $\mathbb{R}^4$. According to [Gom86], this observation was first made by Andrew Casson. This well known result is given as Exercise 9.4.23 of [GS99]. See also Section 8.6 of [OSS15].

A knot $K \subset S^3$ is *smoothly slice* (resp. *topologically slice*) if it is the boundary of a smoothly (resp. topologically) embedded disk $D \subset D^4$ in the 4-ball, i.e. $\partial D = K \subset S^3 = \partial D^4$.

We have the following theorem due to Freedman:

Theorem 2.19 ([FQ90])**.** Any knot in S^3 with Alexander polynomial equal to 1 is topologically slice.

Donaldson's theorem, Theorem 2.17, can be used to show that some topologically slice knots are not smoothly slice. As an example we illustrate the argument for the following:

Proposition 2.20. The $(-3, 5, 7)$-pretzel knot K, shown in Figure 2.5, is topologically slice but not smoothly slice.

Proof. One can check that K has Alexander polynomial 1, and hence is topologically slice by Theorem 2.19.

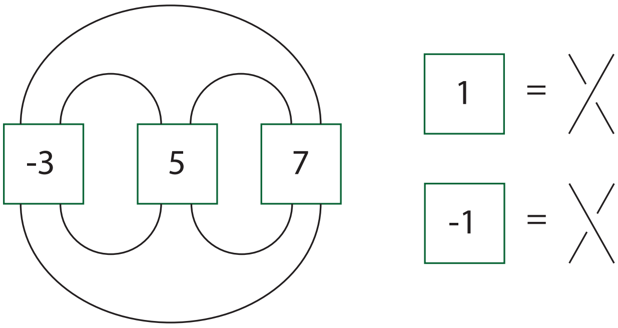

Figure 2.5: $(-3, 5, 7)$-pretzel knot. The green boxes represent a (signed) number of half twists, with the convention for ± 1 shown.

We now argue that K is not smoothly slice. Suppose for sake of contradiction that K is smoothly slice. It is well known that the double branched cover of the 4-ball over a slice disk is a rational homology 4-ball which in this case we denote by U^4. The boundary of U is the double branched cover of S^3 over K, which is given by the surgery diagram shown in Figure 2.6 (this follows from the "Montesinos trick" [Mon76]). Let $M = \partial U$.

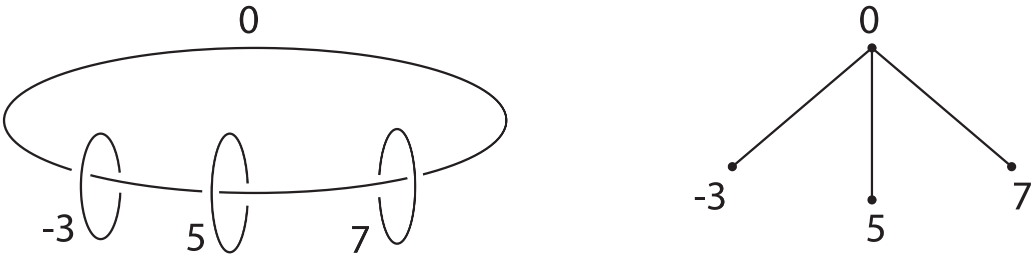

Figure 2.6: On the left is a surgery diagram for the double branched cover of S^3 over the $(-3, 5, 7)$-pretzel knot. On the right is a so-called plumbing diagram schematically representing the same surgery diagram as on the left. Each vertex represents an unknotted component and edges represent linking of components.

The surgery diagram for M can be modified by performing a (left) Rolfsen twist to each of the unknotted components with framings 5 and 7, then inverse slam dunking (see Section 5.3 of [GS99]) the new $-5/4$ and $-7/6$ framed components to obtain the surgery diagram represented as a plumbing diagram in Figure 2.7. Then M is the boundary of the 4-manifold V given by interpreting the surgery presentation given by Figure 2.7 as a Kirby diagram with 2-handles attached to the 4-ball according to the framed link.

By Proposition 2.13, V has intersection matrix given by the linking matrix of the framed link represented by the plumbing diagram Figure 2.7. One can check that the intersection matrix has determinant ± 1, therefore by Proposition 2.14, $H_1(M) = 0$, so M is a homology sphere. Furthermore, the intersection form is negative definite.

The manifold $X = (-U) \cup V$ has intersection form which is the direct sum of the intersection forms for U and V. This follows from the fact that the common boundary of U and V is a homology sphere and the intersection form is additive with respect to gluing along homology spheres (Exercise 1.3.5 [GS99]).

Since U is a rational homology ball, and therefore has trivial intersection form,

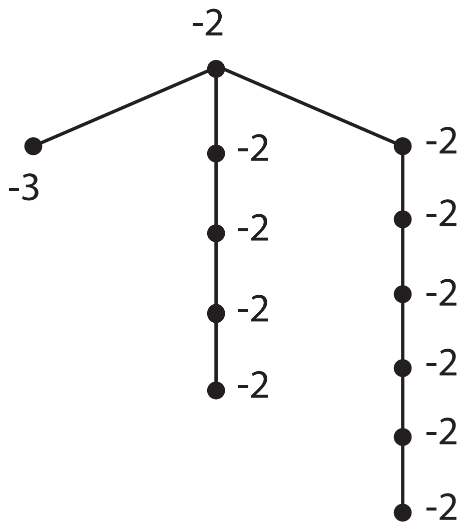

Figure 2.7: A plumbing diagram schematically representing the surgery diagram with each vertex an unknot and edges connect unknots (linking once). The 3-manifold represented is M.

we have that $Q_X \cong Q_V$. By Donaldson's theorem, Theorem 2.17, the intersection form $Q_X \cong Q_V$ must be diagonalisable. Using Proposition 2.13, by appropriately orienting the framed link represented by Figure 2.7, we have a basis $v_1, \ldots, v_{12} \in H_2(V)$, which we can think of as the vertices in Figure 2.7 so that for $i \neq j$, $Q_V(v_i, v_j)$ is 1 if and only if the two vertices are connected by an edge.

Since Q_V is diagonalisable, there is a basis $e_1, \ldots, e_{12}$ for $H_2(V)$ such that $Q_V(e_i, e_j)$ is -1 if $i = j$, and 0 otherwise. We can write each v_i as a linear combination of the e_j's. The element of $H_2(V)$ representing the central (degree 3) vertex, which without loss of generality we assume is v_1, must be a sum of two $\pm e_j$'s in order to have self intersection -2 (no other linear combination of e_j's satisfy this). Thus, without loss of generality we assume $v_1 = e_1 + e_2$. Consider the first vertex in the third column of Figure 2.7, which we without loss of generality assume is v_2.

By the same reasoning, it is a sum of two $\pm e_j$'s, but we also must have $Q_V(v_1, v_2) = 1$. Thus, without loss of generality $v_2 = -e_1 + e_3$. We continue this way down the third column, then second column, whilst at each step ensuring the linear combination we assign pairs via Q_V correctly with previously assigned vertices. We arrive the following assignment shown in Figure 2.8.

When the -3 labelled vertex is written as a linear combination of the e_j's, it must contain either $-e_1$ or $-e_2$ in order to pair to 1 with the central vertex v_1. Say it contains $-e_1$, then it must contain $-e_3$ in order to pair to 0 with v_2 (the first vertex in the third column), but then it must contain $-e_4$ to link correctly with the second vertex in the third column. Similarly, it must contain $-e_5$, but then the self pairing of this linear combination of e_j's is less than -3, a contradiction. Thus K is not smoothly slice. $\square$

We now show that the existence of a knot which is topologically slice but not smoothly slice implies that there exists an exotic $\mathbb{R}^4$. We follow the argument given in [OSS15, Section 8.6], see there for further details.

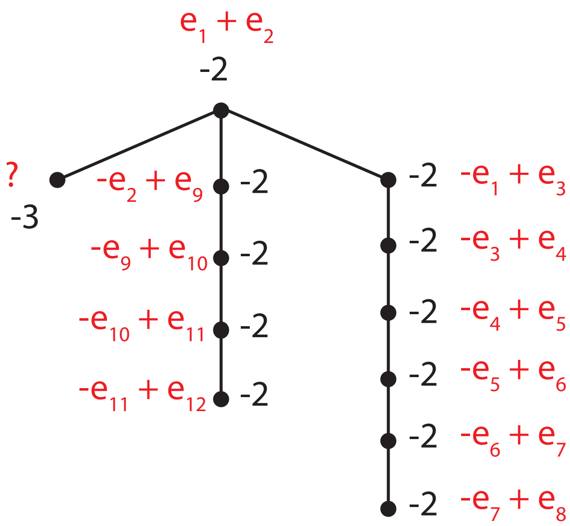

Figure 2.8: Attempt at writing each vertex as a linear combination of the standard basis vectors for a negative definite intersection form of rank 12. There is no way to write the -3 labelled vertex in terms of the e_j.

Proposition 2.21. There exists an exotic $\mathbb{R}^4$, i.e. a smooth 4-manifold homeomorphic to $\mathbb{R}^4$ but not diffeomorphic to $\mathbb{R}^4$ with its standard smooth structure.

Proof. Let $K \subset S^3$ be a topologically but not smoothly slice knot, e.g. as given in Proposition 2.20.

Let X_K denote the smooth 4-manifold given by attaching a 2-handle to D^4 along K with framing 0. It suffices to show that X_K smoothly embeds in a manifold homeomorphic to $\mathbb{R}^4$, but does not smoothly embed in $\mathbb{R}^4$ (with its standard smooth structure).

Suppose for sake of contradiction that X_K smoothly embedded in $\mathbb{R}^4 \subset S^4$. Cone off the knot K in the 0-handle of X_K to get a surface $C \subset D^4$. The link of this surface at the cone point is isotopic to K. Consider the complement in S^4 of a small standardly embedded 4-ball in the 0-handle of X_K centred at the origin (the cone point). This space is smoothly a 4-ball, and the parts of the surface C in this 4-ball, together with the core of the 2-handle of X_K form a smooth slice disk for (the mirror image of) a knot isotopic to K in the boundary. This gives a contradiction. Thus X_K does not embed in $\mathbb{R}^4$.

Now it suffices to construct a 4-manifold homeomorphic to $\mathbb{R}^4$ for which X_K smoothly embeds. Consider $D^4 \subset \mathbb{R}^4$; there is a topological slice disk for K contained in $\mathbb{R}^4 \backslash D^4$. Remove the interior of the union of D^4 and a tubular neighbourhood of the topological slice disk from $\mathbb{R}^4$ (such a tubular neighbourhood exist since the slice disk is topologically flat). Call the resulting 4-manifold Y. Note that we just removed a manifold homeomorphic to the interior of X_K from $\mathbb{R}^4$ to get Y.

The key fact that we use is that since Y is a non-compact topological 4-manifold, it therefore admits a smooth structure by [FQ90]. By identifying Y topologically with $\mathbb{R}^4 \backslash \mathrm{Int}(Y)$, we get a homeomorphism ∂X_K and ∂Y. Isotoping this homeomorphism to a diffeomorphism (every homeomorphism of a 3-manifold is isotopic to a diffeomorphism) allows us to glue Y and X_K to get a smooth manifold X^4. It is homeomorphic to $\mathbb{R}^4$ by construction, and contains X_K smoothly embedded, as required. $\square$

Chapter 3

Cappell-Shaneson homotopy 4-spheres

In this chapter we study Cappell-Shaneson matrices, in particular the question of when different Cappell-Shaneson matrices give rise to diffeomorphic Cappell-Shaneson homotopy 4-spheres. We direct the reader to Section 1.2 for a reminder of the Cappell-Shaneson construction.

3.1 Cappell-Shaneson matrices and homotopy 4-spheres

A matrix $A \in \mathrm{SL}_3(\mathbb{Z})$ is called a *Cappell-Shaneson matrix* if $\det(A - \mathrm{I}) = \pm 1$. In this section we prove Proposition 3.1 which states that the Cappell-Shaneson construction produces a homotopy 4-sphere precisely when the monodromy of the 3-torus bundle is a Cappell-Shaneson matrix. This is Proposition 1 of [CS76b], where the proof is left as an exercise to the reader. We include a proof for completeness.

Proposition 3.1. Let $A \in \mathrm{SL}_3(\mathbb{Z})$, let T_0^3 be a 3-torus with an open ball removed and let $X = T_0^3 \times [0,1]/(x,0) \sim (Ax,1)$ be the T_0^3-bundle over the circle with monodromy A. Let Z be a 4-manifold obtained by gluing $S^2 \times D^2$ to X by any diffeomorphism of their boundaries. Then Z is a homotopy 4-sphere if and only if $\det(A - \mathrm{I}) = \pm 1$.

Proof. Let ϕ be the diffeomorphism of $T_0^3 = (\mathbb{R}^3 - \mathring{N}(\mathbb{Z}^3))/\mathbb{Z}^3$ represented by the matrix A. By isotoping ϕ near ∂T_0^3 we may assume that it fixes ∂T_0^3 pointwise. Pick a point $p \in \partial T_0^3$ and let γ denote the oriented closed curve $p \times [0,1] \subset X$. The fundamental group of T_0^3 is generated by three curves x, y, z based at p which are supported along the x-, y- and z-axes (respectively) except in a small neighbourhood of ∂T_0^3.

The fundamental group of X is given as a HNN extension by

$$\pi_1(X) = \langle x, y, z, \gamma \mid x, y, z \text{ commute}, \gamma w \gamma^{-1} = \phi_*(w) \text{ for every word } w \text{ in } x, y, z \rangle,$$

where x, y, z can be thought of as the three curves which generate $\pi_1(T_0^3)$. In particular $H_1(X) \cong \mathbb{Z}\langle\gamma\rangle \oplus \mathbb{Z}^3/\mathrm{im}(A - \mathrm{I})$.

By van Kampen when we glue $S^2 \times D^2$ to X we kill the image of $\{\mathrm{pt}\} \times \partial D^2 \subset S^2 \times D^2$ in $\pi_1(X)$. However, this curve is isotopic (up to changing orientation) to γ. Hence $\pi_1(Z) \cong H_1(Z) \cong \mathbb{Z}^3/\mathrm{im}(A - \mathrm{I})$. So $\pi_1(Z)$ is trivial if and only if $\det(A - \mathrm{I}) = \pm 1$. Note that Z is a homotopy 4-sphere if and only if $\pi_1(Z)$ is trivial and $H_2(Z) = 0$. Thus, it suffices to check that when $\det(A - \mathrm{I}) = \pm 1$ we also have $H_2(Z) = 0$.

We now assume that $\det(A - \mathrm{I}) = \pm 1$. We will show that $H_2(X) = 0$, which, by a straightforward application of Mayer-Vietoris, implies that $H_2(Z) = 0$. As in Example 2.48 of [Hat02] for bundles over S^1, there is a short exact sequence

$$0 \to \mathrm{coker}(\phi_2 - \mathrm{Id}_2) \to H_2(X) \to \ker(\phi_1 - \mathrm{Id}_1) \to 0,$$

where for $i \in \{1, 2\}$, ϕ_i is the map induced by ϕ on $H_i(T_0^3)$, and Id_i is the identity map on $H_i(T_0^3)$. In coordinates on $H_1(T_0^3) \cong \mathbb{Z}\text{-span}\{x, y, z\}$, the map $\phi_1 - \mathrm{Id}_1$ is given by $A - \mathrm{Id}$, which is injective since $\det(A - \mathrm{I}) = \pm 1$. Hence $\ker(\phi_1 - \mathrm{Id}_1)$ is trivial.

It suffices to show that $\mathrm{coker}(\phi_2 - \mathrm{Id}_2)$ is trivial, i.e. that $\phi_2 - \mathrm{Id}_2$ surjects onto $H_2(T_0^3)$. There is a $\mathbb{Z}$-basis x^*, y^*, z^* for $H_2(T_0^3)$ represented by tori which are dual to the curves x, y, z in the sense that we have the intersection pairings $x^* \cdot x = 1$, $x^* \cdot y = 0$ and $x^* \cdot z = 0$ (and similarly for y^* and z^*). Let B be the matrix representing the map ϕ_2 on $H_2(T_0^3)$. Then notice that, for example, $B_{31} = \phi_*(x^*) \cdot z = x^* \cdot \phi_*^{-1}(z) = (A^{-1})_{13}$. Therefore $B = (A^{-1})^T$ and hence $\det(B - \mathrm{I}) = \det(A^{-1} - \mathrm{I}) = \pm 1$. So $(\phi_2 - \mathrm{Id}_2)$ surjects onto $H_2(T_0^3)$, as required.

□

3.2 Conjugacy classes

Let $A \in \mathrm{SL}_3(\mathbb{Z})$, and let X_A be the 3-torus bundle over the circle with monodromy A. Consider a 4-manifold given by performing a surgery on the zero section of X_A^4. Such a 4-manifold is a homotopy 4-sphere precisely when $\det(A - \mathrm{I}) = \pm 1$, see Proposition 3.1. As this is the case we are interested in for the Cappell-Shaneson construction, we will now assume that $\det(A - \mathrm{I}) = \pm 1$. Moreover, since we are in fact only interested in the diffeomorphism type of the homotopy 4-spheres obtained by surgering the zero section of X_A, and smoothly isomorphic bundles X_A give rise to diffeomorphic homotopy 4-spheres, we aim to understand when different monodromy matrices produce isomorphic bundles.

Notice that X_A and $X_{A^{-1}}$ are smoothly bundle isomorphic (where we reflect the base space S^1 in the isomorphism). Moreover $\det(A^{-1} - \mathrm{I}) = -\det(A - \mathrm{I})$, and hence by replacing A by its inverse A^{-1} if necessary, we may assume that $\det(A - \mathrm{I}) = 1$.

The bundle isomorphism type is also unchanged when we conjugate the monodromy A by a matrix $P \in \mathrm{GL}_3(\mathbb{Z})$. Indeed, X_A and $X_{PAP^{-1}}$ are bundle isomorphic where the isomorphism is given by the bundle map which maps the fiber of X_A above a point $x \in S^1$ to the fiber of $X_{PAP^{-1}}$ above $x \in S^1$ via the diffeomorphism P of the 3-torus fiber.

By a sequence of explicit conjugations, Aitchison-Rubinstein proved the following.

Theorem 3.2 (Theorem A3 of [AR84])**.** Let $A \in \mathrm{SL}_3(\mathbb{Z})$ be a Cappell-Shaneson matrix, i.e. $\det(A - \mathrm{I}) = 1$, and let $a = \mathrm{tr}(A)$. Then A is conjugate in $\mathrm{GL}_3(\mathbb{Z})$ to a matrix of the form

$$A_{a,\lambda,p} = \begin{bmatrix} 0 & 0 & 1 \\ m & \lambda & 0 \\ n & p & a-\lambda \end{bmatrix},$$

where $n = \lambda(a-\lambda)-(a-1)$ and $mp = 1+n\lambda$ (these two conditions on the coefficients correspond to the conditions $\det(A - \mathrm{I}) = 1$ and $\det(A) = 1$). Furthermore, one may either assume $0 \leq \lambda < p$ or else assume $0 \leq \lambda < m$.

The matrices $A_{a,\lambda,p}$ as in Theorem 3.2 may be conjugate for many different values of $\lambda, p \in \mathbb{Z}$. However, for a given conjugacy class one can choose $A_{a,\lambda,p}$ with $(\lambda, p) \in \mathbb{Z}^2_{\geq 0}$ minimal (in the lexicographic order) in the conjugacy class. This picks out a canonical representative of a conjugacy class.

We shall see that conjugacy classes of such matrices A can be understood via ideal classes of a ring. This will help us understand the degeneracy in Theorem 3.2.

3.3 Ideal classes

Let R be an integral domain. Let $\mathrm{Cl}(R)$ be the quotient of the set of non-zero ideals of R by the equivalence relation $I \sim J$ if and only if there exist $a, b \in R\backslash\{0\}$ such that $aI = bJ$. Under this equivalence relation all non-zero principal ideals are equivalent, and hence they form a single element of $\mathrm{Cl}(R)$ which we call the class of principal ideals.

The *ideal class monoid* of R is the monoid $\mathrm{Cl}(R)$ with multiplication given by $[I] \cdot [J] = [IJ]$. The identity element is given by the class of principal ideals. Since R is assumed to be an integral domain, and is therefore commutative, we see that $\mathrm{Cl}(R)$ is an abelian monoid. If $\mathrm{Cl}(R)$ is finite then we call the number of elements in $\mathrm{Cl}(R)$ the *ideal class number* or just the *class number* of $\mathrm{Cl}(R)$.

The following theorem allows us to understand conjugacy classes of matrices in $\mathrm{GL}_n(\mathbb{Z})$ in terms of ideal classes.

Theorem 3.3 ([New72])**.** Let $f \in \mathbb{Z}[x]$ be a monic degree n polynomial which is irreducible over $\mathbb{Q}$, and let $\theta \in \mathbb{C}$ be a root of f. There is a bijection between the conjugacy classes in $\mathrm{GL}_n(\mathbb{Z})$ of matrices A satisfying $f(A) = 0$ and the ideal classes of $\mathbb{Z}[\theta]$.

We shall make the isomorphism in Theorem 3.3 explicit in the case that we are interested in, but before doing so we discuss the appropriate set up.

Let $A \in \mathrm{SL}_3(\mathbb{Z})$ with $\det(A - \mathrm{I}) = 1$. Notice that both the trace of A and the characteristic polynomial of A are conjugacy invariants. Let $f(t) = \det(t\mathrm{I} - A)$ be the characteristic polynomial of A. Then $f(t) = t^3 - \mathrm{tr}(A)t^2 + bt - \det(A)$ for some $b \in \mathbb{Z}$. Now let $a = \mathrm{tr}(A)$ and recall $\det(A) = 1$ by assumption, so we may write $f(t) = t^3 - at^2 + bt - 1$. Furthermore, the condition $\det(A - \mathrm{I}) = 1$ implies that $f(1) = -1$ and so $b = a - 1$. Thus, we may write the characteristic polynomial as

$$f_a(t) = t^3 - at^2 + (a-1)t - 1.$$

We see that the characteristic polynomial gives no more information than the trace.

Following Lemma A4 of [AR84] we show polynomial f_a is irreducible over $\mathbb{Q}$.

Lemma 3.4. The polynomial $f_a(t) = t^3 - at^2 + (a-1)t - 1$, $a \in \mathbb{Z}$ is irreducible over $\mathbb{Q}$.

Proof. Since f_a has degree 3 it is irreducible if and only if it has no root in $\mathbb{Q}$. So suppose $f_a(\frac{p}{q}) = 0$, where $\frac{p}{q} \in \mathbb{Q}$ with $p, q \in \mathbb{Z}$ and $\gcd(p, q) = 1$. Then $p^3 - ap^2q + (a-1)pq^2 - q^3 = 0$. Considering this equation mod 2 and noting that p and q are not both even then leads to a contradiction. $\square$

Corollary 3.5. Let $f_a(t) = t^3 - at^2 + (a-1)t - 1$, $a \in \mathbb{Z}$. A matrix $A \in \mathrm{GL}_3(\mathbb{Z})$ satisfies $f_a(A) = 0$ if and only if $\det(A) = 1$, $\det(A - \mathrm{I}) = 1$ and $\mathrm{tr}(A) = a$.

Proof. Suppose $f_a(A) = 0$. Since f_a is irreducible over $\mathbb{Q}$ we get that f_a is the characteristic polynomial of A. Hence we may read off the trace and determinant from f_a. Furthermore, $f_a(1) = -1$ immediately implies $\det(A - \mathrm{I}) = 1$. The converse was shown above. $\square$

Let $a \in \mathbb{Z}$ and suppose we are trying to understand the conjugacy classes in $\mathrm{SL}_3(\mathbb{Z})$ of matrices A with trace a and $\det(A - \mathrm{I}) = 1$. By Theorem 3.3 and Lemma 3.5 these conjugacy classes are in bijection with the ideal classes of $\mathbb{Z}[\theta]$ where $\theta \in \mathbb{C}$ is a root of $f_a(t) = t^3 - at^2 + (a-1)t - 1$.

The bijection can be described as follows. Let $A \in \mathrm{SL}_3(\mathbb{Z})$ be a representative of such a conjugacy class. Since $A - \theta\mathrm{I}$ has entries in the field $\mathbb{Q}[\theta] = \mathbb{Q}(\theta)$, corresponding to the eigenvalue θ of A we can find an eigenvector $(x_1, x_2, x_3)^t \in (\mathbb{Q}[\theta])^3$. By scaling if necessary we assume that $x_1, x_2, x_3 \in \mathbb{Z}[\theta]$. The element of the ideal class monoid $\mathrm{Cl}(\mathbb{Z}[\theta])$ corresponding to the conjugacy class containing A is then given by the ideal class $[(x_1, x_2, x_3)] \in \mathrm{Cl}(\mathbb{Z}[\theta])$.

Proposition 3.6 ([AR84])**.** The matrix

$$A_{a,\lambda,p} = \begin{bmatrix} 0 & 0 & 1 \\ m & \lambda & 0 \\ n & p & a-\lambda \end{bmatrix},$$

as in Theorem 3.2, corresponds to the ideal class with representative $(m, \theta - \lambda) \subset \mathbb{Z}[\theta]$.

Proof. We compute an eigenvector x corresponding to the eigenvalue θ of $A_{a,\lambda,p}$. We have

$$\begin{bmatrix} 0 & 0 & 1 \\ m & \lambda & 0 \\ n & p & a-\lambda \end{bmatrix} \begin{bmatrix} x_1 \\ x_2 \\ x_3 \end{bmatrix} = \theta \begin{bmatrix} x_1 \\ x_2 \\ x_3 \end{bmatrix}.$$

Thus, $x_3 = \theta x_1$ and $mx_1 + \lambda x_2 = \theta x_2$. Taking $x_1 = \theta - \lambda$, we obtain $x_2 = m$ and $x_3 = \theta(\theta - \lambda)$. Hence, a representative for the ideal is given by $(\theta - \lambda, m, \theta(\theta - \lambda)) = (m, \theta - \lambda)$. $\square$

A *number field* is a finite field extension of $\mathbb{Q}$. For example $\mathbb{Q}(\theta) = \mathbb{Q}[\theta]$ is a degree 3 field extension of $\mathbb{Q}$ with $\mathbb{Q}$-basis $\{1, \theta, \theta^2\}$. The *ring of integers* $\mathcal{O}_K$ of a number field K is the subring of K consisting of all elements which are roots of monic polynomials with integer coefficients. An *order* of K is a subring of K which is a free $\mathbb{Z}$-module of rank $[K : \mathbb{Q}]$. It is a basic result in algebraic number theory that $\mathcal{O}_K$ is an order and every other order is contained in $\mathcal{O}_K$, so that $\mathcal{O}_K$ is the maximal order, e.g. see [Ste08, Theorem 2.2].

The ideal class monoid of the ring of integers of a number field is a group. One of the main results in algebraic number theory is that the ideal class group of the ring of integers of a number field is finite. It is true more generally that the ideal class monoid of an order is finite, see Theorem 20.6 of [CR06]. Thus, for a given trace there are only finitely many conjugacy classes of Cappell-Shaneson matrices in $\mathrm{SL}_3(\mathbb{Z})$.

In our specific case, we have that the ring $\mathbb{Z}[\theta]$ is an order of $\mathbb{Q}(\theta)$, indeed it is the free $\mathbb{Z}$-submodule generated by $\{1, \theta, \theta^2\}$. However, in general $\mathbb{Z}[\theta]$ is not equal to $\mathcal{O}_{\mathbb{Q}(\theta)}$. For example, when $a = 27$ and $f_a(x) = x^3 - 27x^2 + 26x - 1$, the element $\frac{1}{7}(2\theta^2 + 6\theta + 1)$ is not in $\mathbb{Z}[\theta]$ but it is in $\mathcal{O}_{\mathbb{Q}(\theta)}$ since one can check that it is a root of $x^3 - 217x^2 + 303x - 47$.

Fortunately, for many values of a, it is the case that $\mathbb{Z}[\theta] = \mathcal{O}_{\mathbb{Q}(\theta)}$, in which case the ideal class monoid is in fact a group (all ideal classes are invertible). Aitchison and Rubinstein (Table 1 of [AR84]), compute the class number for all values of the trace betweeen -9 and 14 inclusive, except for $a = -8, 13$ for which they were unable to determine if $\mathbb{Z}[\theta]$ is the maximal order. The computer software SageMath [Dev17] is able to determine if $\mathbb{Z}[\theta]$ is the maximal order and if so, compute the ideal class group. Using SageMath it is straightforward to check that for $a = -8, 13$ the ring $\mathbb{Z}[\theta]$ is the maximal order. We discuss this further in the next section.

3.4 Ideal class groups in SageMath

In this section we briefly illustrate how the computer software SageMath [Dev17] can be used to compute the ideal class group of the ring of integers of a number field. For many values of the trace, this allows us to compute representatives for the conjugacy classes of Cappell-Shaneson matrices with that trace.

Consider, as in the previous section, $\mathbb{Z}[\theta]$, where $\theta \in \mathbb{C}$ is a root of $f_a(t) = t^3 - at^2 + (a-1)t - 1$, $a \in \mathbb{Z}$. The ideal classes of $\mathbb{Z}[\theta]$ are in one to one correspondence with the conjugacy classes of trace a Cappell-Shaneson matrices.

We display a short interactive session inside SageMath. For $a = 13$, we check that $\mathbb{Z}[\theta]$ is the ring of integers of the number field $K = \mathbb{Q}(\theta)$. We then compute the class number and ideal class group of $\mathbb{Z}[\theta]$ (listing its elements).

SageMath code 3.1:

```
sage: a = 13; K.<t> = NumberField(x^3 - a*x^2 + (a-1)*x - 1)
sage: O = K.order(t)
sage: O == K.ring_of_integers()
True
sage: O.class_number()
3
sage: G = O.class_group(); G
```

```
Class group of order 3 with structure C3 of Number Field in t with
defining polynomial x^3 - 13*x^2 + 12*x - 1
sage: [z for z in G]

[Trivial principal fractional ideal class,
 Fractional ideal class (3, t^2 - 12*t + 5),
 Fractional ideal class (11, -5*t^2 + 61*t - 20)]
```

We see that there are three conjugacy classes of Cappell-Shaneson matrix with trace $a = 13$.

As another example, we can determine whether the trace 3 matrices

$$A_{3,1,1} = \begin{bmatrix} 0 & 0 & 1 \\ 1 & 1 & 0 \\ 0 & 1 & 2 \end{bmatrix}, \quad A_{3,4,1} = \begin{bmatrix} 0 & 0 & 1 \\ -23 & 4 & 0 \\ -6 & 1 & -1 \end{bmatrix},$$

are conjugate by determining whether $(1, \theta - 1)$ and $(-23, \theta - 4)$ (see Proposition 3.6) are in the same ideal class as follows. After first running SageMath code 3.1 with $a = 3$, we check:

SageMath code 3.2:

```
sage: G(K.ideal((1, t-1))) == G(K.ideal((-23, t-4)))
True
```

Hence the two matrices are in fact conjugate.

In fact, we can enumerate a list of representatives for the Cappell-Shaneson conjugacy classes of trace 3. Using Theorem 3.2, for $\lambda = 0, 1, 2, \ldots$, we set p to range over all (of the finitely many) factors of $1 + n\lambda$. We record the ideal class of matrices we encounter until every ideal class in the ideal class group is accounted for. In SageMath, this works more generally for any trace in which $\mathbb{Z}[\theta]$ is the ring of integers of $K = \mathbb{Q}(\theta)$. Note that at the time of this writing SageMath cannot enumerate the ideal classes for orders which are not maximal (in that case the ideal class monoid is not a group).

3.5 Fishtail surgery trick

A *fishtail neighbourhood* is a compact 4-manifold given by a product torus neighbourhood $T^2 \times D^2$ with a 2-handle glued onto $(S^1 \times \{pt\}) \times D^2 \subset T^2 \times D^2$ via a ± 1 twist. If there is a fishtail neighbourhood Q embedded in a smooth 4-manifold X then one can cut out $T^2 \times D^2 \subset Q \subset X$ and glue it back in by the diffeomorphism of $T^2 \times S^1$ given by a k-fold Dehn twist along T^2 parallel to $S^1 \times \{pt\}$, and the identity map in the remaining S^1 factor. We refer to this operation as a fishtail surgery. It is well-known that a fishtail surgery does not change the diffeomorphism type of the 4-manifold, see for example Lemma 2.2 of [Gom10].

Note that this is an example of an operation in which we remove a neighbourhood of a torus in a 4-manifold and glue it back in by some diffeomorphism. Such an operation is often called a torus surgery, logarithmic transform or Luttinger surgery.

In [Gom10], Gompf locates fishtail neighbourhoods in Cappell-Shaneson homotopy spheres under some algebraic conditions. By then performing fishtail surgery he shows that a Cappell-Shaneson homotopy sphere corresponding to a different monodromy is then obtained. This shows that many Cappell-Shaneson spheres are in fact diffeomorphic.

More precisely Gompf shows the following. Suppose that the monodromy in the construction of a Cappell-Shaneson homotopy sphere is given by a matrix

$$A = \begin{bmatrix} 0 & a & b \\ 0 & c & d \\ 1 & e & f \end{bmatrix}.$$

Let

$$\delta = \begin{bmatrix} 1 & -1 & 0 \\ 0 & 1 & 0 \\ 0 & 1 & 1 \end{bmatrix}.$$

Then left or right multiplication of the monodromy matrix A by δ^k, $k \in \mathbb{Z}$ does not change the diffeomorphism type of the corresponding Cappell-Shaneson homotopy 4-sphere with the same framing. This new operation allows us to change the trace of the monodromy matrix without changing the diffeomorphism type. In fact, this operation allows us to change the trace by any multiple of d. For example it immediately applies to show that the Cappell-Shaneson homotopy 4-spheres corresponding to the well-studied infinite family

$$A_m = \begin{bmatrix} 0 & 1 & 0 \\ 0 & 1 & 1 \\ 1 & 0 & m+1 \end{bmatrix}, \quad m \in \mathbb{Z}$$

are all diffeomorphic to the A_0 case. To see this note that $d = 1$ so we can change the trace of A_m to have trace 2 then finally note that there is only one conjugacy class of Cappell-Shaneson matrices with trace 2 [AR84]. Since the Cappell-Shaneson spheres with monodromy A_0 and both framings were shown to be diffeomorphic to S^4, this proves the Cappell-Shaneson spheres A_m, $m \in \mathbb{Z}$ are all diffeomorphic to S^4, a result first proved by Akbulut [Akb10].

Conjecture (Gompf): This fishtail surgery operation together with conjugation in $\mathrm{SL}_3(\mathbb{Z})$ can be used to show that all Cappell-Shaneson homotopy 4-spheres are diffeomorphic to the A_0 case, and hence are diffeomorphic to the standard 4-sphere.

Using SageMath we checked that for all conjugacy classes of Cappell-Shaneson matrices $A = \left(\begin{smallmatrix} 0 & a & b \\ 0 & c & d \\ 1 & e & f \end{smallmatrix}\right)$ with $-21 \leq \mathrm{tr}(A) \leq 26$, $\mathrm{tr}(A) \neq 0$, we can find a representative Cappell-Shaneson matrix in the conjugacy class with $0 < d < 2|\mathrm{tr}(A)|$. We can use Gompf's operation on such a representative to decrease $|\mathrm{tr}(A)|$. Hence, the corresponding Cappell-Shaneson spheres are diffeomorphic to the $\mathrm{tr}(A) = 0$ case, and hence are diffeomorphic to the standard 4-sphere. This shows the following:

Proposition 3.7. Let A be a Cappell-Shaneson matrix with $-21 \leq \mathrm{tr}(A) \leq 26$, then the two associated Cappell-Shaneson spheres are diffeomorphic to the standard 4-sphere.

Proposition 3.7 can not easily be extended using our computer code since for $\mathrm{tr}(A) = -22, 27$, the ideal class monoid is not a group, and so SageMath can not be used to understand the conjugacy classes. However, very recently, the paper [KY17] was posted on the arXiv, in which the authors extend Proposition 3.7. They show that all Cappell-Shaneson spheres corresponding to Cappell-Shaneson matrices A with $-64 \leq \mathrm{tr}(A) \leq 69$ are diffeomorphic to S^4. This is done by understanding the ideal class monoid in cases where it is not a group. Furthermore, they show a new infinite family of Cappell-Shaneson homotopy 4-spheres are diffeomorphic to S^4.

Chapter 4

Triangulation once-punctured 2-torus bundles

In this chapter we describe the Floyd-Hatcher triangulations of once punctured torus bundles over the circle [FH82]. The monodromy of an (oriented) once punctured torus bundle can be thought of as an element $A \in \mathrm{SL}_2(\mathbb{Z})$. We triangulate those bundles with $\mathrm{tr}(A) > 2$ (the case $\mathrm{tr}(A) < 2$ is similar) for which the monodromy homeomorphism is pseudo-Anosov. For nice expositions of this material see also [Gué06] or [Lac03].

4.1 Farey Tessellation

In order to triangulate once-punctured torus bundles, we first factor the monodromy matrix (up to conjugation, which does not change the bundle) into a convenient canonical form (Theorem 4.1). From this canonical form we can read off instructions which tell us how construct the triangulation.

Theorem 4.1. Let A be a matrix in $\mathrm{SL}_2(\mathbb{Z})$ with $\mathrm{tr}(A) > 2$. Then there exist $B \in \mathrm{SL}_2(\mathbb{Z})$, $n \in \mathbb{Z}$, and non-negative integers $a_1, \ldots, a_n, b_1, \ldots, b_n$ such that

$$BAB^{-1} = L^{a_1} R^{b_1} L^{a_2} R^{b_2} \cdots L^{a_n} R^{b_n},$$

where

$$L = \begin{pmatrix} 1 & 1 \\ 0 & 1 \end{pmatrix} \text{ and } R = \begin{pmatrix} 1 & 0 \\ 1 & 1 \end{pmatrix}.$$

We prove this using properties of the Farey tessellation of the hyperbolic upper half plane. Relevant sources for this section include [Bon09, Chapter 9], [Ser85a] and [Ser85b].

Definition 4.2. The *upper-half plane model of the hyperbolic plane* is the metric space

$$\mathbb{H}^2 = \{(x, y) \in \mathbb{R}^2 = \mathbb{C} \mid y > 0\}$$

with distance function

$$d(a, b) = \inf\{\ell(\gamma) \mid \gamma : [0, 1] \to \mathbb{H}^2 \text{ smooth}, \gamma(0) = a, \gamma(1) = b\}$$

where

$$\ell(\gamma) = \int_0^1 \frac{\sqrt{x'(t)^2 + y'(t)^2}}{y(t)} dt$$

is the *hyperbolic length* of the curve $\gamma(t) = (x(t), y(t))$.

The *geodesics* of $\mathbb{H}^2$ are vertical lines and semicircles centred on a point in $\mathbb{R} \subseteq \mathbb{C}$. An *ideal hyperbolic triangle* is the region of $\mathbb{H}^2$ bounded by the geodesics pairwise joining three distinct points in $\mathbb{R} \cup \{\infty\}$ which is homeomorphic to a triangle with its vertices removed.

Convention 1. When considering an element $\frac{p}{q} \in \mathbb{Q} \cup \{\infty\}$ we assume that p and q are coprime and $q > 0$, with the exception of ∞ which we consider to be $\infty = \frac{1}{0} = \frac{-1}{0}$.

Definition 4.3. The elements $\frac{p}{q}, \frac{p'}{q'} \in \mathbb{Q} \cup \{\infty\}$ form a *Farey pair* if $pq' - p'q = \pm 1$.

Definition 4.4. The *Farey tessellation* is the set of hyperbolic ideal triangles which are bounded by the geodesics whose endpoints in $\mathbb{Q} \cup \{\infty\}$ form Farey pairs.

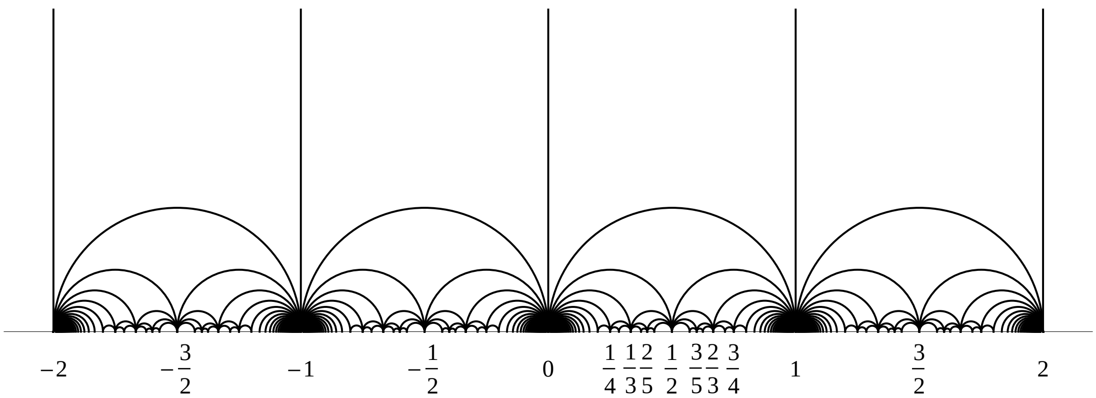

Figure 4.1: Part of the Farey tessellation

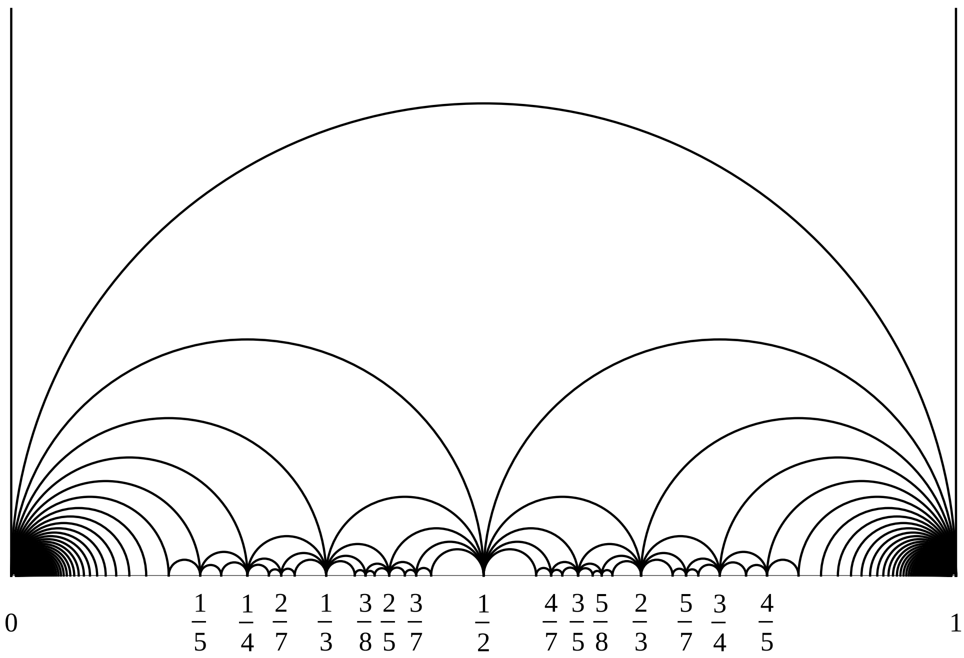

Figure 4.2: $[0, 1]$ region of the Farey tessellation

Lemma 4.5. If T is a Farey triangle, then the set of vertices of T is $\{\frac{a}{b}, \frac{c}{d}, \frac{a+c}{b+d}\}$, for some $\frac{a}{b}, \frac{c}{d} \in \mathbb{Q} \cup \{\infty\}$.

Proof. Let $\frac{a}{b} > \frac{e}{f} > \frac{c}{d}$ be the three vertices of T. Then $af - be = 1$, $ed - fc = 1$ and $ad - bc = 1$. Solving for e and f in the first two equations, then using the third equation to simplify the result, we obtain $e = a + c$ and $f = b + d$ as required. □

Lemma 4.6. If $\varphi(z) = \frac{az+b}{cz+d}$, where $ad - bc = 1$, is in $\mathrm{PSL}(2, \mathbb{Z})$ then A preserves the Farey tessellation, that is, if $\frac{u}{v}, \frac{s}{t} \in \mathbb{Q} \cup \{\infty\}$ are a Farey pair then $\varphi(\frac{u}{v}), \varphi(\frac{s}{t})$ form a Farey pair.

Proof. Since $\varphi(\frac{u}{v}) = \frac{au+bv}{cu+dv}$ and $\varphi(\frac{s}{t}) = \frac{as+bt}{cs+dt}$, we have

$$(au + bv)(cs + dt) - (cu + dv)(as + bt) = (ad - bc)(ut - vs) = \pm 1,$$

as required. □

Proof of Theorem 4.1.

Step 1. Given a matrix $M \in \mathrm{SL}_2(\mathbb{Z})$ let φ_M denote the induced isometry of the upper half plane given by

$$A = \left(\begin{smallmatrix} a & b \\ c & d \end{smallmatrix}\right) \mapsto \varphi_A(z) = \frac{az + b}{cz + d}.$$

Since $\mathrm{tr}(A) > 2$, the isometry φ_A is hyperbolic and fixes a geodesic axis G with repelling fixed point α_- and attracting fixed point α_+. Furthermore, α_- and α_+ are irrational real numbers, so G does not coincide with any edge of the Farey tessellation. We give G an orientation from repelling to attracting fixed point. As we traverse the oriented geodesic G there is a bi-infinite sequence of triangles of the Farey tessellation which are crossed by G.

Claim. There exists an isometry $h \in \mathrm{PSL}_2(\mathbb{Z})$ such that the oriented geodesic axis G' of $h \circ \varphi_A \circ h^{-1}$ crosses the vertical geodesic joining 0 to ∞ from left to right, i.e. so that the attracting fixed point of G' is a positive real number.

Proof of claim. Pick a Farey triangle T crossed by G and let the vertices be given by $\frac{p}{q}, \frac{r}{s}, \frac{p+r}{q+s}$ in clockwise order. The isometry $f(z) = \frac{qz-p}{-sz+r}$, which is in $\mathrm{PSL}_2(\mathbb{Z})$, maps T to the triangle Δ with vertices $0, \infty, 1$. Furthermore, the isometry $\theta(z) = \frac{1}{1-z}$ which is in $\mathrm{PSL}_2(\mathbb{Z})$ acts on the Farey tessellation by rotating Δ by $2\pi/3$ counter-clockwise, that is, cyclically permuting its vertices counter-clockwise. Hence, the isometry $\theta^i \circ f$, where $i \in \{0, 1, 2\}$ is appropriately chosen, sends the oriented geodesic G to an oriented geodesic which crosses the vertical geodesic from 0 to ∞ from left to right. Therefore, the isometry $h = \theta^i \circ f$ has the property stated in the claim.

Step 2. Let $\varphi' = h \circ \varphi_A \circ h^{-1}$, where h is the isometry from Step 1. Let

$$(\ldots, \Delta_{-1}, \Delta_0, \Delta_1, \Delta_2, \ldots)$$

be the bi-infinite sequence of Farey triangles crossed by the oriented geodesic axis G' of φ', where $\Delta_0 = \Delta$ is the triangle with vertices $0, \infty, 1$. For each triangle Δ_j we distinguish the edge in which G' enters Δ_j. For $f \in \mathrm{PSL}_2(\mathbb{Z})$, we will use the notation $f(\Delta_j) = \Delta_k$ to mean that f sends Δ_j to Δ_k as a set, and preserves the distinguished edge. Observe that f is completely specified by the equation $f(\Delta_j) = \Delta_k$, as this determines f on the vertices of Δ_j.

When the oriented geodesic G' enters a triangle Δ_i there are exactly two possible edges for which it can exit Δ_i and enter Δ_{i+1}, either through the edge to the left or to the right of where it enters. In this way we associate a matrix A_i to Δ_i which is L (resp. R) if G' exits Δ_i to the left (resp. right) of where it enters.

Since φ' acts as a translation along its geodesic axis, and sends Farey triangles to Farey triangles, there exists $m \in \mathbb{Z}$ such that $\varphi'(\Delta_0) = \Delta_m$.

Claim. Let $k \in \mathbb{Z}_{\geq 0}$ and let ψ_k be the isometry induced by $A_0 A_1 A_2 \cdots A_k$. Then $\psi(\Delta_0) = \Delta_k$.

Assume the claim. Then $\psi_m(\Delta_0) = \varphi'(\Delta_0) = \Delta_m$, and so $\varphi' = \psi_m$. Therefore A and $M := A_0 A_1 A_2 \cdots A_m$ are conjugate in $\mathrm{PSL}_2(\mathbb{Z})$, i.e. there exists $P \in \mathrm{PSL}_2(\mathbb{Z})$ such that $PAP^{-1} = \pm M$ as matrices in $\mathrm{SL}_2(\mathbb{Z})$. We know that $\mathrm{tr}(M) > 0$, and by assumption $\mathrm{tr}(A) > 2$, therefore $PAP^{-1} = M$, which completes the proof.

Proof of claim by induction on $k \in \mathbb{Z}_{\geq 0}$.

Base case $k = 0$.

(a) If $A_0 = L$ then $\psi_0(z) = z + 1$, hence $(0, \infty, 1) \mapsto (1, \infty, 2)$ as required.

(b) If $A_0 = R$ then $\psi_0(z) = \frac{z}{z+1}$, therefore $(0, \infty, 1) \mapsto (0, 1, \frac{1}{2})$ as required.

Assume the claim is true for $k \in \mathbb{Z}_{\geq 0}$. Assume first that $A_{k+1} = L$. We know that $\psi_k(\Delta_0) = \Delta_k$, so by continuity ψ_k maps the triangle to the left of Δ_0 to the triangle to the left of Δ_k, preserving the distinguished edge. Hence

$$(\psi_k \circ \varphi_L)(\Delta_0) = \psi_k(\varphi_L(\Delta_0)) = \Delta_{k+1}.$$

Since $\psi_k \circ \varphi_L$ is induced by $(A_0 \cdots A_k)L = A_0 \cdots A_{k+1}$, so $\psi_{k+1} = \psi_k \circ \varphi_L$. Therefore $\psi_{k+1}(\Delta_0) = \Delta_{k+1}$, as required. The case $A_{k+1} = R$ is analogous.

Example 4.7. Let
$$A = \begin{pmatrix} -4 & 11 \\ -3 & 8 \end{pmatrix} \in \mathrm{SL}_2(\mathbb{Z}).$$

The oriented geodesic axis G of the isometry given by A is shown in Figure 4.3. It cuts through the Farey triangle with vertices $2, 3, \infty$. By translating left two units G is sent to G', which cuts the Farey triangle $0, 1, \infty$. Conjugating A by this translation we obtain,

$$A' = \begin{pmatrix} 1 & -2 \\ 0 & 1 \end{pmatrix} \begin{pmatrix} -4 & 11 \\ -3 & 8 \end{pmatrix} \begin{pmatrix} 1 & -2 \\ 0 & 1 \end{pmatrix}^{-1} = \begin{pmatrix} 2 & -1 \\ -3 & 2 \end{pmatrix}.$$

We see that G' is oriented from right to left, hence we cyclically rotate the Farey triangle $0, 1, \infty$ twice sending G' to G''. Conjugating the matrix A' by this rotation we obtain,
$$A'' = \begin{pmatrix} 0 & 1 \\ -1 & 1 \end{pmatrix}^2 \begin{pmatrix} 2 & -1 \\ -3 & 2 \end{pmatrix} \begin{pmatrix} 0 & 1 \\ -1 & 1 \end{pmatrix}^{-2} = \begin{pmatrix} 3 & 2 \\ 1 & 1 \end{pmatrix}.$$
Finally, the isometry given by A'' sends the Farey triangle $0, 1, \infty$ to $2, 3, \frac{5}{2}$, so we may read off from Figure 4.3 the cutting sequence of A'' as LLR. Hence, $A'' = LLR$. Combining these steps, we can check that,

$$\begin{pmatrix} -1 & 3 \\ -1 & 2 \end{pmatrix} A \begin{pmatrix} -1 & 3 \\ -1 & 2 \end{pmatrix}^{-1} = LLR,$$

where L and R are as given in Theorem 4.1.

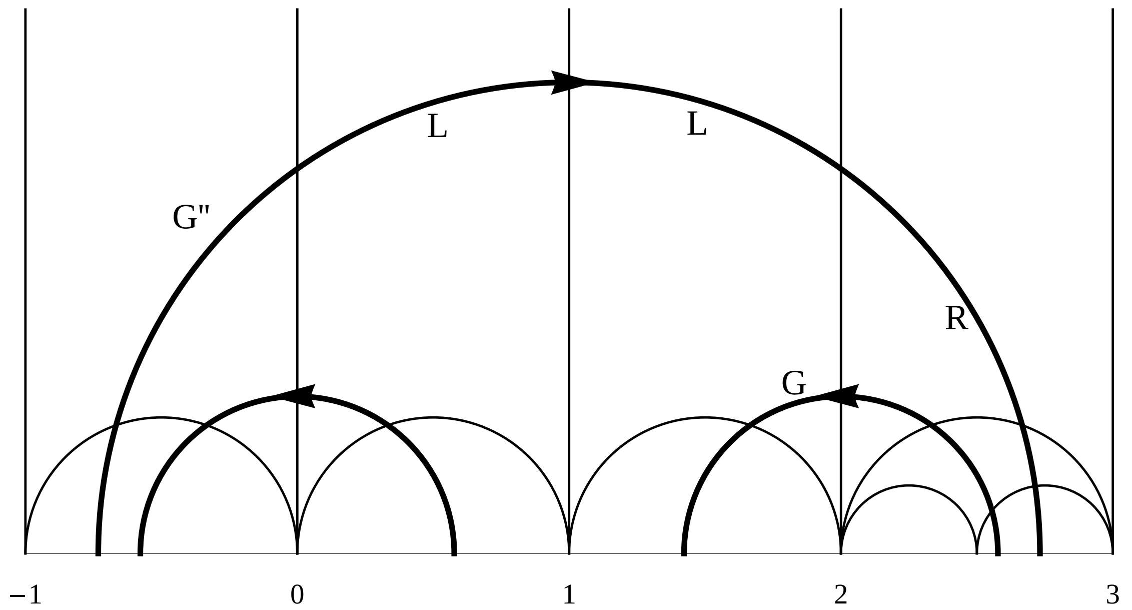

Figure 4.3: Geodesic axes and cutting sequence

4.2 Ideal triangulations of once-punctured torus bundles

Let $A \in \mathrm{SL}_2(\mathbb{Z})$ be a linear transformation of $\mathbb{R}^2$. Then A descends to a homeomorphism of the torus T. In fact, since A preserves the lattice $\mathbb{Z}^2$ which projects to a single point p in the torus, the homeomorphism A restricts to a homeomorphism of the punctured torus $T^\circ = T\backslash\{p\} = (\mathbb{R}^2\backslash\mathbb{Z}^2)/\mathbb{Z}^2$.

Let $A = LR = \left(\begin{smallmatrix} 2 & 1 \\ 1 & 1 \end{smallmatrix}\right)$, where $L = \left(\begin{smallmatrix} 1 & 1 \\ 0 & 1 \end{smallmatrix}\right)$ and $R = \left(\begin{smallmatrix} 1 & 0 \\ 1 & 1 \end{smallmatrix}\right)$. We will show how to obtain an ideal triangulation of the once-punctured torus bundle with monodromy A. From Theorem 4.1 an element $B \in \mathrm{SL}_2(\mathbb{Z})$ with $\mathrm{tr}(B) > 2$ is conjugate to a product of matrices which are equal to either L or R, which can be used to obtain an ideal triangulation of the once-punctured torus with monodromy B; see [Gué06] for details.

Step 1. Ideally triangulate the surface T°.

An *ideal triangle* is a topological space homeomorphic to a triangle with its vertices removed. An *ideal triangulation* of $T^\circ = T\backslash\{p\}$ is a decomposition of T° along ideal arcs into ideal triangles, where an ideal arc is the image $\alpha((0,1)) \subseteq T^\circ$ of a simple closed curve $\alpha : [0,1] \to T$ based at p.

A matrix $M \in \mathrm{SL}_2(\mathbb{Z})$ defines an ideal triangulation of T° described as follows. The columns of the matrix define two vectors u, v in $\mathbb{R}^2$. The vectors u, v form a parallelogram with diagonal $u+v$. The parallelogram, excluding its vertices, defines a fundamental domain for T°.

Furthermore, the edges of the parallelogram (excluding the vertices), together with the diagonal $u + v$ project to curves in T° which bound two ideal triangles, where an ideal triangle is a topological triangle with its vertices removed.

Taking M to be the identity matrix we obtain a triangulation of T° as shown in Figure 4.4.

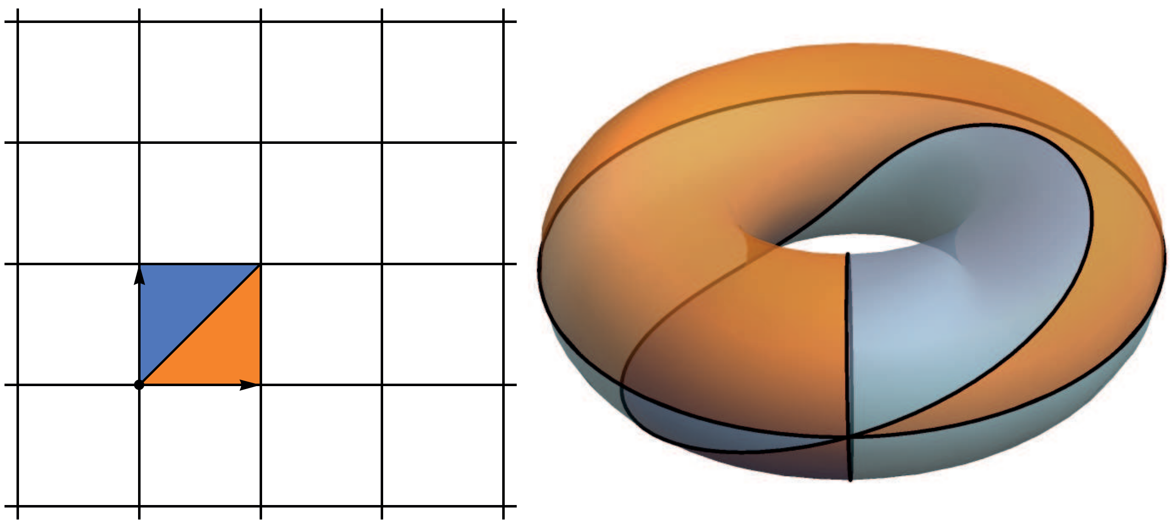

Figure 4.4: Layer 0 triangulation of T°. Note that in the image on the right, the vertex where the triangles meet in the torus is a puncture point, although this is not shown.

Step 2. Interpolate between $\mathcal{T}_0$ and $A(\mathcal{T}_0)$ by diagonal exchanges.

We obtain two more triangulations, one for each letter in the word representation of A, i.e. LR. Let M_0 denote the identity matrix, which induces triangulation $\mathcal{T}_0$. Define $M_1 = M_0 L$ and $M_2 = M_1 R$, and denote their induced triangulations on T° by $\mathcal{T}_1$ and $\mathcal{T}_2$ respectively, see Figures 4.5 and 4.6. (More generally, if $A = A_0 A_1 \cdots A_k$ where each A_i is either L or R, then we would define $M_{n+1} = M_n A_n$ for $n \in \{0, 1, \ldots, k\}$.)

What is the effect of each multiplication on the right by L or R on the induced triangulation? Suppose that we start with a parallelogram defined by the vectors (x_1, y_1) and (x_2, y_2), with diagonal $(x_1 + x_2, y_1 + y_2)$. Multiplying on the right by R we obtain

$$\begin{pmatrix} x_1 & x_2 \\ y_1 & y_2 \end{pmatrix} \begin{pmatrix} 1 & 0 \\ 1 & 1 \end{pmatrix} = \begin{pmatrix} x_1 + x_2 & x_2 \\ y_1 + y_2 & y_2 \end{pmatrix},$$

which gives a parallelogram defined by the vectors $(x_1 + x_2, y_1 + y_2)$ and (x_2, y_2), with diagonal $(x_1 + 2x_2, y_1 + 2y_2)$. Hence, the effect on the level of triangulations is that the edge joining the origin to (x_1, y_1) is removed and replaced by the edge joining the origin to $(x_1, y_1) + 2(x_2, y_2)$.

The effect of multiplication on the right by L is similar, in this case (x_2, y_2) is replaced by $2(x_1, y_1) + (x_2, y_2)$.

Notice that the columns $x, y \in \mathbb{R}^2$ of $M_2 = LR = A$ are precisely the image of the vectors $(1, 0)$ and $(0, 1)$ under the linear transformation A. Therefore, the triangulation induced by M_2 is equal to the image of $\mathcal{T}_0$ under the homeomorphism A.

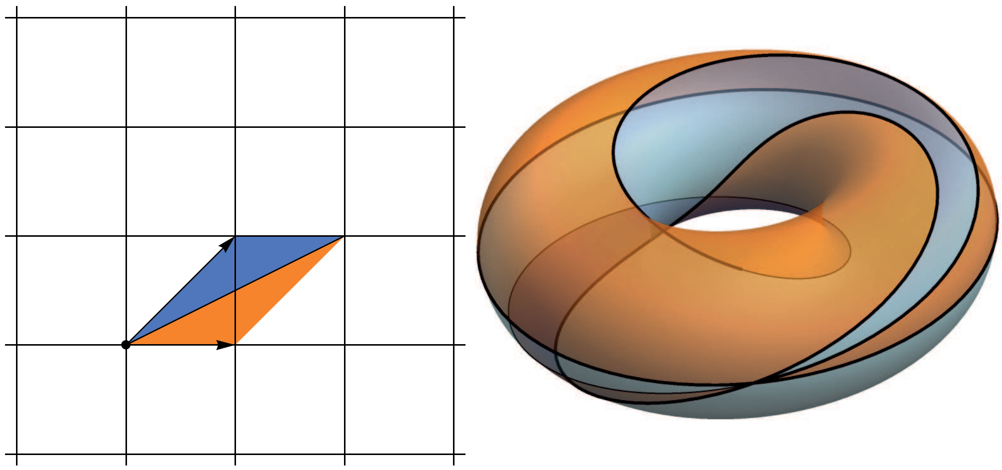

Figure 4.5: Layer 1 triangulation $\mathcal{T}_1$.

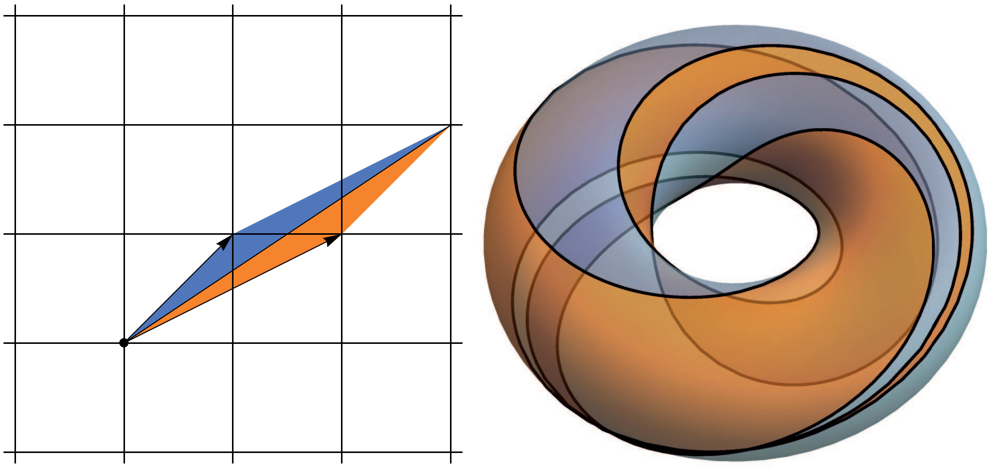

Figure 4.6: Layer 2 triangulation $\mathcal{T}_2$.

Step 3. Insert ideal tetrahedra between layers of surface triangulations.

The removal of an edge adjacent with two triangles in a triangulation of T°, followed by the addition of the other edge which forms a diagonal with the two triangles is known as a diagonal exchange or Whitehead move, see Figure 4.7. In Step 2 we saw that each successive triangulation obtained by multiplication by R or L corresponds to such a diagonal exchange.

For each diagonal exchange we attach an ideal tetrahedron to the two triangles which are removed, see Figure 4.7. Roughly speaking, the tetrahedron is thought of as being very close to flat so that the dihedral angle at the exchanged edges are close to π and the remaining dihedral angles are close to 0. It has two bottom faces attached to the triangles of $\mathcal{T}_0$ and two top faces attached to the triangles of $\mathcal{T}_1$.

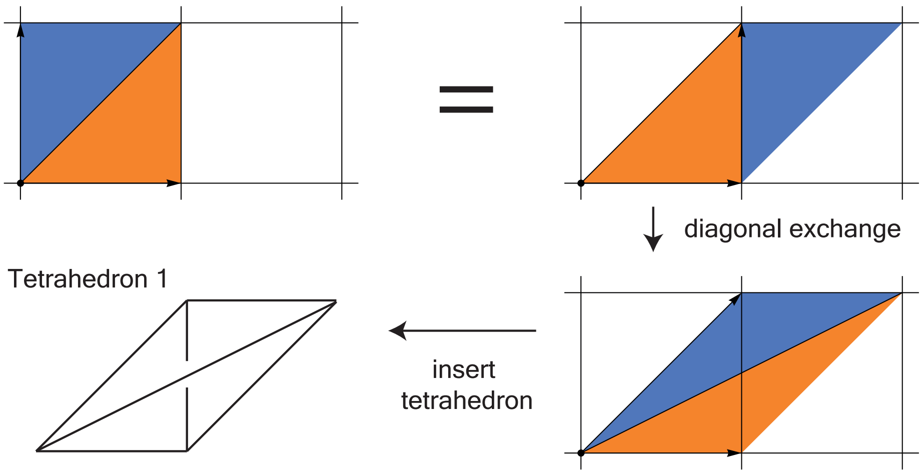

Figure 4.7: $\mathcal{T}_1$ is obtained by a diagonal exchange of an edge of $\mathcal{T}_0$, induced by multiplication on the right by L.

Similarly we insert a tetrahedron between the triangulations $\mathcal{T}_1$ and $\mathcal{T}_2$, as shown in Figure 4.8.

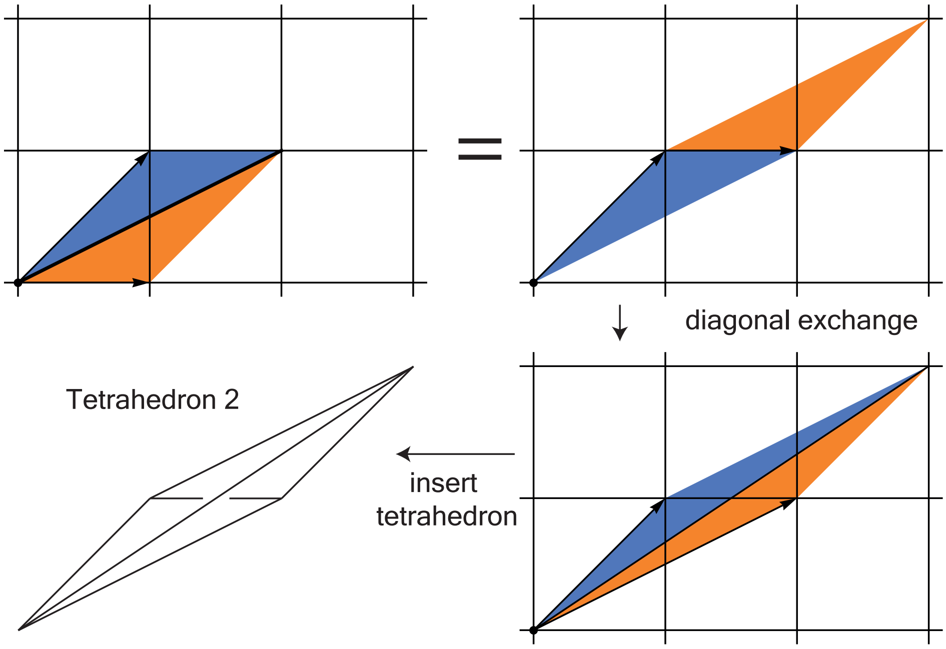

Figure 4.8: $\mathcal{T}_2$ is obtained by a diagonal exchange of an edge of $\mathcal{T}_1$, induced by multiplication on the right by R.

Step 4. Determine the face pairings between tetrahedra.

The front two faces, i.e. faces which are facing the reader in Figure 4.7, of tetrahedron 1 are paired to the back faces of tetrahedron 2 via $\mathcal{T}_1$. Since $A(\mathcal{T}_0) = \mathcal{T}_2$ and the back faces of tetrahedron 1 are paired with the front faces of tetrahedron 2 via the monodromy. The result is a topological ideal triangulation of the mapping torus with monodromy A.

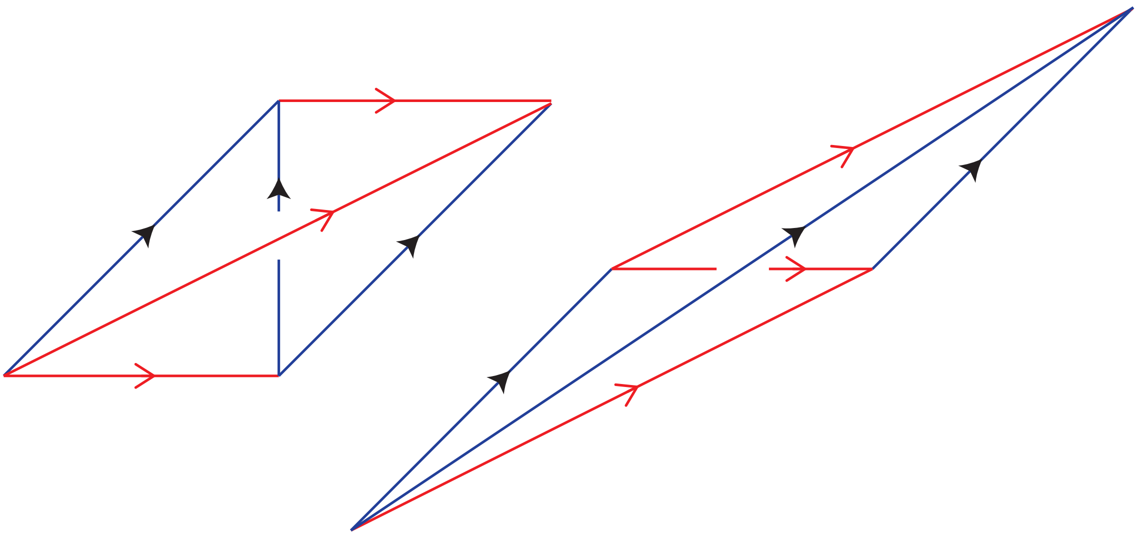

Figure 4.9: Faces with the same arrow pattern are glued, or paired, in such a way that the edge patterns are respected.

Remark 4.8. The mapping torus with monodromy A, which we triangulated, is homeomorphic to the figure eight knot complement in the three sphere $S^3 = \mathbb{R}^3 \cup$

$\{\infty\}$ (compare with the triangulations in [Thu97, Example 1.4.8] or [Fra87, Chapter 8].)

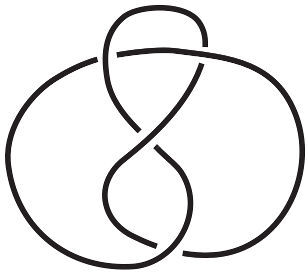

Figure 4.10: The figure eight knot.

Chapter 5

Triangulating once-punctured 3-torus bundles

In this chapter we explain how to construct layered triangulations of once-punctured 3-torus bundles. Our strategy is similar to constructing triangulations of once-punctured 2-torus bundles, so we recommend the reader acquaint themselves with the material in Chapter 4 before reading this chapter. One difference with the once-punctured torus bundle case is that the triangulations we obtain are not canonical, i.e. they depend on the choice of conjugacy class representative of the monodromy in $\mathrm{GL}_3(\mathbb{Z})$. In fact, even for a fixed representative, there are choices along the way which give rise to different triangulations of the same bundle.

In an enumeration of 4-dimensional triangulations, Budney, Burton and Hillman [BBH12] found a very interesting two 4-simplex ideal triangulation. They prove that this triangulation is *homeomorphic* to a once-punctured 3-torus bundle with monodromy $A = \begin{bmatrix} 0 & 0 & 1 \\ 1 & 0 & 0 \\ 0 & 1 & -1 \end{bmatrix}$. However, their argument relies on Freedman's results on topological surgery, and hence only proves that the triangulated manifold is *homeomorphic* to the bundle with monodromy A. They ask whether the triangulated manifold is in fact PL equivalent to the bundle with monodromy A.

We are able to recover the triangulation of Budney, Burton, Hillman starting from the monodromy matrix by directly triangulating the bundle as a layered triangulation. We can also obtain their triangulation by first using our general method for triangulating once-punctured 3-torus bundles and then simplifying the resulting triangulation. This shows that the triangulation they found is PL homeomorphic to the bundle with monodromy A, answering their question affirmatively. This is explained in Section 5.1.

Theorem 5.1. The two ideal 4-simplex triangulation of Budney-Burton-Hillman [BBH12] (see Figure 1.1 for a description) is PL-homeomorphic to the once-punctured 3-torus bundle over S^1 with monodromy matrix $A = \begin{bmatrix} 0 & 0 & 1 \\ 1 & 0 & 0 \\ 0 & 1 & -1 \end{bmatrix}$.

As mentioned earlier, for a fixed monodromy our strategy depends on choices along the way, and if we apply the general algorithm, described in Section 5.2 which works for any given monodromy to the monodromy A, we will obtain a much larger triangulation of the bundle. The minimal triangulation found by Budney, Burton, Hillman is instead obtained by making carefully selected choices when constructing the triangulation. We describe these choices in Section 5.1. Since this is one of the simplest examples of a layered triangulation of a once punctured 3-torus bundle, Section 5.1 is a useful starting point in understanding the more general construction.

We now give an outline of the steps needed to triangulate the once-punctured 3-torus bundle with monodromy $A \in \mathrm{GL}_3(\mathbb{Z})$.

(i) Fix a carefully selected highly symmetric ideal triangulation of the 3-torus which we denote by $\mathcal{T}_0$. This triangulation is independent of the monodromy.

(ii) Write the monodromy matrix $A \in \mathrm{GL}_3(\mathbb{Z})$ as a product of a permutation matrix and unit shear matrices. See Theorem 5.2.

(iii) Use the matrix factorisation to find a sequence of Pachner moves interpolating between the initial triangulation $\mathcal{T}_0$ and its image under the monodromy $A(\mathcal{T}_0)$. Each unit shear matrix will give rise to four Pachner moves on the punctured 3-torus. The symmetry of our initial triangulation $\mathcal{T}_0$ will imply that it is invariant under the permutation matrix.

(iv) Finally, we use the sequence of Pachner moves to construct a triangulation of the bundle. We start by triangulating $T^3 \times [0,1]$, where $T^3 = (\mathbb{R}^3 - \mathbb{Z}^3)/\mathbb{Z}^3$ is the once-punctured 3-torus. This is done in such a way that the induced 3-dimensional boundary triangulations of $T^3 \times \{0,1\}$ are given by $\mathcal{T}_0 \times \{0,1\}$. Then each Pachner move interpolating between $\mathcal{T}_0$ and $A(\mathcal{T}_0)$ will give rise to one 4-simplex which is layered onto a stack of 4-simplices on top of $T^3 \times [0,1]$. Finally the two ends are glued together via the monodromy.

We implemented the above steps as a Python program which takes as input a monodromy matrix in $\mathrm{GL}_3(\mathbb{Z})$ and builds the bundle triangulation. The triangulation can then be output as either an isomorphism signature or a custom file format which is a simple generalisation of the SnapPy [CDGW] 3-manifold triangulations file format (essentially the raw facet pairing data).

5.1 Triangulating the bundle of Budney, Burton and Hillman

In this section, we describe how the triangulation described by Budney, Burton, Hillman [BBH12] may be constructed directly as a layered triangulation starting with the monodromy of the bundle. Let $T = (\mathbb{R}^3 - \mathbb{Z}^3)/\mathbb{Z}^3$ be the once-punctured 3-torus, (ideally) triangulated by six ideal tetrahedra as shown in Figure 5.1. We denote this triangulation by $\mathcal{T}_0$.

Let

$$A = \begin{bmatrix} 0 & 0 & 1 \\ 1 & 0 & 0 \\ 0 & 1 & -1 \end{bmatrix}$$

be the monodromy matrix. The image of the triangulation of T under A is shown in the left of Figure 5.2. We denote this triangulation of T by $\mathcal{T}_2 := A(\mathcal{T}_0)$. In Figure 5.1, the action of A on $\mathcal{T}$ can be seen in Figure 5.1 as rotating 120 degrees

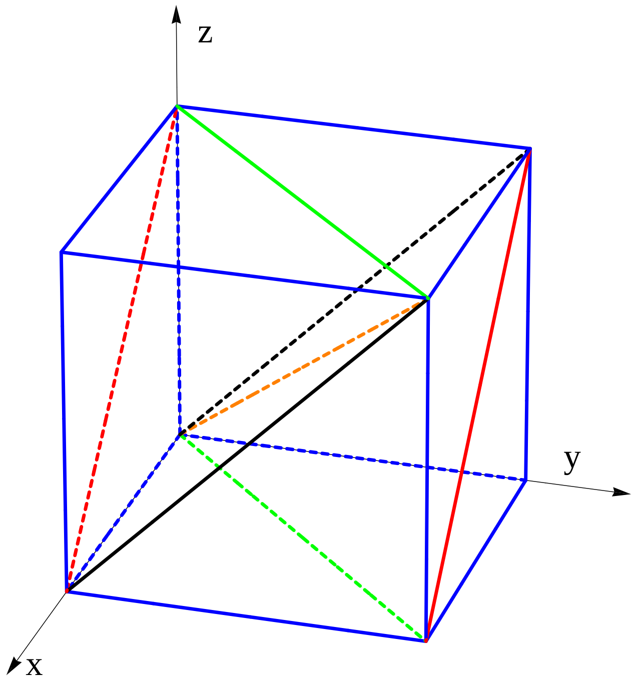

Figure 5.1: Triangulation of the (punctured) 3-torus. Only a unit cube fundamental domain is shown. Whenever 4 vertices of the cube are pairwise joined by edges (including edges of the unit cube) they form a tetrahedron.

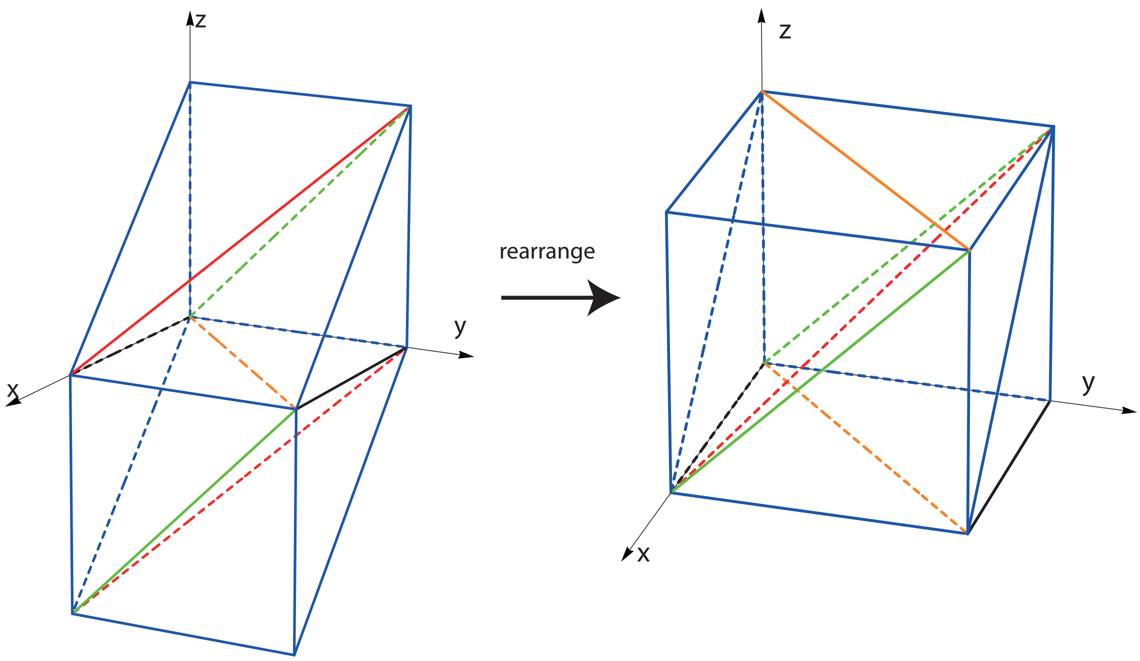

Figure 5.2: Image of the triangulation of Figure 5.1 under the monodromy.

about the axis spanned by the orange edge from $(0,0,0)$ to $(1,1,1)$, then shearing the triangulated cube one unit downwards. This corresponds to the matrix factorisation $A = \begin{bmatrix} 1 & 0 & 0 \\ 0 & 1 & 0 \\ -1 & 0 & 1 \end{bmatrix} \cdot \begin{bmatrix} 0 & 0 & 1 \\ 1 & 0 & 0 \\ 0 & 1 & 0 \end{bmatrix}$, as a product of a permutation matrix and a shear matrix. In the right of Figure 5.2 we have redrawn the triangulation $\mathcal{T}_2$ inside the unit cube fundamental domain.

We aim to find a sequence of Pachner 3-2 and 2-3 moves to interpolate between the triangulations $\mathcal{T}_0$ and $\mathcal{T}_2$. Notice that the edges of the triangulations $\mathcal{T}_0$ and $\mathcal{T}_2$ all coincide, except for the diagonals of the unit cube fundamental domain, i.e. the orange edge in Figure 5.1 and the red edge in the right of Figure 5.2. Each of these diagonal edges is common to four tetrahedra which together form a solid octahedron with common octahedral boundary. Replacing the orange edge with the red edge corresponds to replacing an internal edge of the octahedron with another internal edge, which changes the triangulation by replacing four tetrahedra with four other tetrahedra making up the octahedron, and is sometimes called a *4-4 move*. Although a 4-4 move is not a Pachner move it can be realised as a sequence of two Pachner moves, namely a 2-3 move followed by a 3-2 move, as shown in Figures 5.3 and 5.4. We denote by $\mathcal{T}_1$ the triangulation obtained after performing the first 2-3 move on $\mathcal{T}_0$.

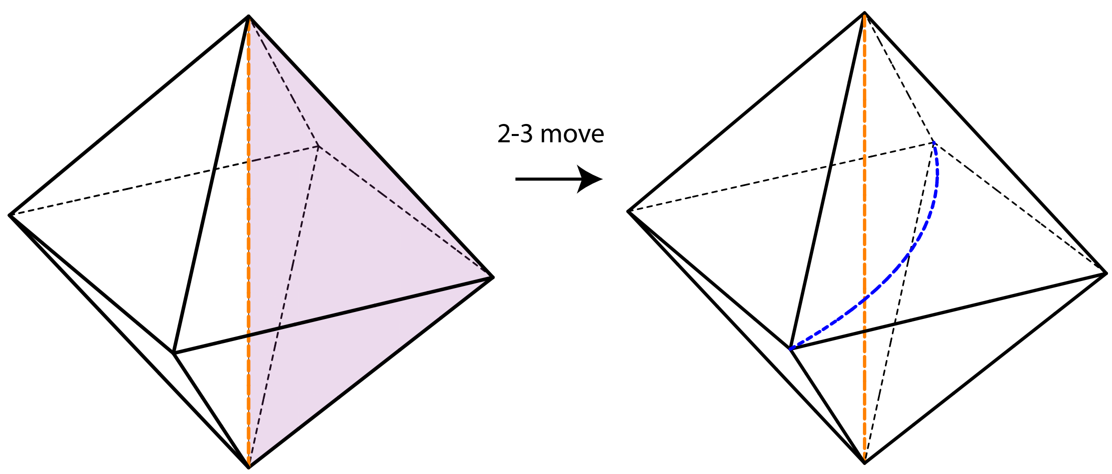

Figure 5.3: Pachner 2-3 move, replacing shaded face by blue dual edge.

In Figures 5.5 and 5.6, we show the tetrahedral facets of the two pentachora which interpolate between $\mathcal{T}_0$ and $\mathcal{T}_2$. We label the vertices of each pentachoron. Let P_i denote pentachoron i for $i \in \{1, 2\}$, so that P_i is thought of as interpolating between $\mathcal{T}_{i-1}$ and $\mathcal{T}_i$.

We now determine the facet pairings of the layered triangulation determined by P_1 and P_2. We will refer to the tetrahedral facet opposite vertex $i \in \{0, 1, 2, 3, 4\}$ by facet i. For example, facet 4 of P_1 has vertices $0, 1, 2, 3$. Pentachoron P_1 has two "bottom" facets, namely facets 0 and 4. Facets 0 and 4 of P_1 can be seen in Layer 0 of Figure 5.7, while the other three facets can be seen in Layer 1.

Facet 4 of P_1 has vertices $0, 1, 2, 3$ which are represented by the coordinates B,C,A,C' in $\mathcal{T}_0$ of Figure 5.7. To simplify notation, we simply write that 0123 of P_1 is represented by coordinates BCAC' in $\mathcal{T}_0$, where we think of 0123 and BCAC' as representing tetrahedra with the order of vertices being kept track of. Since facet 4 of P_1 is a "bottom" facet, in order to determine what it is glued to we work our way through the triangulations $\mathcal{T}_i$ reducing i cyclically (i.e. think of $i \in \mathbb{Z}_3$), keeping

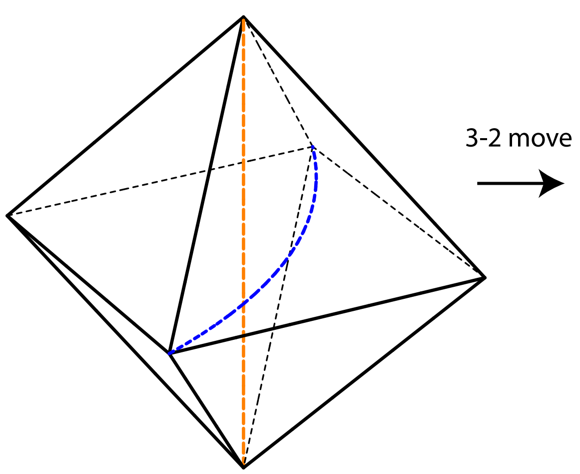

Figure 5.4: Pachner 3-2 move, replacing orange edge by a dual face.

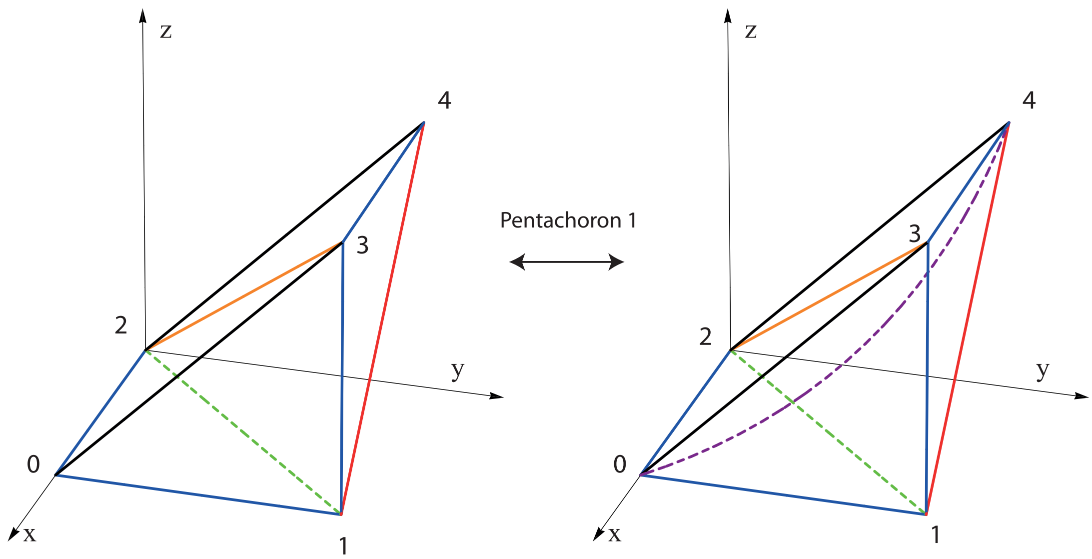

Figure 5.5: Tetrahedral facets of pentachoron 1.

track of the tetrahedron in each layer which this facet is identified with, until finally we encounter a “top” facet of a pentachoron which it glues to.

BCAC’ of Layer 0 is identified by the monodromy with the tetrahedron DD’AC in $\mathcal{T}_2$ of Figure 5.7. Tetrahedron DD’AC of Layer 2 remains tetrahedron DD’AC in Layer 1 and in Layer 0. Again, applying the monodromy we see that DD’AC of Layer 0 gets identified with tetrahedron A’BAD’ of Layer 2, which is facet 3 of P_2 as can be seen in Figure 5.6. More precisely A’BAD’ of Layer 2 is tetrahedral facet 1024 of P_2. Thus, we see that the facet 0123 of P_1 is glued to 1024 of P_2, where the order of the vertices is respected in the gluing map, e.g. vertex 0 of P_1 gets glued to vertex 1 of P_2 in this facet pairing.

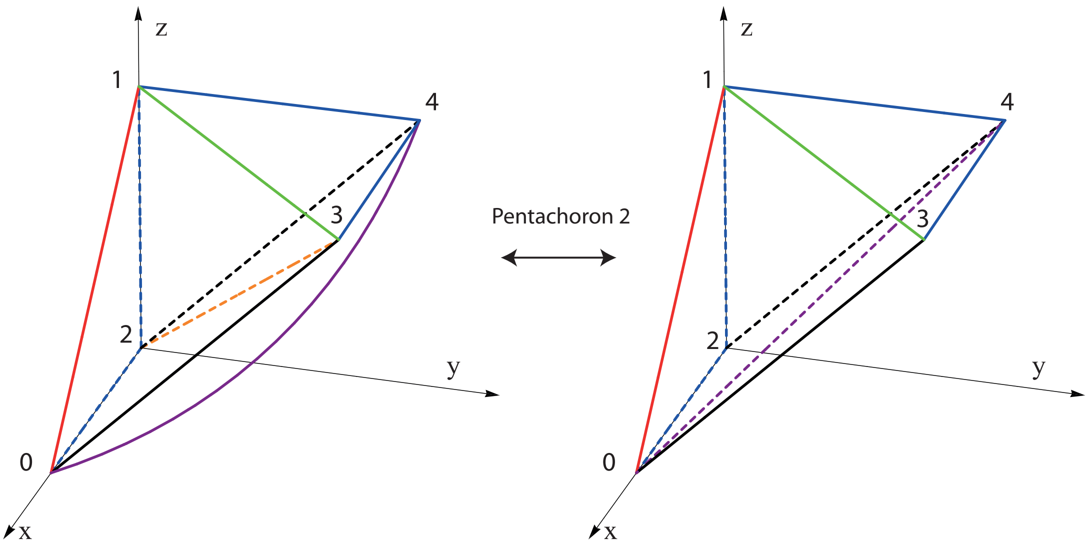

Figure 5.6: Tetrahedral facets of pentachoron 2.

We summarise the above computation by writing

$$\begin{aligned}(0123, P_1) &\leftrightarrow (BCAC', \mathcal{T}_0) \leftrightarrow (DD'AC, \mathcal{T}_2) \leftrightarrow (DD'AC, \mathcal{T}_1)\\ &\leftrightarrow (DD'AC, \mathcal{T}_0) \leftrightarrow (A'BAD', \mathcal{T}_2) \leftrightarrow (1024, P_2),\end{aligned}$$

where, for example, $(0123, P_1)$ denotes tetrahedral facet 0123 of P_1 and $(BCAC', \mathcal{T}_0)$ denotes tetrahedron $BCAC'$ of triangulation $\mathcal{T}_0$ as can be seen in Figure 5.7. We repeat the above procedure for the other "bottom" facets of P_1 and P_2 to determine all the face pairings of the triangulation. This computation is shown in Table 5.1.

Table 5.1: Layered triangulation facet pairing

Bottom facet	Identification sequence	Top facet
$(0123, P_1)$	$(BCAC', \mathcal{T}_0) \leftrightarrow (DD'AC, \mathcal{T}_2) \leftrightarrow (DD'AC, \mathcal{T}_1)$ $\leftrightarrow (DD'AC, \mathcal{T}_0) \leftrightarrow (A'BAD', \mathcal{T}_2)$	$(1024, P_2)$
$(1234, P_1)$	$(CAC'D', \mathcal{T}_0) \leftrightarrow (D'ACB, \mathcal{T}_2)$	$(4210, P_1)$
$(0123, P_2)$	$(BA'AC', \mathcal{T}_1) \leftrightarrow (BA'AC', \mathcal{T}_0) \leftrightarrow (D'BA'C', \mathcal{T}_2)$	$(4013, P_2)$
$(1234, P_2)$	$(A'AC'D', \mathcal{T}_1) \leftrightarrow (A'AC'D', \mathcal{T}_0) \leftrightarrow$ $(BA'C'B', \mathcal{T}_2) \leftrightarrow (BA'C'B', \mathcal{T}_1) \leftrightarrow$ $(BA'C'B', \mathcal{T}_0) \leftrightarrow (D'BC'C, \mathcal{T}_2) \leftrightarrow (D'BC'C, \mathcal{T}_1)$	$(4031, P_1)$
$(0234, P_2)$	$(BAC'D', \mathcal{T}_1)$	$(0234, P_1)$

Figure 5.8 is a diagram of the layered triangulation described by the face pairings given in Table 5.1, see Figure 1.1 and surrounding text for an explanation of the diagram. In order to see that this triangulation is combinatorially isomorphic to the triangulation obtained by Budney-Burton-Hillman shown in Figure 1.1, first relabel the vertices of pentachoron P_1 by the permutation $(0, 1, 2, 3, 4) \mapsto (1, 3, 0, 4, 2)$ and relabel the vertices of pentachoron P_2 by $(0, 1, 2, 3, 4) \mapsto (2, 1, 0, 4, 3)$. Then observe that the diagram of Figure 5.8 is transformed precisely to the diagram of Figure 1.1. This completes the proof of Theorem 5.1.

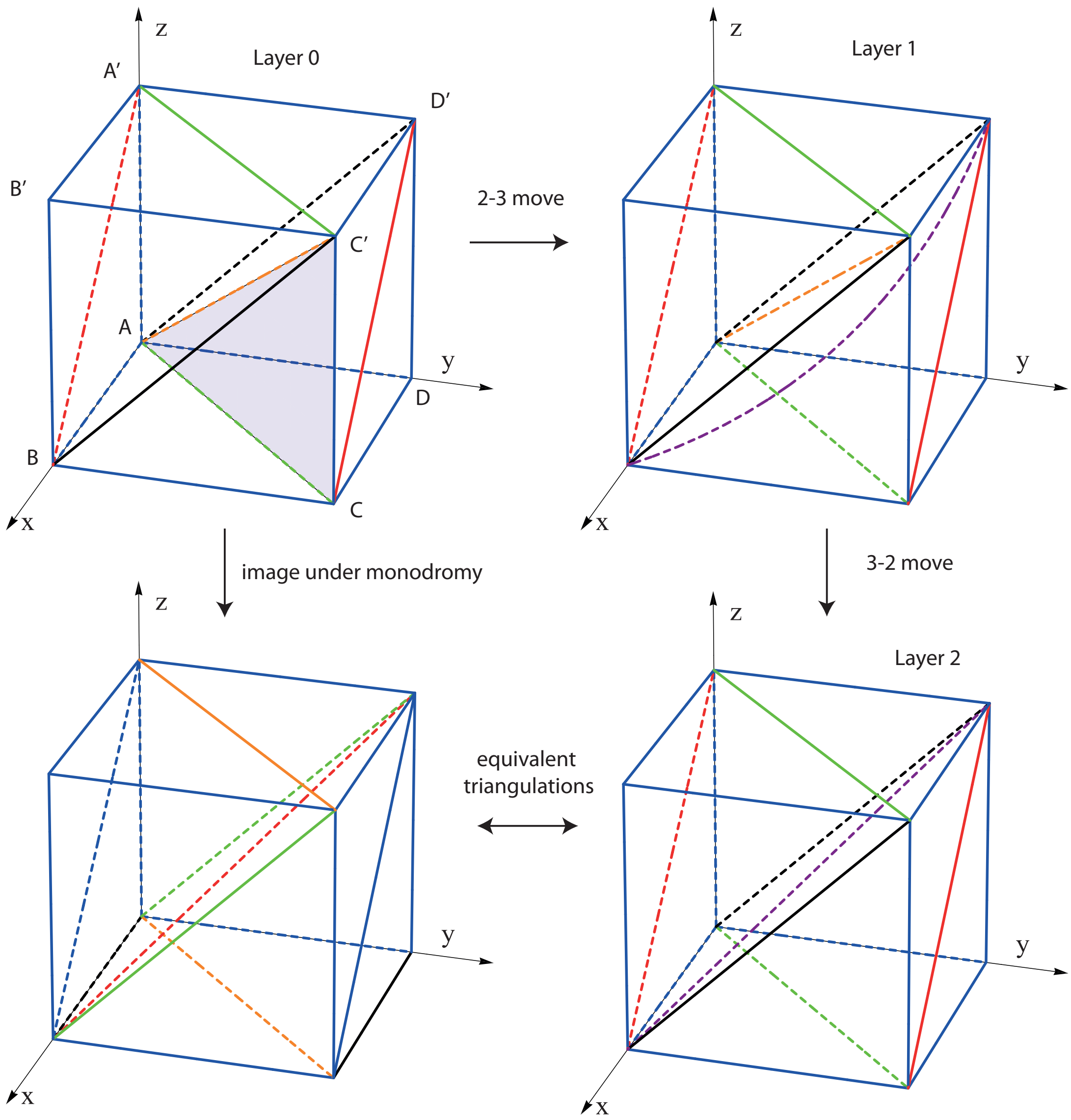

Figure 5.7: Sequence of Pachner moves interpolating between $\mathcal{T}_0$ and $\mathcal{T}_2 = A(\mathcal{T}_0)$. In Layer 0, we have shaded the face common to two tetrahedra in which the 2-3 move is performed.

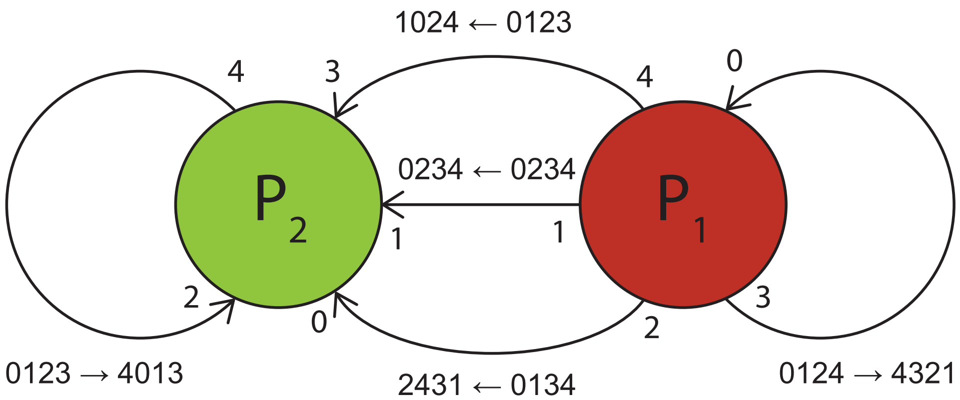

Figure 5.8: Diagram of the triangulation of the Budney-Burton-Hillman bundle which we obtained by layering tetrahedra.

5.2 General case

In this section we describe how to obtain a layered triangulation of any given once-punctured 3-torus bundle with monodromy in $A \in \mathrm{GL}_3(\mathbb{Z})$. We first obtain a useful factorisation of A given by the following theorem.

Theorem 5.2. Let $A \in \mathrm{GL}_3(\mathbb{Z})$. Then A can be written as

$$A = PA_1A_2 \cdots A_n, \quad n \geq 0$$

where

(i) For all i, A_i is a unit shear matrix, i.e. obtained from the identity matrix by changing a single non-diagonal entry to 1 or -1.

(ii) P is a permutation matrix.

Proof. By row reduction over $\mathbb{Z}$, we can write A as a product of elementary matrices. An elementary matrix is one of three types:

(i) a permutation matrix which exchanges rows,

(ii) a shear matrix which adds an integer multiple of one row to another,

(iii) or a matrix which scales a row by a multiplicative unit of $\mathbb{Z}$, i.e. ± 1.

An elementary matrix of the third type is either the identity or obtained from the identity by changing a single diagonal element to -1. Such a matrix may be written as a product of matrices of the first two types. For example,

$$\begin{pmatrix} -1 & 0 & 0 \\ 0 & 1 & 0 \\ 0 & 0 & 1 \end{pmatrix} = \begin{pmatrix} 1 & 0 & 0 \\ 1 & 1 & 0 \\ 0 & 0 & 1 \end{pmatrix} \begin{pmatrix} 1 & -1 & 0 \\ 0 & 1 & 0 \\ 0 & 0 & 1 \end{pmatrix} \begin{pmatrix} 1 & 0 & 0 \\ 1 & 1 & 0 \\ 0 & 0 & 1 \end{pmatrix} \begin{pmatrix} 0 & 1 & 0 \\ 1 & 0 & 0 \\ 0 & 0 & 1 \end{pmatrix}.$$

The other two cases with -1 entries in the second or third diagonal entry are similar to this one. Thus, we can write A as a product of elementary matrices of the first two types.

An elementary matrix of the second type (a shear matrix) can be written as a power of a unit shear matrix since adding an integer multiple $c \in \mathbb{Z}$ of one row to another is the same as adding that row to the other c times (for $c < 0$ we instead subtract $|c|$ times). Hence we may write A as a product of unit shear matrices and permutation matrices which exchange two rows.

Let T be a permutation matrix which permutes rows according to a permutation $\tau \in S_n$, and let A_{ij} be the unit shear matrix obtained from the identity by setting its (i,j) entry to ± 1. Then $TA_{ij}T^{-1} = A_{\tau(i),\tau(j)}$, where $A_{\tau(i),\tau(j)}$ is the unit shear matrix obtained from the identity by setting the $(\tau(i),\tau(j))$ entry to ± 1. Hence we have $TA_{ij} = A_{\tau(i),\tau(j)}T$. This relation allows us to commute permutation matrices with unit shear matrices, and hence we may write A as a product of a permutation matrix followed by a finite sequence of unit shear matrices, as required. $\square$

Remark 5.3. The proof of Theorem 5.2 provides a method to obtain an appropriate matrix factorisation of A. The number of 4-simplices in the triangulations of the once-punctured 3-torus bundles we obtain depends linearly on the number of matrices in the factorisation (n in Theorem 5.2). It would be interesting to investigate how to keep n small while keeping A in a fixed conjugacy class.

Let $A \in \mathrm{GL}_3(\mathbb{Z})$ be a monodromy matrix. Write $A = PA_1A_2 \cdots A_n$ as in Theorem 5.2. We will explain how to construct an ideal triangulation of the punctured 3-torus bundle over S^1 with monodromy given by A. This is a two step process, first we explain how to obtain a sequence of 3-dimensional Pachner moves interpolating between a triangulation and its image under the monodromy. We then explain how these Pachner moves can be used to obtain a triangulation of the bundle.

Let $\mathcal{T}_0$ be the triangulation of the punctured 3-torus T shown in Figure 5.9. This is a triangulation using six ideal tetrahedra. We will use the matrix factorisation of A to find a sequence of Pachner moves interpolating between the triangulation $\mathcal{T}_0$ and its image under the monodromy, $A(\mathcal{T}_0)$.

Define $\mathcal{T}'_k$, $0 \leq k \leq n$ to be the triangulation induced by the action of $PA_1A_2 \cdots A_k$ on the initial triangulation $\mathcal{T}_0$, i.e. let $\mathcal{T}'_k = PA_1A_2 \cdots A_k(\mathcal{T}_0)$.

Observe that since we chose the initial triangulation $\mathcal{T}_0$ in such a way that it is symmetric with respect to the x, y and z-axes, it is invariant under the action of permutation matrices. Hence we have $\mathcal{T}'_0 = P\mathcal{T}_0 = \mathcal{T}_0$. By definition, we also have that $\mathcal{T}'_n = A(\mathcal{T}_0)$ which is the image of the initial triangulation under the monodromy. Thus, in order to find a sequence of Pachner moves interpolating between $\mathcal{T}_0$ and $A(\mathcal{T}_0)$ it suffices to show there is a sequence of Pachner moves interpolating between $\mathcal{T}'_k$ and $\mathcal{T}'_{k+1}$, for $0 \leq k < n$. In fact, for any given k we will show that four Pachner moves suffice.

Proposition 5.4. Let $S = \begin{pmatrix} 1 & 0 & 0 \\ 0 & 1 & 0 \\ -1 & 0 & 1 \end{pmatrix}$. Then there is a sequence of four Pachner moves interpolating between $\mathcal{T}_0$ and $S(\mathcal{T}_0)$.

Before proving Proposition 5.4, we show that this specific computation is enough to interpolate between triangulations differing by a general type of shear.

Corollary 5.5. Let $S' \in \mathrm{GL}_3(\mathbb{Z})$ be any unit shear matrix, i.e. S' is obtained from the identity matrix by replacing a single non-diagonal entry with ± 1. Then there is a sequence of four Pachner moves interpolating between $\mathcal{T}_0$ and $S'(\mathcal{T}_0)$.

Proof of Corollary 5.5. This corollary follows by using the symmetry of the triangulation $\mathcal{T}_0$ under a permutation of the x, y and z-axes to conjugate the sequence of moves in Proposition 5.4. In more detail, suppose first that S' is obtained from the identity by changing an entry to -1. Then $S' = PSP^{-1}$ for some permutation matrix P, where S is as in Proposition 5.4. Then conjugating the sequence of Pachner moves from Proposition 5.4 by P gives a sequence of Pachner moves interpolating between $P\mathcal{T}_0$ and $P(S\mathcal{T}_0) = PSP^{-1}(P\mathcal{T}_0) = S'(P\mathcal{T}_0)$. Since $P\mathcal{T}_0 = \mathcal{T}_0$, we see this is just a sequence of moves between $\mathcal{T}_0$ and $S'\mathcal{T}_0$ as required.

Now suppose that S' is obtained from the identity by changing an entry to $+1$. This case can be deduced from the above case by thinking of the Pachner moves in

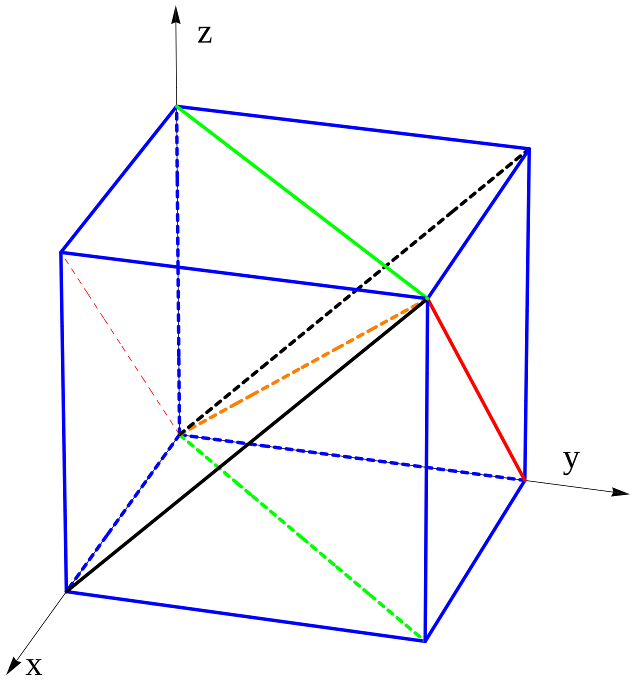

Figure 5.9: Initial triangulation $\mathcal{T}_0$ of punctured 3-torus.

reverse order and conjugating appropriately. More precisely, from the above case we obtain a sequence of Pachner moves from $\mathcal{T}_0$ to $S'^{-1}\mathcal{T}_0$. Conjugating the sequence of Pachner moves by S' gives a sequence from $S'\mathcal{T}_0$ to $S'(S'^{-1}\mathcal{T}_0) = \mathcal{T}_0$. Reversing the Pachner moves gives the desired sequence of moves from $\mathcal{T}_0$ to $S'\mathcal{T}_0$. $\square$

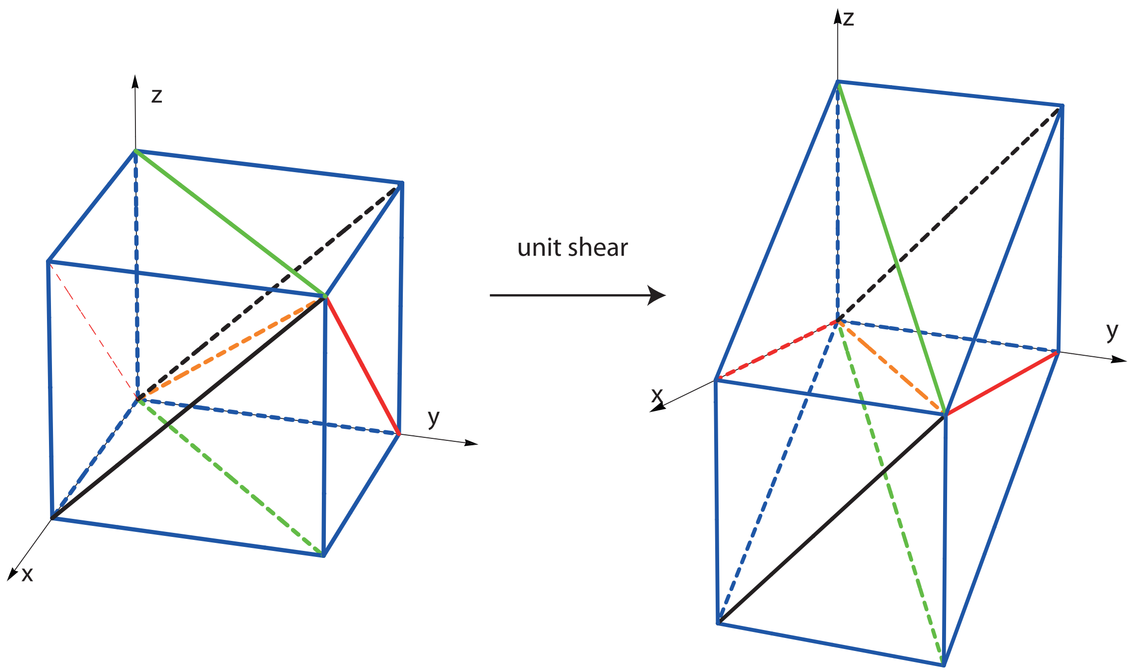

Figure 5.10: Effect of unit shear S on initial triangulation $\mathcal{T}_0$.

Proof of Proposition 5.4. The triangulation $S(\mathcal{T}_0)$ can be seen in the right of Figure 5.10. We can view this triangulation inside the standard fundamental domain $[0,1]^3 \subset \mathbb{R}^3$ by translating the tetrahedra below the xy-plane by one unit upwards in the positive z direction, shown in the bottom left of Figure 5.11.

Figure 5.11 shows a sequence of two 4-4 moves interpolating between $\mathcal{T}_0$ and $S(\mathcal{T}_0)$. Recall that each 4-4 move can be decomposed into a 2-3 move followed by a 3-2 move, as shown in Figures 5.3 and 5.4. The first 4-4 move is performed on the octahedron consisting of the four tetrahedra around the edge coloured red in the top left of Figure 5.11. The red edge is replaced by a new diagonal of the octahedron, also coloured red, shown in the top right of Figure 5.11. Similarly, the next 4-4 move is done on the octahedron consisting of the four tetrahedra around the edge coloured orange in the top right of Figure 5.11. □

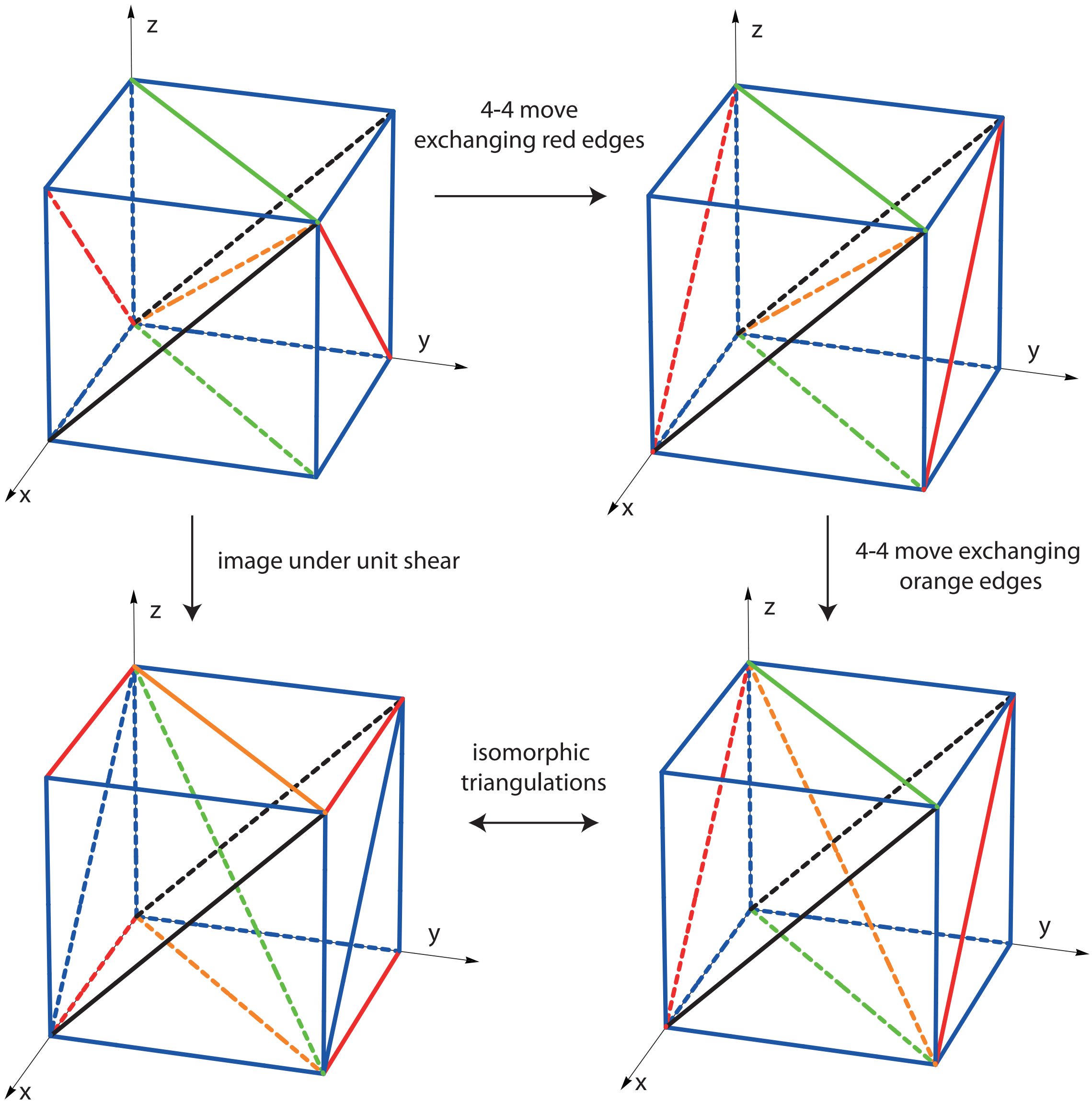

Figure 5.11: Interpolating between triangulation $\mathcal{T}_0$ and its image under a unit shear (as given in Prop 5.4) using two Pachner 4-4 moves.

From interpolation to triangulation

In the previous section, we saw how starting with a monodromy matrix $A \in \mathrm{GL}_3(\mathbb{Z})$ we may obtain a sequence of n 3-dimensional Pachner moves interpolating between an initial triangulation $\mathcal{T}_0$ of the punctured 3-torus, and the triangulation $\mathcal{T}_n = A(\mathcal{T}_0)$. We denote by $\mathcal{T}_i$ the triangulation in the sequence obtained after performing $0 \le i \le n$ Pachner moves.

By conjugating this sequence of Pachner moves by A^k, $k \in \mathbb{Z}$, we obtain a sequence of n Pachner moves interpolating between $A^k(\mathcal{T}_0)$ and $A^{k+1}(\mathcal{T}_0)$. We denote the corresponding sequence of triangulations by $\mathcal{T}_{nk}, \mathcal{T}_{nk+1}, \ldots, \mathcal{T}_{n(k+1)}$. Doing this for all $k \in \mathbb{Z}$ we obtain a bi-infinite sequence of triangulations $\mathcal{T}_i$ for $i \in \mathbb{Z}$.

Let $T^3 = (\mathbb{R}^3 - \mathbb{Z}^3)/\mathbb{Z}^3$ denote the punctured 3-torus and consider the product space $T^3 \times \mathbb{R}$. Triangulate the slice $T^3 \times \{0\} \subset T^3 \times \mathbb{R}$ as in Figure 5.9 so that it has triangulation $\mathcal{T}_0$. This slice is two-sided, we call the side bounding $T^3 \times \mathbb{R}_{\ge 0}$ the "top" side and the side bounding $T^3 \times \mathbb{R}_{\le 0}$ the "bottom" side.

Suppose that a Pachner 2-3 move interpolates between $\mathcal{T}_0$ and $\mathcal{T}_1$. Then we may immerse an ideal 4-simplex $\Delta^4_{0,1}$ in $T^3 \times \mathbb{R}_{\ge 0}$ so that two tetrahedral facets of $\Delta^4_{0,1}$ lie on the slice $T^3 \times \{0\}$. This is done in such a way that these two facets are mapped onto the two ideal tetrahedra of $\mathcal{T}_0$ (the triangulation of the slice) involved in the Pachner move. The case of a 3-2 Pachner instead of a 2-3 Pachner move is similar.

The slice $T^3 \times \{0\}$, together with the immersed 4-simplex separates $T^3 \times \mathbb{R}$ into two pieces, the bottom piece with boundary triangulation $\mathcal{T}_0$ and the top piece with boundary triangulation $\mathcal{T}_1$. In this way a 4-simplex can be thought of as the trace of a 3-dimensional Pachner move. We can then immerse another 4-simplex $\Delta^4_{1,2}$ inside the top piece to interpolate between the triangulations $\mathcal{T}_1$ and $\mathcal{T}_2$. Continuing in this way, we immerse a 4-simplex $\Delta^4_{i,i+1}$ for the Pachner move interpolating between $\mathcal{T}_i$ and $\mathcal{T}_{i+1}$ for all $i \in \mathbb{Z}$ (for $i < 0$ a 4-simplex is immersed in the bottom piece).

Suppose that $n > 0$ so that we now obtain a bi-infinite stack of ideal 4-simplices immersed in $T^3 \times \mathbb{R}$. Consider $U_N = \bigcup_{i=-N}^{N} \Delta^4_{i,i+1}$ for $N \ge 0$. Suppose that for N large, U_N is PL-homeomorphic to $T^3 \times [0,1]$. Then $U := \bigcup_{i=-\infty}^{\infty} \Delta^4_{i,i+1}$ is PL-homeomorphic to $T^3 \times \mathbb{R}$ and there is a PL-homeomorphism $q : U \to U$ which sends $\Delta^4_{i,i+1}$ to $\Delta^4_{i+n,i+n+1}$ and acts like the monodromy matrix in the $\mathbb{R}$ direction. The quotient U/q of U by q is then a PL triangulation of the standard once-punctured 3-torus bundle with monodromy A.

Note that U_N may fail to be PL-homeomorphic to $T^3 \times [0,1]$ for N large, for example if there is some edge in the triangulation $\mathcal{T}_0$ of the slice $T^3 \times \{0\} \subset T^3 \times \mathbb{R}$ which is never involved in a 3-dimensional Pachner move (so U_N can be thought of as "pinched" along the edge).

This difficulty can be avoided as follows. The PL structure of $T^3 \times [0,1]$ (with its standard smooth structure) is given by the Cartesian product of the PL manifolds T^3 and $[0,1]$ in the category of PL manifolds. Equipping T^3 with the triangulation $\mathcal{T}_0$ and $[0,1]$ with its triangulation consisting of one edge and two vertices, we can obtain a product PL triangulation $\mathcal{T}$ of $T^3 \times [0,1]$. The boundary triangulations of $T^3 \times \{0,1\}$ are given by $\mathcal{T}_0 \times \{0,1\} \subset \mathcal{T}$. Then we may use the sequence of Pachner moves interpolating between $\mathcal{T}_0$ and $\mathcal{T}_n$ to layer ideal 4-simplices onto $\mathcal{T}_0 \times \{1\} \subset \mathcal{T}$ to obtain a triangulation $\mathcal{T}' = \mathcal{T} \cup \bigcup_{i=0}^{n-1} \Delta^4_{i,i+1}$. Then $\mathcal{T}'$ has boundary triangulations

$\mathcal{T}_0$ and $\mathcal{T}_n$ and we may glue these two boundary components via the monodromy A to obtain a triangulation of the punctured 3-torus bundle with monodromy A, as required.

In order to triangulate $T^3 \times [0,1]$ note that crossing each ideal tetrahedron in the triangulation $\mathcal{T}_0$ of T^3 with an interval gives a decomposition of $T^3 \times [0,1]$ into "prisms". One merely needs to subdivide each prism into ideal 4-simplices in a consistent way.

In practice in our computer program, in order to triangulate $T^3 \times [0,1]$ we start with the initial symmetric triangulation $\mathcal{T}_0$ of T^3 then layer on a sequence of ideal 4-simplices corresponding to a sequence of a Pachner move directly followed by its inverse Pachner move (this ensures the induced triangulation on $T^3 \times \{1\}$ is also $\mathcal{T}_0$). This is done in such a way that every edge of $\mathcal{T}_0$ is involved in a 3-2 Pachner move, which guarantees that this is a triangulation of $T^3 \times [0,1]$. The following proposition shows that in fact this triangulation is a PL triangulation of $T^3 \times [0,1]$ with its standard smooth structure.

Proposition 5.6. Let $\mathcal{T}$ be a triangulation of $T^3 \times [0,1]$ with its standard smooth structure. Let $\mathcal{T}'$ be a triangulation homeomorphic to $T^3 \times [0,1]$ obtained by layering simplices. Suppose that the two triangulations have combinatorially isomorphic triangulations along their boundaries $T^3 \times \{0,1\}$. Then $\mathcal{T}'$ is a triangulation of $T^3 \times [0,1]$ with its standard smooth structure.

Proof. Let X^4 be the smooth 4-manifold obtained by gluing $\mathcal{T}$ and $\mathcal{T}'$ along one of their boundary components. Then X^4 is homeomorphic to $T^3 \times [0,1]$ and its smooth structure may be thought of in two ways. First, it is obtained by gluing a standard $T^3 \times [0,1]$ to $\mathcal{T}'$, which has the same smooth structure as $\mathcal{T}'$. Next, it is obtained by starting with $\mathcal{T}$ then layering a sequence of ideal 4-simplices onto the boundary of $\mathcal{T}$. Layering an ideal 4-simplex does not change the smooth structure, and so X also has the smooth structure of $\mathcal{T}$ (this is analogous to inverse elementary shellings preserving the PL-type in the non-ideal case [Pac91]). Therefore $\mathcal{T}$ and $\mathcal{T}'$ are PL equivalent, as required. $\square$

Chapter 6

Gluck twisting via triangulations

A natural analogue of Dehn surgery in 3-dimensions is given by performing surgery on surfaces in 4-manifolds. More precisely, given a surface smoothly embedded in a smooth 4-manifold one can perform surgery on the surface to obtain a new 4-manifold, that is, we drill out a neighbourhood of the surface and glue it back in via a diffeomorphism of its boundary.

When the surface is T^2, such a surgery is often called a torus surgery or a logarithmic transform. This is an important operation on 4-manifolds. For example, it is known that any exotic pair of simply-connected 4-manifolds are related by a sequence of torus surgeries [BS13]. It is an interesting open question to determine which 4-manifolds can be obtained by surgery on a link of tori in S^4, see [Lar15].

In this section we will be interested in the case where the surface is S^2. An important special case of this is surgery along a smoothly embedded S^2 in S^4.

6.1 Gluck twisting 2-knots

Given a 2-knot K in S^4, i.e. a smoothly embedded $S^2 \hookrightarrow S^4$, we can perform surgery on K.

Proposition 6.1. The normal bundle to K is trivial. In particular, a closed tubular neighbourhood of K is diffeomorphic to $S^2 \times D^2$.

Proof. The normal bundle to K is an $\mathbb{R}^2$-bundle over S^2, and is therefore determined up to isomorphism by its Euler number. The Euler number of the normal bundle is equal to the self-intersection number of $K \subset S^4$. Since S^4 has trivial intersection form, this self-intersection number is 0. Thus the normal bundle is trivial. □

More generally, we can perform surgery along a 2-knot in any 4-manifold, as long as it has a closed tubular neighbourhood diffeomorphic to $S^2 \times D^2$.

We drill out an open tubular neighbourhood $\nu(K) \cong S^2 \times \mathring{D}^2$ from S^4 to get a compact 4-manifold with boundary $\partial(S^2 \times D^2) = S^2 \times S^1$. We can then reglue the tubular neighbourhood of K via a diffeomorphism $S^2 \times S^1 \to S^2 \times S^1$. Note that if we choose this diffeomorphism to be the identity map, we get back the manifold we started with, namely S^4. We now show that there is essentially only one diffeomorphism for which the surgery could potentially result in a manifold other than S^4.

Let $\mathcal{D}(S^2 \times S^1)$ be the diffeotopy group of $S^2 \times S^1$, i.e. the quotient group of (not necessarily orientable) diffeomorphisms of $S^2 \times S^1$ quotiented out by isotopy.

Theorem 6.2 (Gluck [Glu62])**.** $\mathcal{D}(S^2 \times S^1) \cong \mathbb{Z}_2 \times \mathbb{Z}_2 \times \mathbb{Z}_2$. Moreover, each $\mathbb{Z}_2$ factor is generated (respectively) by the following three diffeomorphisms:

(i) Reversing the S^1 direction:

$$\begin{aligned} \phi_1 : S^2 \times S^1 &\to S^2 \times S^1 \\ (x, \theta) &\mapsto (x, \overline{\theta}), \end{aligned}$$

where $\theta \in S^1 \subset \mathbb{C}$, and $\overline{\theta}$ is the complex conjugate of θ.

(ii) Antipodal map on S^2 factor:

$$\begin{aligned} \phi_2 : S^2 \times S^1 &\to S^2 \times S^1 \\ (x, \theta) &\mapsto (-x, \theta), \end{aligned}$$

where $x \in S^2 \subset \mathbb{R}^3$, the unit sphere in $\mathbb{R}^3$.

(iii) Gluck twist:

$$\begin{aligned} \mu : S^2 \times S^1 &\to S^2 \times S^1 \\ (x, \theta) &\mapsto (\mathrm{rot}_\theta(x), \theta), \end{aligned}$$

where rot_θ is rotation of $S^2 \subset \mathbb{R}^3$ by an angle of θ about the z-axis.

Since the first two diffeomorphisms in Theorem 6.2 extend to diffeomorphisms of $S^2 \times D^2$, gluing $S^2 \times D^2$ to the 2-knot exterior via a diffeomorphism (class) in $\mathcal{D}(S^2 \times S^1)$ generated by the first two diffeomorphisms trivially results in a manifold diffeomorphic to S^4. Thus, up to composition with the first two diffeomorphisms, only the Gluck twist could result in a manifold not diffeomorphic to S^4 after gluing.

We will now show that Gluck twisting along a 2-knot in S^4 returns a manifold *homeomorphic* to S^4.

Proposition 6.3. Suppose $K \subset S^4$ is a 2-knot in S^4. Let $X = S^4 \backslash \nu(K)$ and let $M^4 = X \cup_\phi (S^2 \times D^2)$, where ϕ is a self-diffeomorphism of $S^2 \times S^1$. Then

(i) M is simply connected, and

(ii) $H_2(M) = 0$.

Proof. It suffices to prove this for ϕ a Gluck twist as in Theorem 6.2 (iii). Observe that $S^2 \times D^2$ can be built from a single 2-handle and a 0-handle. Turning this upside down, we see that M is obtained from X by attaching a 2-handle then a 4-handle. In this upside down picture, the 2-handle can be seen as $N \times D^2 \subset S^2 \times D^2$, where N is the northern hemisphere of $S^2 \subset D^2$. The attaching region is the solid torus given by $N \times \partial D^2$ and the core of the 2-handle is $\{n\} \times D^2 \subset S^2 \times D^2$, where $n = (0,0,1)$ is the north pole. The attaching circle is $\{n\} \times \partial D^2$.

A 2-handle $D^2 \times D^2$ deformation retracts onto its core $D^2 \times \{0\}$. Thus, up to homotopy attaching a 2-handle is the same as attaching a 2-cell which can be taken to be the core disk of the 2-handle. However, notice that the attaching circle is exactly the same whether ϕ is the identity map, or ϕ is a Gluck twist. Visually, this is because the north pole is fixed under rotation about the z-axis. Thus the homotopy type of $M \backslash D^4$ is the same for both ϕ the identity map, and ϕ a Gluck twist. Thus $\pi_1(M) \cong \pi_1(M\backslash D^4) \cong \pi_1(S^4) = 0$. Similarly, $H_2(M) \cong H_2(M\backslash D^4) \cong H_2(S^4\backslash D^4) \cong H_2(S^4) = 0$, where the first and last equality follow since attaching a 4-handle i.e. a 4-ball, does not change the second homology. □

Corollary 6.4. Gluck twisting along a 2-knot in S^4 produces a manifold homeomorphic to S^4.

Proof. By Freedman's celebrated theorem, the homeomorphism type of a closed smooth simply-connected 4-manifold is determined by its intersection form. By Proposition 6.3, the manifold obtained by Gluck twisting along a 2-knot is simply-connected and has trivial intersection form, hence is homeomorphic to S^4. □

Proposition 6.5 (cf. Exercise 5.2.7 of [GS99])**.** Let X be a simply connected closed 4-manifold. Let M be the result of Gluck twisting along a *null-homologous* 2-knot K in X. Then M is homeomorphic to X.

Proof. Our proof of Proposition 6.3 shows that M is simply connected. Since K is null-homologous, using the Mayer-Vietoris sequence we see that $H_2(X\backslash\nu(K)) \cong H_2(X)$, where the isomorphism is induced by the inclusion map. Thus, we can pick a basis for $H_2(X) \cong H_2(M)$ consisting of surfaces contained in $X\backslash\nu(K)$. Since the surfaces are contained in a common compact submanifold of both X and M, the intersection pairing of these surfaces is the same for both X and M. Hence X and M have the same intersection form. By Freedman's theorem, this implies that M and X are homeomorphic. □

Q: (Gluck [Glu62]) Does Gluck twisting a 2-knot in S^4 always produce a manifold diffeomorphic to the standard S^4?

This question remains open. In fact, this is currently one of the most promising ways of producing an exotic S^4.

Let $S^3 \tilde{\times} S^1$ denote the non-orientable twisted S^3-bundle over S^1, i.e. with monodromy a reflection of $S^3 \subset \mathbb{R}^4$ across a hyperplane. In [Akb88], it is shown that there is a smoothly embedded sphere in $(S^3 \tilde{\times} S^1)\#(S^2 \times S^2)$ such that Gluck twisting along it produces an exotic $(S^3 \tilde{\times} S^1)\#(S^2 \times S^2)$. However, there are currently no known examples of an exotic pair of orientable 4-manifolds related by a Gluck twist. It remains an interesting question to find such an exotic pair.

Q: Does Gluck twisting a 2-sphere in a closed orientable 4-manifold X ever produce an exotic copy of X?

There are some families of 2-knots in S^4 for which Gluck twisting is known to return the standard S^4. For spun knots, this was shown by Gluck [Glu62]. Gordon

[Gor76] then showed this for the more general class of twist-spun knots. In [NS12], a 2-parameter infinite family of 2-knots is introduced, and it is shown that these also return S^4.

We say that 2-knots $K_1, K_2 \subset S^4$ are 0-*concordant* if there is a smooth proper embedding $f : S^2 \times [0,1] \to S^4 \times [0,1]$, with $f(K_i) = f(S^2 \times \{i\})$, $i = 1, 2$ such that each regular level set image$(f) \cap S^4 \times \{t\}$ consists of a finite collection of 2-spheres. In his thesis [Mel77], Melvin proved that Gluck twisting 2-knots which are 0-concordant to the unknotted 2-sphere produces S^4. See also [Sun15] for a different proof and a generalisation.

One final case we would like to mention is a corollary of Exercise 6.2.11 (b) of [GS99], which implies that Gluck twisting along a 2-knot obtained by doubling a ribbon 2-disk returns the standard S^4.

6.2 Ideal to finite vertex triangulations

In order to perform Gluck twisting combinatorially on the level of triangulations we will need to be able to convert an ideal vertex triangulation to a finite vertex triangulation, which we now describe.

Given a compact manifold M^n with boundary, we consider two types of triangulations associated to M. First, we can find a triangulation of M consisting of a finite collection of n-simplices with some of their facets glued in pairs by affine maps. The "open" facets of n-simplices, that is, those which are not glued to any other facet, form an $(n-1)$-dimensional triangulation of ∂M. We call such a triangulation a *finite vertex triangulation* of M.

Second, we can find a triangulation of the interior of M consisting of a finite collection of n-simplices with their vertices removed, where all the facets of n-simplices are affinely glued in pairs (away from the vertices). Such a triangulation is called an *ideal triangulation*.

Each type of triangulation has its own benefits and disadvantages. For example, ideal triangulations can be very efficient in terms of the number of simplices needed to triangulate a given manifold. As an example, the figure eight knot complement has an ideal triangulation consisting of two ideal tetrahedra [Thu97], whereas a minimal finite vertex triangulation of the figure eight knot exterior has ten tetrahedra [JR14]. On the other hand, if we want to glue triangulated manifolds along their boundary to obtain a triangulation, it seems most natural to use finite vertex triangulations.

Since we would like to glue a triangulated $S^2 \times D^2$ to certain ideally triangulated once-punctured 3-torus bundles, it will be useful to be able to truncate the vertices of an ideal triangulation to convert it to a finite vertex triangulation. In this section we will describe one way an ideal triangulation can be converted to a finite vertex triangulation.

Before we give such a description, we would like to point out that using the method we outline, the finite vertex triangulations we obtain for 4-manifolds contain 145 times more 4-simplices than the original ideal triangulation. This large blow up in the size of the triangulations is one of the main limiting factors to eventually simplifying triangulations of Cappell-Shaneson homotopy 4-spheres in a reasonable amount of computer time. Thus, from a practical standpoint it seems prudent to come up with more efficient methods to convert from ideal to finite vertex triangulations.

In 3-dimensions, Jaco and Rubinstein [JR14] found an operation on ideal triangulations dual to crushing a triangulation of a 3-manifold along its boundary. They call this operation *inflation*. This leads to an efficient way to convert an ideal triangulation to a finite vertex triangulation. In fact, they show that for the two tetrahedron ideal triangulation of figure 8 knot complement, there's an inflation which produces a minimal 10 tetrahedron finite vertex triangulation of the figure 8 knot exterior. Similarly, there's an inflation of the one tetrahedron ideal triangulation of the non-orientable Gieseking manifold giving a minimal finite vertex triangulation with 7 tetrahedra. We leave the following as an interesting problem.

Problem: Work out how to perform inflations on 4-dimensional triangulations.

Converting an ideal triangulation to a finite vertex triangulation

Our strategy for converting a 4-dimensional ideal triangulation to a finite vertex triangulation is analogous to that used in the computer software Regina [BBP+14] for 3-dimensional triangulations. In all dimensions the idea is the same: truncate the ideal vertices then subdivide the resulting polytope into simplices. We first describe how this is done for 2 and 3-dimensional triangulations as it is easiest to visualise for these cases. After completing this work it was pointed out to us that Regina 5.0 [BBP+14] supports converting ideal triangulations to finite vertex triangulations for 4-manifolds.

2-dimensions

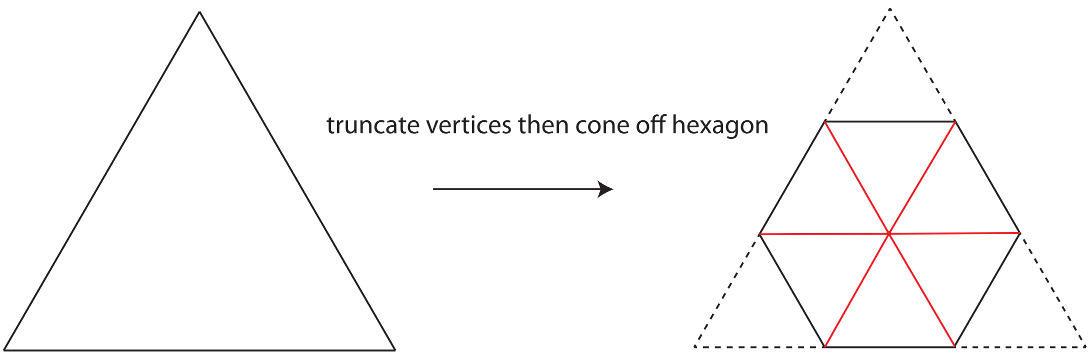

Figure 6.1: Truncating ideal vertices in 2 dimensions.

Given an ideal triangulation of a 2-manifold for each ideal triangle we do the following:

1. Cut out a small triangular neighbourhood of each ideal vertex. More precisely, each ideal vertex is incident to two edges of the triangle, cut along a line

connecting points one third of the length of each of the two edges (measured away from the vertex in question), see Figure 6.1. Note that since edges in our ideal triangulation are glued via affine maps, the truncated edges (now a third of the length they used to be) remain glued consistently. We now have a decomposition of our associated compact surface into hexagons.

2. Cone off each hexagon into 6 finite vertex triangles. That is, introduce a vertex at the centre of each hexagon and an edge connecting the centre to a vertex for each of the six vertices of the hexagon, see Figure 6.1. We now have a finite vertex triangulation with 6 times as many triangles as our original ideal triangulation.

3-dimensions

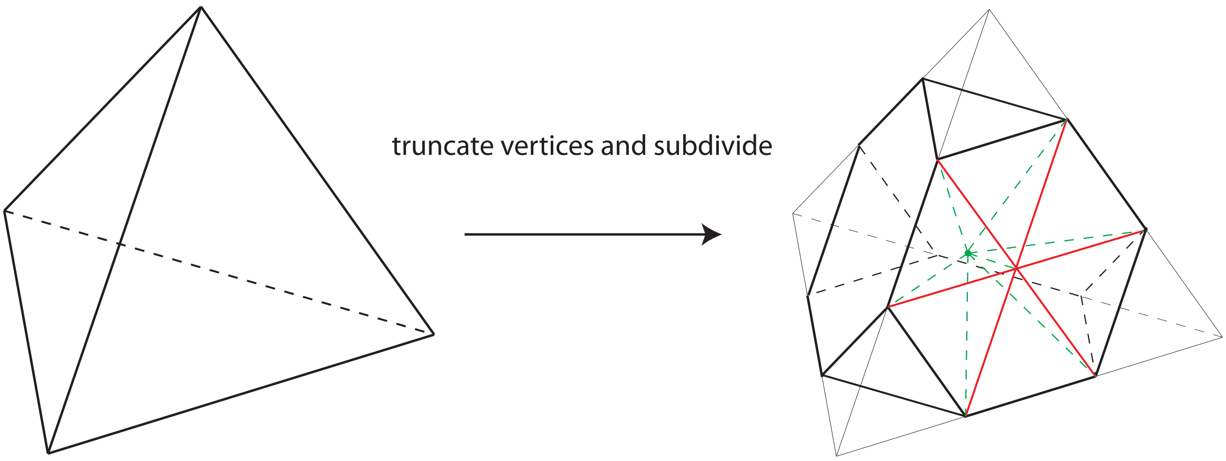

Figure 6.2: Truncating ideal vertices in 3 dimensions. In order to avoid cluttering our diagram only subdivisions involving a single face are shown.

Given an ideal triangulation of a 3-manifold for each ideal tetrahedron we do the following (see Figure 6.2):

1. Analogous to the 2-dimensional case, we cut out a small neighbourhood of each ideal vertex, see Figure 6.2. We now have a polytope with four hexagonal faces and four triangular faces.
2. Cone off each hexagonal face from the centre of the face into 6 triangles as in the 2-dimensional case. Now we have a polytope with $6 \cdot 4 + 4 = 28$ triangular faces.
3. Cone off each face from the centre of the polytope. We now have a finite vertex triangulation with 28 times as many tetrahedra as our original ideal triangulation.

4-dimensions

Given an ideal triangulation of a 4-manifold for each ideal pentachoron we do the following:

1. Cut out a small pentachoral neighbourhood of each ideal vertex. We now have a polytope with five truncated-tetrahedral (i.e. tetrahedron with neighbourhoods of four vertices cut out as in the right side of Figure 6.2) facets and five tetrahedral facets (one for each of the five ideal vertex of the pentachora).

2. Subdivide each truncated tetrahedron facet into 28 3-dimensional simplices as in the 3-dimensional case above. Now we have a polytope with $28 \cdot 5 + 5 = 145$ tetrahedral facets.

3. Finally, cone off each tetrahedral facet from the centre of the polytope. We now have a finite vertex triangulation with 145 times as many pentachora as our original ideal triangulation.

6.3 Triangulating Cappell-Shaneson homotopy 4-spheres

In this section our goal is to perform the Cappell-Shaneson construction in the PL category, to obtained triangulated homotopy 4-spheres.

Let $A \in \mathrm{SL}_3(\mathbb{Z})$ be a monodromy matrix such that $\det(A - I) = \pm 1$. Let $E^4 = T^3 \times [0,1]/(x,1) \sim (Ax,0)$ be the 3-torus bundle with monodromy A. Remove an open tubular neighbourhood of the 0-section $\{0\} \times S^1 \subset E$ from E, and call the resulting manifold M. Then M is a compact 4-manifold with boundary $S^2 \times S^1$.

There are essentially two ways to glue $S^2 \times D^2$ to M along their boundary, differing by a Gluck twist (see Section 6.1). Performing the two possible gluings, we obtain an unordered pair of Cappell-Shaneson homotopy 4-spheres, for which we would like to obtain triangulations. We now describe the steps needed to triangulate one of the two Cappell-Shaneson homotopy 4-spheres. In the following subsection we explain how we may triangulate both of the Cappell-Shaneson homotopy 4-spheres.

1. We first triangulate M and $S^2 \times D^2$. We may obtain a finite vertex triangulation of M by first ideally triangulating the once-punctured 3-torus bundle with monodromy A, as in Chapter 5. This is an ideal triangulation of $E\backslash$(0-section). We then convert the ideal triangulation to a finite vertex triangulation as in Section 6.2 which gives a finite vertex triangulation of M. We obtain a finite vertex triangulation of $S^2 \times D^2$ using *simpcomp* [ES], a GAP package for working with simplicial complexes. The package *simpcomp* contains a vast library of triangulations, in particular one for $S^2 \times D^2$.

2. We would now like to glue the triangulations of M and $S^2 \times D^2$ via a PL-homeomorphism of their boundary $S^2 \times S^1$. If the triangulations of ∂M and $\partial(S^2 \times D^2)$ are combinatorially isomorphic, i.e. equal up to a relabelling of the vertices, then any combinatorial isomorphism induces a PL-homeomorphism $\phi : \partial M \to \partial(S^2 \times D^2)$. Moreover, we can use such a combinatorial isomorphism to identify the open facets of the triangulations of M and $S^2 \times D^2$ to obtain a triangulation of $M \cup_\phi (S^2 \times D^2)$.

   In general, the boundaries will not be combinatorially isomorphic. However, we can modify the triangulations so that their boundaries are combinatorially isomorphic. We now describe how this can be done. The manifold $S^2 \times S^1$ has a unique minimal triangulation with two tetrahedra. This can be verified by observing that there is only a single minimal triangulation listed for $S^2 \times S^1$ in the enumeration of minimal triangulations included in Regina [BBP+14]. In fact, there is a one tetrahedron triangulation of the solid torus. It is given by taking a tetrahedron then gluing two faces by an orientation reversing map which rotates a triangle by $2\pi/3$ (where no twisting corresponds to folding along the common edge of the two faces). Doubling this one tetrahedron triangulation of the solid torus, i.e. taking two copies and gluing them by the identity map along their boundaries gives the two tetrahedron triangulation of $S^2 \times S^1$.

Consider a sequence of 3-dimensional Pachner moves from the triangulation $\partial(S^2 \times D^2)$ to the minimal triangulation of $S^2 \times D^2$. For each Pachner move, we can layer on a 4-simplex onto the boundary of the triangulation of $S^2 \times D^2$ in such a way that the boundary triangulation changes by exactly the Pachner move desired. This increases the size of the triangulation of $S^2 \times D^2$ by one for each Pachner move on the boundary which we do. This is analogous to the layered triangulations of surface bundles where we start with a surface and layer on tetrahedra which essentially performs Pachner moves on the induced triangulation on the surface. Similarly, if we find a sequence of 3-dimensional Pachner moves from the triangulation of ∂M to the minimal two tetrahedron triangulation of $S^2 \times S^1$, we can realise it by layering on 4-simplices.

3. Once the boundaries of M and $S^2 \times D^2$ have combinatorially isomorphic boundaries we can glue the two manifolds together. In this way, we obtain a triangulation of the one of the two Cappell-Shaneson homotopy 4-spheres associated with the monodromy A. In the following subsection we discuss how triangulations for both Cappell-Shaneson homotopy 4-spheres can be obtained.

6.3.1 Gluck twisting via triangulations

Suppose M^4 is a manifold with boundary $S^2 \times S^1$ triangulated by two tetrahedra. We saw that we can glue a triangulated $S^2 \times D^2$ to obtain a triangulation of $M \cup_\partial (S^2 \times D^2)$, where the gluing map is induced by some combinatorial isomorphism of their boundary triangulations. The goal of this section is to explain how we can obtain the unordered pair of triangulated manifolds $M \cup_\phi (S^2 \times D^2)$, where ϕ is either the identity map or the Gluck twist. We first discuss preliminary material on S^2-bundles over S^2.

S^2-bundles over S^2

We would like to understand S^2-bundles over S^2. We briefly describe the clutching construction.

Let $p : X^4 \to S^2$ be a smooth S^2-bundle over S^2, with structure group $\mathrm{Diff}(S^2)$, the group of (not necessarily orientation preserving) diffeomorphisms of S^2. Let $L, U \subset S^2$ be the closed disks which are the southern and northern hemispheres of the base space S^2. If we restrict the bundle p to the southern hemisphere of the base, i.e. $p|_L : p^{-1}(L) \to L$, then we obtain an S^2-bundle over a disk which is necessarily the trivial bundle, since all fiber bundles over a contractible space are trivial. Similarly, $p|_U$ is the trivial S^2-bundle over a disk. Fix trivialisations of p over the southern and northern hemispheres.

Then X^4 may be recovered by gluing the two trivial bundles $S^2 \times L$ and $S^2 \times U$ along the equator by a map

$$\begin{aligned} S^2 \times \partial L &\to S^2 \times \partial U \\ (x, \theta) &\mapsto (\bar{\phi}_\theta(x), \theta), \end{aligned}$$

where

$$\begin{aligned} \bar{\phi} : S^1 &\to \mathrm{Diff}(S^2) \\ \theta &\mapsto \bar{\phi}_\theta \end{aligned}$$

is a smooth map. The map $\bar{\phi}$ is called the *clutching map*. The bundle p (up to bundle isomorphism) is determined by the homotopy class of the clutching map $\bar{\phi}$.

Notice that the homotopy class of $\bar{\phi}$ depends on the trivialisations we chose. Suppose that the clutching map is orientation reversing. Then can change trivialisations, for example, by the bundle map $S^2 \times L \to S^2 \times L$ which is the identity on the base but is a reflection in the S^2 factor, so that the resulting clutching map $\bar{\phi}$ maps into the subgroup $\mathrm{Diff}^+(S^2)$ of orientation preserving diffeomorphisms. Thus, we can without loss of generality assume that $\bar{\phi}_\theta \in \mathrm{Diff}^+(S^2)$ for all $\theta \in S^1$. Since $\mathrm{Diff}^+(S^2)$ is connected, we may identify the collection of homotopy class of clutching maps with $\pi_1(\mathrm{Diff}^+(S^2))$.

Theorem 6.6 ([Sma59])**.** The group $\mathrm{Diff}^+(S^2)$ of orientation preserving smooth diffeomorphisms of S^2 deformation retracts onto the rotation group $\mathrm{SO}(3)$.

As a corollary of the above theorem, we see that $\pi_1(\mathrm{Diff}^+(S^2)) = \pi_1(\mathrm{SO}(3)) = \mathbb{Z}_2$. Hence, we have the following:

Lemma 6.7. There are at most two S^2-bundles over S^2.

Handle decompositions of S^2-bundles over S^2

We saw (Lemma 6.7) that there are at most two S^2-bundles over S^2. We now describe handle decompositions of the two bundles.

The manifold $S^2 \times D^2$ has a handle decomposition consisting of a 0-handle and a 2-handle. To see this it will be convenient to think of the 0-handle as $D^4 = D^2 \times D^2$, so that it looks like a 2-handle. We attach the 2-handle $D^2 \times D^2$ to the 0-handle so that the attaching region $\partial(D^2) \times D^2$ of the 2-handle is glued to the 0-handle by the identity map. The attaching circle $\partial(D^2) \times 0$ of the 2-handle is unknotted in the boundary of the 0-handle, since $\partial(D^2) \times 0$ is the unknot in $\partial(D^2 \times D^2) = S^3$. Furthermore, two parallel copies of the core disk are unlinked in S^3. Thus, a Kirby diagram for $S^2 \times D^2$ is given by a single unknotted component with framing 0 as shown in Figure 6.3.

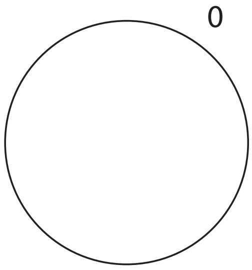

Figure 6.3: Kirby diagram for handle decomposition of $S^2 \times D^2$ into a 0-handle and a 2-handle. The 2-handle is attached with framing 0.

Let M, N be two copies of $S^2 \times D^2$. Let $X^4 = M \cup_\phi N$, where ϕ is a diffeomorphism. We shall find a handle decomposition of X^4. Although we will not need it, the reader may find Example 5.5.8 of [GS99] useful for a general discussion of obtaining handle decompositions under gluings. We endow M, N with its handle decomposition given as described above. We now turn the handle decomposition of N upside down, so that N consists of a (dualised) 2-handle and a 4-handle. Thus, X has a handle decomposition with a 0-handle, two 2-handles and a 4-handle.

Since 4-handles are glued uniquely, it suffices to understand how the dualised 2-handle of N attaches to M. When a 2-handle is turned upside down, the role of the core and cocore are interchanged. The cocore in the (non-dualised) handle decomposition of $N = S^2 \times D^2$ is $n \times D^2$, where n is the north pole of S^2. Thus, this is the core in the 2-handle we want to attach. In particular, the attaching circle is $n \times \partial(D^2) \subset N$.

Regardless of whether $\phi : M \to N$ is the identity map or the Gluck twist map, $\phi^{-1}(n \times \partial(D^2)) = n \times \partial(D^2)$. Therefore, the 2-handle is attached to the belt circle of the 2-handle of M. However, the belt circle is isotopic in M to $s \times \partial(D^2) \subset S^2 \times D^2 = M$, where s is the south pole of S^2. This is precisely $0 \times D^2 \subset D^2 \times D^2$ of the 0-handle of M. Thus, the 2-handle of M is attached along $\partial(D^2) \times 0$ of the 0-handle, and the 2-handle coming from N is attached to the 0-handle of M along $0 \times \partial(D^2)$. These two curves form a Hopf link in S^3, the boundary of the 0-handle.

It suffices to compute the framing of the 2-handle. Consider the two oriented curves $\gamma_i = p_i \times \partial(D^2) \subset S^2 \times D^2 = N$, $i = 1, 2$, $p_1 \neq p_2$. Pulling back these curves to $S^3 = \partial(0\text{-handle})$ under ϕ, the linking number of the two curves in S^3 gives the framing of the 2-handle attachment. If ϕ is the identity map we see that the two circles in S^3 are unlinked, so the framing is 0. If ϕ is a Gluck twist, then the two curves link exactly once, and thus the framing is ± 1. The resulting manifold is independing of whether one takes ϕ or ϕ^{-1} (since ϕ and ϕ^{-1} are in fact isotopic), so the sign of the framing can without loss of generality be taken to be 1.

Proposition 6.8. There are exactly two S^2-bundles over S^2 (in particular, the two bundles described below are not isomorphic, in fact not even homotopy equivalent):

1. The trivial bundle $S^2 \times S^2$ obtained by gluing two copies of $S^2 \times D^2$ along their boundary by the identity map. The intersection form is given by

$$Q_{S^2 \times S^2} = \begin{bmatrix} 0 & 1 \\ 1 & 0 \end{bmatrix}.$$

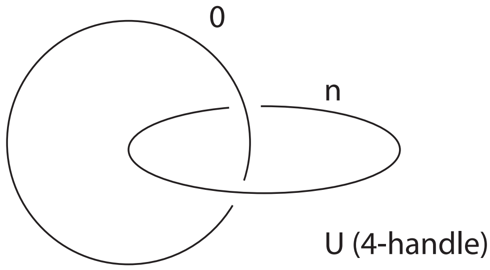

Figure 6.4: Kirby diagram for S^2-bundles over S^2. If $n = 0$, then this is $S^2 \times S^2$. If $n = 1$, then this is the twisted S^2-bundle over S^2.

2. A twisted S^2-bundle over S^2, denoted $S^2 \tilde{\times} S^2$, obtained by gluing two copies of $S^2 \times D^2$ along their boundary by a Gluck twist. The intersection form is given by
$$Q_{S^2 \tilde{\times} S^2} = \begin{bmatrix} 0 & 1 \\ 1 & 1 \end{bmatrix}.$$

Proof. Note that from the discussion preceding Proposition 6.8 we see that there are at most two S^2-bundles over S^2. Their Kirby diagrams are shown in Figure 6.4. Since there are no 1- or 3-handles, we can read off the intersection form as the linking matrix for the framed link of 2-handle attachments. Since the intersection form of $S^2 \times S^2$ is even and the intersection form of $S^2 \tilde{\times} S^2$ is odd, their intersection forms are inequivalent and hence the total spaces of the bundles are not even homotopy equivalent. $\square$

Gluck twisting via triangulations

Now that we have the appropriate background on S^2-bundles over S^2 described in Section 6.3.1, we return to the problem of gluing triangulations. Suppose M^4 is a triangulated manifold with boundary which we identify with $S^2 \times S^1$, where the boundary is triangulated by two tetrahedra. We want to obtain triangulations for the unordered pair of triangulated manifolds $M \cup_\phi (S^2 \times D^2)$, where ϕ is either the identity map or the Gluck twist. This can be done using the following proposition:

Proposition 6.9. Let M^4 be a triangulated 4-manifold with boundary $S^2 \times S^1$. Let T_1, T_2 be finite vertex triangulations of $S^2 \times D^2$. Suppose the following hold:

(i) T_1 and T_2 have combinatorially isomorphic triangulated boundaries consisting of two tetrahedra. Let $\phi : \partial T_1 \to \partial T_2$ be the PL-homeomorphism induced by such a combinatorial isomorphism.

(ii) $T_1 \cup_\phi T_2$ is the twisted S^2-bundle over S^2.

(iii) The boundary triangulation of M is combinatorially isomorphic to T_1 (and therefore also T_2). Let $\psi : \partial M \to \partial T_1$ be the PL-homeomorphism induced by such a combinatorial isomorphism.

Then $M \cup_\psi T_1$ and $M \cup_{\phi \circ \psi} T_2$ correspond to the two possible (a priori different) ways to glue $S^2 \times D^2$ to M.

Proof. Let $\mu : \partial(S^2 \times D^2) \to \partial(S^2 \times D^2)$ be a Gluck twist, or more generally, a diffeomorphism which does not extend over $S^2 \times D^2$.

If $f : \partial M \to \partial(S^2 \times D^2)$ is a PL-homeomorphism then the two ways to glue $S^2 \times D^2$ to M correspond precisely to $M \cup_f (S^2 \times D^2)$ and $M \cup_{\mu \circ f} (S^2 \times D^2)$.

Thus, it suffices to show that $\phi : \partial T_1 \to \partial T_2$ is a diffeomorphism which does not extend over T_1. If ϕ did extend over T_1 then $T_1 \cup_\phi T_2$ would necessarily be PL-homeomorphic to the trivial bundle $S^2 \times S^2$, contradicting our assumption that it is the twisted S^2-bundle over S^2 (they are non-isomorphic by Proposition 6.8). □

In order to use Proposition 6.9, we need to find a pair of triangulations T_1, T_2 of $S^2 \times D^2$ with combinatorially isomorphic boundary, such that gluing them via a combinatorial isomorphism of their boundary gives $S^2 \widetilde{\times} S^2$. We are able to find such a pair by doing the following:

1. Start with a finite vertex triangulation T_1 of $S^2 \times D^2$ with induced triangulation on the boundary consisting of two tetrahedra. We described how we obtained such a triangulation in Section 6.3.

2. Randomly layer on a sequence of pentachora to the boundary of T_1. Each pentachora that is layered on changes the boundary triangulation by a Pachner move. Call the resulting triangulation T_2'.

3. Simplify the boundary triangulation of T_2' to the minimal two tetrahedron triangulation layering on an appropriately chosen sequence of penctachora to the boundary of T_2'. We continue to denote the resulting triangulation by T_2'. Glue T_1 and T_2' by a combinatorial isomorphism of their boundary. If the resulting manifold is $S^2 \widetilde{\times} S^2$ then let $T_2 = T_2'$, we are done. Otherwise, go back to Step 2.

Remark 6.10.

- In Step 3, we know that the manifold we obtain from the gluing is one of the two S^2-bundles over S^2. From Proposition 6.8, these two bundles are distinguished by the parity of their intersection forms. We compute the intersection form of the closed manifold via its triangulation. We explain this in Section 6.3.2.

- In the triangulations T_1, T_2 that we find, it does not matter which combinatorial isomorphism $\phi : \partial(T_1) \to \partial T_2$ is chosen, $T_1 \cup_\phi T_2$ is always the twisted S^2-bundle over S^2.

- The above algorithm is not guaranteed to terminate. However, heuristically, if in Step 2 the boundary triangulation was randomised sufficiently well, we might expect the probability that Step 3 then terminates to be roughly $\frac{1}{2}$ (so there's a $\frac{1}{2}$ chance to obtain each of the two S^2-bundles over S^2). Thus, we'd expect to perform Step 2 only two twice on average. This is roughly what seems to happen in practice.

- After simplification using Pachner moves, we obtain triangulations T_1, T_2 each of which has 6 pentachora. They have isomorphism signatures given by `gHfMAQcbbdedefffaa5a5aaabaeapbpbca` and `gALAAIaaacdddeff2aoaMaobyayamaaaGa`.

6.3.2 Computing the intersection form using triangulations

In this section we briefly explain how one can compute the intersection form of a closed oriented 4-manifold M via a triangulation of M.

Recall that the intersection form of M is the symmetric bilinear form

$$Q : (H_2(M)/\mathrm{tor}) \times (H_2(M)/\mathrm{tor}) \to \mathbb{Z}$$

defined as follows. Let $[\alpha], [\beta] \in H_2(M)$, where α and β are representative 2-cycles which intersect transversely in a finite number of points. Then $Q([\alpha], [\beta])$ is the signed count of intersection points between α and β.

Let $\mathcal{T}$ be a fixed triangulation of M. This triangulation has a dual cellulation which we denote by $\mathcal{T}^\perp$. Each i-dimensional cell of $\mathcal{T}$ is dual to precisely one $(4-i)$-dimensional cell in $\mathcal{T}^\perp$ and moreover these cells intersect transversely in M. Thus, if α, β are 2-cycles such that α is a linear combination of 2-cells of $\mathcal{T}$ and β is a linear combination of 2-cells of $\mathcal{T}^\perp$. Then the two 2-cells intersect transversely and one can easily compute the signed intersection of points between α and β, which equals $Q([\alpha], [\beta])$.

Let $\alpha_1, \ldots, \alpha_k$ be representative 2-cycles for a basis of $H_2(M)/\mathrm{tors}$ with respect to cellular homology of $\mathcal{T}$. Thus, $\alpha_1, \ldots, \alpha_k$ live in the 2-skeleton of $\mathcal{T}$. By bilinearity, in order to compute the intersection form it suffices to compute $Q([\alpha_i], [\alpha_j])$, $i, j \in \{1, \ldots, k\}$. Thus, we would like to homotope the 2-cycles so that they become 2-cycles living in the 2-skeleton of $\mathcal{T}^\perp$. In theory this can be done using the following theorem:

Theorem 6.11 (Cellular approximation)**.** If $f : X \to Y$ is a continuous map between CW-complexes, then f is homotopic to a cellular map, i.e. a map f' which maps the k-skeleton of X into the k-skeleton of Y for all k.

We note that there is also an analogous approximation theorem for simplicial complexes. However, as the triangulations we deal with are generally not simplicial, we work in the more general setting of CW-complexes.

We use Theorem 6.11 by letting $f : M \to M$ be the identity map, and we consider the domain to have CW-decomposition given by $\mathcal{T}$, and the codomain to have CW-decomposition $\mathcal{T}^\perp$. Then f is homotopic to a map f' which is cellular. Thus, the image of the 2-cycles $\alpha_1, \ldots, \alpha_k$ under f' give 2-cycles in the 2-skeleton of $\mathcal{T}^\perp$ which represent the same class in $H_2(M)/\mathrm{tor}$.

In practice, it turns out to be more convenient to instead consider the identity map $g : M \to M$, where the domain has CW-decomposition $\mathcal{T}^\perp$ and codomain has CW-decomposition $\mathcal{T}$ (opposite to that of f considered above). Then g is homotopic to a cellular map g' which maps 2-cells to linear combinations of 2-cells. Importantly, g' can be easily computed. Before discussing how g' may be algorithmically computed, we describe how g' may be used to compute the intersection form.

Let $C_2(\mathcal{T})$ denote the collection of 2-chains, i.e. the $\mathbb{Z}$-span of the 2-cells of $\mathcal{T}$. Similarly we have $C_2(\mathcal{T}^\perp)$. Then g' induces a map $g' : C_2(\mathcal{T}^\perp) \to C_2(\mathcal{T})$, which descends to an isomorphism on second homology. Thus, via linear algebra over $\mathbb{Z}$

one can find 2-cycles $\beta_1, \ldots, \beta_k \in C_2(\mathcal{T}^\perp)$ which map to $\alpha_1, \ldots, \alpha_k$ under g'. Then $\mathbb{Q}([\alpha_i], [\alpha_j])$ is given by the signed count of intersection points between α_i and β_j.

Finally, we describe how g' may be algorithmically computed. The triangulation $\mathcal{T}$ and its dual cellulation $\mathcal{T}^\perp$ have a common subdivision given by the barycentric subdivision of $\mathcal{T}$, denoted by $\mathcal{T}_{\text{bar}}$. Our strategy is to homotope g (the identity map) to a map g' which is in fact a cellular map from $\mathcal{T}_{\text{bar}}$ to $\mathcal{T}$. Then g' is necessarily also cellular as a map from $\mathcal{T}^\perp$ to $\mathcal{T}$ as required. We do this in such a way that the restriction of g' to any simplex (of any dimension) of the barycentric subdivision will be an affine map. Hence, in order to specify g' it suffices to specify where g' maps the vertices of $\mathcal{T}_{\text{bar}}$. By definition the vertices of $\mathcal{T}_{\text{bar}}$ are precisely the centres of simplices (of all dimensions) of $\mathcal{T}$. If σ is an i-simplex of $\mathcal{T}$, then map the vertex at the centre of σ to an arbitrarily chosen vertex of σ. This specifies g'.

The map g' is homotopic to the identity map because it can be thought of a composition of a sequence of homotopies starting with the identity map. Homotope the identity map so that the centre of each 4-simplex of $\mathcal{T}$ is sent to one of its five (before identifications) vertices. Then homotope the resulting map so that the centre of each 3-simplex of $\mathcal{T}$ is sent to one of its vertices, and so on. Finally composing with a homotopy which fixes the vertices but makes the resulting map affine on each simplex gives g'.

Example 6.12 (Half-dimensional case)**.** Let T be a closed oriented surface. Then T has an associated intersection pairing, which is a bilinear anti-symmetric map

$$\begin{aligned} Q : H_1(T) \times H_1(T) &\to \mathbb{Z} \\ (\alpha, \beta) &\mapsto Q(\alpha, \beta) = \alpha \cdot \beta, \end{aligned}$$

where $\alpha \cdot \beta$ is the algebraic intersection number between transversely intersecting 2-cycle representatives of α and β.

The ideas discussed to compute the intersection form of a closed oriented 4-manifold from a triangulation can also be used to compute the intersection pairing of a surface. We illustrate this on the torus.

Let $T = T^2$ denote the 2-dimensional torus with the two-triangle triangulation $\mathcal{T}$ as shown in black in the left of Figure 6.5. In the left of Figure 6.5 in red, we see the dual cellulation $\mathcal{T}^\perp$ of $\mathcal{T}$, which can be seen to be a hexagon with its edges identified (in particular, it is not a triangulation). We have oriented the edges for convenience.

The right of Figure 6.5 (including both the red and black edges) shows the barycentric subdivision of $\mathcal{T}$, which we denote by $\mathcal{T}_{\text{bar}}$. The barycentric subdivision is a common subdivision of both $\mathcal{T}$ and $\mathcal{T}^\perp$. Let $g : \mathcal{T}_{\text{bar}} \to \mathcal{T}$ denote the identity map. We homotope g so that the vertices of $\mathcal{T}_{\text{bar}}$ are homotoped to the vertices of $\mathcal{T}$ according to the green arrows in Figure 6.5, and at the end of the homotopy we obtain a map g' which is affine on each simplex (in particular it's determined by where it maps vertices). Then $g' : \mathcal{T}^\perp \to \mathcal{T}$ is a cellular map, which maps cells as follows: $g'(e_1) = E_2, g'(e_2) = E_1$ and e_3 is mapped into the vertex.

Thus, on the level of homology, $g'([e_1 - e_3]) = E_2$ and $g'([e_2 + e_3]) = E_1$. Using $[E_1], [E_2] \in H_1(T)$ as a basis, we now compute the intersection form. Note that

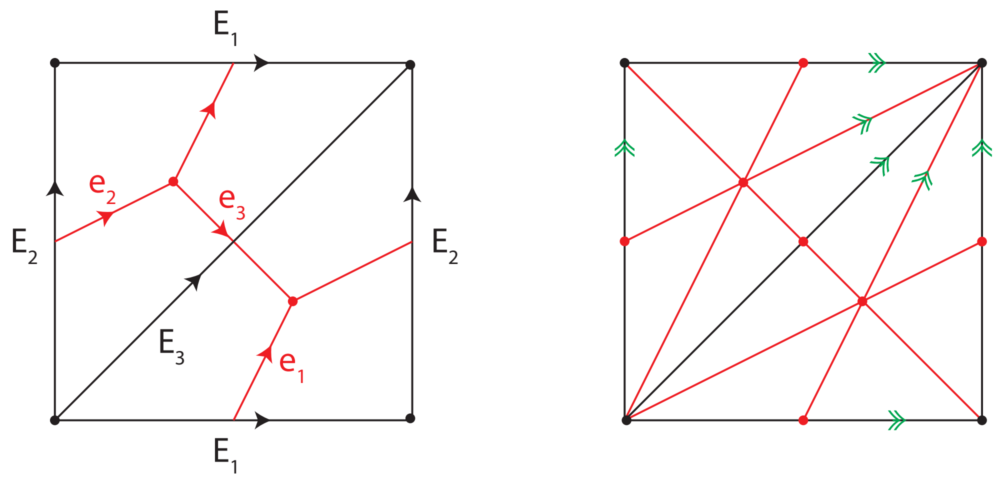

Figure 6.5: Opposite sides of each square are identified to get the torus.

$E_1 \cdot e_1 = 1$ and $E_2 \cdot e_2 = -1$.

$$\begin{aligned}
Q([E_1],[E_1]) &= Q([E_1], g'^{-1}([E_1])) \\
&= Q([E_1],[e_2+e_3]) = E_1 \cdot e_2 + E_1 \cdot e_3 = 0 + 0 = 0, \\
Q([E_1],[E_2]) &= Q([E_1],[e_1 - e_3]) = 1, \\
Q([E_2],[E_1]) &= -Q([E_1],[E_2]) = -1, \\
Q([E_2],[E_2]) &= Q([E_2],[e_1 - e_3]) = 0.
\end{aligned}$$

Therefore $Q(p[E_1] + q[E_2], r[E_1] + s[E_2]) = ps - qr$, as is well known.

Chapter 7

Computations and further work

In this chapter we document our attempt to systematically enumerate, construct and simplify triangulations of Cappell-Shaneson homotopy 4-spheres. Some of this data is included in Table 7.2. We also discuss some possible avenues for future research.

7.1 Outline of computations

As a test of the techniques developed in this thesis, we attempted to, and succeeded in, computing triangulations of all Cappell-Shaneson homotopy spheres with monodromy matrix having trace between 0 and 20 (inclusive), a total of 78 triangulations. Note that we verified that all these Cappell-Shaneson spheres are standard via Gompf's fishtail neighbourhood argument, see Proposition 3.7. For some of these triangulations of Cappell-Shaneson homotopy spheres we were able to use Pachner moves to simplify them to triangulations of the standard S^4. We briefly discuss how this was carried out and include some data, for example see Table 7.2. The relevant computer code we wrote includes over 3000 lines of Python and SageMath code. Both the code and data are available from the author upon request[1].

Our first step was to obtain matrix representatives for each conjugacy class of Cappell-Shaneson matrices with trace between 0 and 20. Fortunately, for all of these values of the trace the conjugacy classes can be understood in terms of ideal class groups as discussed in Chapter 3. We wrote a SageMath script to perform this enumeration, see Section 3.4. Note that the matrix representatives we chose are in the form of the transpose of those given by Aitchison-Rubinstein in Theorem 3.2, this turned out to be useful in keeping the triangulations small in the next step.

Our next step was to construct a triangulation of the once-punctured 3-torus bundle for each monodromy matrix using the method described in Section 5.2. Some of these triangulations were rather large with approximately 200 4-simplices. We left our triangulation simplification code running for a few days to simplify these triangulations using Pachner moves, with the size and isomorphism signature of the simplified bundle triangulations as shown in Table 7.2. Most of this time was spent simplifying a few cases which seemed to get stuck in deep local minima. In one case

[1]Send an email to ahmadissa@gmail.com.

we simply restarted our simplification procedure from the initial triangulation which avoided getting stuck in the same local minimum. Note that these triangulations may not be minimal, further simplification may still be possible.

Once we had triangulations of the once-punctured 3-torus bundles we converted the ideal vertex triangulations to finite vertex triangulations as described in Section 6.2. This blows up the number of 4-simplices by a factor of 145. For each triangulation we then layer 4-simplices to the boundary to simplify the boundary triangulation to the unique minimal two tetrahedron triangulation of $S^1 \times S^2$. Note that by the uniqueness, we only need to simplify the boundary triangulation to have two tetrahedra. We then glue in each of the two triangulations of $S^2 \times D^2$ with isomorphism signatures given by `gHfMAQcbbdedefffaa5a5aaabaeapbpbca` and `gALAAIaaacdddeff2aoaMaobyayamaaaGa`. Both of these triangulations have six 4-simplices. This results in the unordered pair of Cappell-Shaneson spheres for each monodromy matrix. This step, starting with the triangulations of the bundles and finally obtaining triangulations of the Cappell-Shaneson spheres, took several hours of computer time to complete.

7.1.1 Simplifying triangulations of Cappell-Shaneson spheres

The final and most computationally expensive step is to try to simplify the triangulations of the Cappell-Shaneson spheres to that of the 4-sphere.

In dimensions $n \leq 2$ the problem of algorithmically recognising the n-sphere is trivial. In dimension 3, Rubinstein [Rub95] gave an algorithm to recognise the 3-sphere, which was later simplified by Thompson [Tho94]. In contrast, Novikov showed that there is no general algorithm to recognise a PL n-sphere for $n \geq 5$, see Section 10 of [VKF74]. Whether there exists an algorithm to recognise a PL 4-sphere remains open.

In our computer program, we use heuristic methods to attempt to simplify a Cappell-Shaneson sphere to a target simple 4-sphere triangulation using Pachner moves. Heuristic methods to simplify n-spheres has been studied by Joswig, Lutz, Tsuruga [JLT14]. Note, however, that they deal with simplicial complexes which are less general than the type of triangulations we use, and so we are unable to directly use their software on our examples. In her PhD thesis [Tsu15], Tsuruga attempts to simplify triangulations of Akbulut-Kirby spheres using such heuristic methods.

The standard 4-sphere has a simple triangulation consisting of two 4-simplices glued along their boundary by the identity map, with isomorphism signature `cPkbbbbaaaaaaaa`. We take this triangulation to be the target triangulation when simplifying the triangulations of Cappell-Shaneson spheres. Note that this triangulation has five vertices, and so when simplifying triangulations we only perform 5-1 Pachner moves (which decrease the number of vertices) and its inverse until there are precisely five vertices in the triangulation.

We attempted to simplify the triangulations of Cappell-Shaneson spheres corresponding to monodromy matrices with trace between 0 and 5 (inclusive). Appendix A contains pseudocode illustrating our heuristic simplification algorithm. Using it, we were able to simplify the four triangulations corresponding to traces 0 and 1 to our target triangulation of S^4. For each of the traces 3, 4 and 5, we were able to simplify precisely one of the two corresponding triangulations. This data is given in Table 7.1, where we also include the isomorphism signatures of the simplified triangulations.

As an example, for the trace 1 triangulation with framing 1 (an arbitrary labelling), on a random run[2], our computer program took 4 hours and 17 minutes to simplify the triangulation to our target 4-sphere triangulation. We note that this seemed to be the easier of the two framings with trace 1 to simplify using our program. We never needed to increase the size of the triangulation beyond 608 pentachora in order to simplify it. On this run, our program called the Pachner move subroutine $2,436,584$ times. However, we needed only about 88 thousand moves to simplify the triangulation to 34 pentachora, at which point it became hard to simplify further. It took another 700 thousand moves to simplify to 32 pentachora. Interestingly, we noticed that for many of the examples our program seemed to get stuck at two points when simplifying, first when it reached some point at around 30–36 pentachora, and then again at about 10–18 pentachora. At these points, our program would typically expand the triangulation, increasing the number of pentachora by up to about 80, while performing random 3-3 moves (which do not change the number of pentachora), then attempt to simplify again. After a number of rounds of this expansion and contraction, our program was often able to simplify past these difficult local minima. Finally, we point out that the running time is highly variable on the particular run, and it sometimes seemed better to restart the simplification from the original triangulation than to continue a bad run.

Observe that even in the cases we were not able to simplify completely to our target S^4 triangulation, the triangulations we obtained (see Table 7.1) have relatively few 4-simplices and yet they seemed to resist our attempts to simplify them to the two 4-simplex triangulation of S^4. Our attempts to simplify these triangulations include repeatedly increasing the size of the triangulations by performing random 2-4 and 3-3 Pachner moves until the triangulations had expanded by about 80 4-simplices then simplifying the resulting triangulation. In [Bur11], Burton presents experimental work showing that for small one-vertex triangulations of 3-manifolds, he never needed to add more than two tetrahedra in order to simplify (reduce the number of tetrahedra in) a non-minimal triangulation. In contrast, our failed simplification attempts might suggest that for non-minimal triangulations of S^4 simplification might require first greatly increasing the size of the triangulation. Indeed, for triangulations of n-manifolds, n-manifolds $n \geq 4$, this was shown to be true [Nab96], [LN16]. Finally, it may very well also be the case that further improvement to our simplification algorithm would lead to simplification of the triangulations in Table 7.1.

[2]Run on a single core of a laptop with an i5 6440-HQ processor.

Table 7.1: Results of attempt to simplify Cappell-Shaneson sphere triangulations. Note that the second column is an arbitrary labelling of the two Cappell-Shaneson spheres coming from a single conjugacy class. The fourth column is the smallest number of 4-simplices in the triangulation found so far.

Trace	CS sphere #	# simplices in original CS tri.	# simplices in simplified CS tri.	Simplifies to S^4	Isomorphism signature of simplified CS tri.
0	1, 2	308	2	Yes	`cPkbbbbaaaaaaaa`
1	1, 2	604	2	Yes	`cPkbbbbaaaaaaaa`
2	1	734	12	No	`mLLALQQvPQQabdcdfegfggkkjllkllfafaqbPbfaJafa bbPbcaPbtbtbRaratbmbtbIb`
2	2	734	2	Yes	`cPkbbbbaaaaaaaa`
3	1	1162	2	Yes	`cPkbbbbaaaaaaaa`
3	2	1162	14	No	`oAvLLAAQQPMPkaaeeifihhikkkkilllnnnnyafa2aHbr bUbLaobvbuabababababatbpapapapapapapa`
4	1	1854	14	No	`oAMwLLPAQzQPkaabccfijijijhjillllnnnnyacayaday aDa8aZaZahaaaqaUajasaZbZbZbZbZbZbZb`
4	2	1854	2	Yes	`cPkbbbbaaaaaaaa`
5	1	1646	18	No	`sLAAMPvLLvQPQQQQbbbdddfffkjoolmqorqrqorppppr aaaaaaaaaaaaaaaaaaXa1bDaZbXb0bVbkbDbqaDbkaLb Ga1b1b1b1b5a`
5	2	1646	2	Yes	`cPkbbbbaaaaaaaa`

7.2 Further work

Much of the work developed in this thesis to triangulate once-punctured 3-torus bundles should generalise to triangulate arbitrary once-punctured n-torus bundles. However, one step which needs additional thought is to work out a sequence of Pachner moves triangulating between an initial triangulation and its image under a unit shear matrix. Even more generally it would be interesting to investigate how one can construct M^n-bundles over S^1 for an arbitrary manifold M^n. Ideally this would be implemented as a computer program.

Another important source of potentially exotic 4-spheres comes from removing a tubular neighbourhood of a knot in S^4 then gluing it back in via a Gluck twist. If we had ideal triangulations of 2-knot complements, then we could use them as input into our program to perform this Gluck twist surgery combinatorially, and again test whether the resulting homotopy 4-sphere is standard. Hence, it would be useful to work out an algorithm to construct an ideal triangulation of a 2-knot complement, given a description of the 2-knot, for example as a Yoshikawa diagram [Yos94].

Thurston observed that the complement of a knot in S^3 is the union of two 3-balls along strata in their boundary, and that this can be used to triangulate the knot complement [Thu97], [Wee05]. One should be able to carry this out for 2-knot complements as well. For the trivial 2-knot, we were able to carry this out to obtain a 64 4-simplex mixed triangulation (i.e. with both ideal and finite vertices). We note that in order to do this we had to complicate the usual movie picture for the trivial 2-knot to introduce additional strata to work with. Finally, we simplified the triangulation to a minimal two 4-simplex ideal triangulation of the trivial 2-knot complement, i.e. the interior of $B^3 \times S^1$. Generalising this to arbitrary 2-knots could form an interesting future project.

There are a number of improvements that can be made concerning the efficiency of our methods. Perhaps the most important for keeping the triangulations small would be an efficient way to convert an ideal vertex to a finite vertex triangulation. As discussed in Section 6.2, perhaps the best approach way would be to work out how to perform inflation (see [JR14]) in 4-dimensions.

It would be interesting to improve the algorithms and computer programs to simplify more triangulations of Cappell-Shaneson spheres. Even a simple rewrite of our algorithm making use of Regina's [BBP+14] Pachner move routines is likely to result in a very significant speedup over our Python implementation. We pose as a challenge to simplify all 78 triangulations of Cappell-Shaneson spheres described in this chapter.

7.3 Table of triangulation data

Table 7.2: The third column is the number of 4-simplices in the triangulation of the punctured 3-torus bundle. The fourth column is number of 4-simplices in the triangulation of each of the two corresponding Cappell-Shaneson homotopy spheres.

Trace	Monodromy	# Simp. in bundle	# Simp. in unsimplified CS-spheres	Isomorphism signature of bundle triangulation
0	$\begin{pmatrix} 0 & 1 & 1 \\ 0 & 0 & 1 \\ 1 & 0 & 0 \end{pmatrix}$	2	308	`cMkabbb+aAa3blb`
1	$\begin{pmatrix} 0 & 1 & 0 \\ 0 & 0 & 1 \\ 1 & 0 & 1 \end{pmatrix}$	4	604	`eLMQcbbcdcddGbvbgbVa5aIbNa`
2	$\begin{pmatrix} 0 & 1 & -1 \\ 0 & 0 & 1 \\ 1 & 0 & 2 \end{pmatrix}$	4	734	`eLAQcbbcdddd0bRbhaRb8azbEb`
3	$\begin{pmatrix} 0 & 1 & -2 \\ 0 & 0 & 1 \\ 1 & 0 & 3 \end{pmatrix}$	6	1162	`gvLQQQcefddefeff+a+aSaMbHbraHb+araSa`
4	$\begin{pmatrix} 0 & 1 & -3 \\ 0 & 0 & 1 \\ 1 & 0 & 4 \end{pmatrix}$	10	1854	`kvLAALQQQcedfeghijhgjihijjIbtbtbIbJbkblarbla` `sb0bMacbJaFbUb`
5	$\begin{pmatrix} 0 & 1 & -4 \\ 0 & 0 & 1 \\ 1 & 0 & 5 \end{pmatrix}$	10	1646	`kvLLAPQQQcfehggeihjiijhjijNaQbhbhbaasaIaZbhb` `aahbaaZb1aubsa`
6	$\begin{pmatrix} 0 & 1 & -5 \\ 0 & 0 & 1 \\ 1 & 0 & 6 \end{pmatrix}$	12	2640	`mvLLLLQQQQfdgjiikhjjkllkiilklJaCa8aaaSb-anb` `Da-anbaa0a2aLbgb1bwaLbSa`
7	$\begin{pmatrix} 0 & 1 & -6 \\ 0 & 0 & 1 \\ 1 & 0 & 7 \end{pmatrix}$	14	2502	`ovLvAzPQPQQQkdgfklmhjlmnkmlknlkjnmn1btaBalaW` `b0aVbDa0aaaNaibMbjaibibmbNaYbib6a1b`

8	$\begin{pmatrix} 0 & 1 & -7 \\ 0 & 0 & 1 \\ 1 & 0 & 8 \end{pmatrix}$	18	2826	`svLvLAAMzAMQQQQQegigikjiknjnjorqlpomrnqprqrq`
				`FaLaLaaa0a0a3aaa0a1bjaFaCbXataVbga1b6aKahbCb`
				`aa6a-aiaiaia`

9	$\begin{pmatrix} 0 & 1 & -8 \\ 0 & 0 & 1 \\ 1 & 0 & 9 \end{pmatrix}$	20	3646	`uvLLLPLPLQzAQAQQQkedgkjijkkmimirlppqontrotststrssFaFaLavbaa3avbaajaFajaqbjaWbmbmbFa0bfa0aaaEa+aUaMa7aMambYbMbMb`
10	$\begin{pmatrix} 0 & 1 & -9 \\ 0 & 0 & 1 \\ 1 & 0 & 10 \end{pmatrix}$	24	4240	`yvLvLAAMPAMPLQwAAQQQQegigikjiklnjnjqrorqnpsutvvxswxtwuvxwxFaLaLaaa0a0a3aaa0aWb1bjaFaCbtaWb6aDbhbCbaaPakbIbCbCbjboaXadbga6aQbPbaa5a0b`
10	$\begin{pmatrix} 0 & 5 & 7 \\ 0 & 2 & 3 \\ 1 & 0 & 8 \end{pmatrix}$	18	3206	`svLLLPLPLQzQQQQQedgkjijkkmimirlqppornoprqqrqFaFaLavbaa3avbaajaFajaqbjaWbmbUambFaLbdb0a6a6aEaZadbdbma`
11	$\begin{pmatrix} 0 & 1 & -10 \\ 0 & 0 & 1 \\ 1 & 0 & 11 \end{pmatrix}$	26	4072	`AvLLLPLzPAAAQzPMMAMQQQkedgkfijkmiminlkpoprqrstsuwvuxzxvzywyxzyzFaFaLavbXa3a3ajaFajaqbja1ambcbmbVaXa3aZaWbDbaa3axbCa1a0ambDbmbja0a3aPbMaFaaaZbca`
12	$\begin{pmatrix} 0 & 1 & -11 \\ 0 & 0 & 1 \\ 1 & 0 & 12 \end{pmatrix}$	28	4798	`CLLAMPPLPPwwLwLAMAPQQPQQccdecdghghgkilklknoptvwqvryAutxyzAxzxAzBBABBAbybXaXaFaaahbZbwaybEabahbWabambaaQapazbaa0bbaEa1bWaDb0bqapabaVa9aXbVaFbyafa7aMa1bsbpa`
12	$\begin{pmatrix} 0 & 7 & 16 \\ 0 & 3 & 7 \\ 1 & 0 & 9 \end{pmatrix}$	22	3948	`wvLLLLwAAAAAQLPQQQQcefgkfihjjinppklomosrtusvursuvrvtvuFaPbLa3acb3aZaebmbjaqb7axaXa0a0a0acbRbaaobobMaaaPbbbmb0acbYbbb0a0acb`
13	$\begin{pmatrix} 0 & 1 & -12 \\ 0 & 0 & 1 \\ 1 & 0 & 13 \end{pmatrix}$	30	4880	`EvLLLPLPLQMzAwQMPzMMQMQPQQedgkjijkknimnilpporrvtssvryxxABzvyAxCBCDABCDDDFaFaLavbaa3avbaaja1bjaqbFaCbmbmbFafatatanbDbMaMaqbjaHafb0aaakbLaBaeaDbmbpalaqbXaBaMbCaububNa`
13	$\begin{pmatrix} 0 & 3 & 10 \\ 0 & 2 & 7 \\ 1 & 0 & 11 \end{pmatrix}$	22	3454	`wvLLLPLPPAMzQzAQQQQcedgkfijlkmimiqkssrnpqrsuvuvruttvvuFaFaLavbXa3a3aaajaFajaqbjaWbcbaakb3a0aqaEakb3aDb7aYbFaqbqbMbmbubSaFb`
13	$\begin{pmatrix} 0 & 7 & 10 \\ 0 & 2 & 3 \\ 1 & 0 & 11 \end{pmatrix}$	22	3454	`wvLLLPLPLALAAQMQQQQcedgkjijkkmiislpponqrsrurtvttsuvuvvFaFaLavbaa3avbaajaFajaCbtambmbFafa0aaamaQaZaDbWbMa7aMa2a2a2aXbxbHbKa`
14	$\begin{pmatrix} 0 & 1 & -13 \\ 0 & 0 & 1 \\ 1 & 0 & 14 \end{pmatrix}$	32	5068	`GLLAMPPLPPwAzLQMvQLAzLPQQQQkcdecdghghgkilklknmnqsrtsqxwvzyuvABACFEADBCDFEFEEFAbybXaXaFaaahbZbwaybEabahbWabambaaba0bPbzbXaaarb1baaIaaaaazb1aoaWbRb-aaa6aXbKasa1aPbyaVanavalblblb`

14	$\begin{pmatrix} 0 & 23 & 32 \\ 0 & 5 & 7 \\ 1 & 0 & 9 \end{pmatrix}$	22	3582	`wvLLLPLPLPLAQMPQQQQcedgkjijkkimislpproqvupqu qttsuvtvuvFaFaLavbaa3avbaajajaqbCbtambmbFaeb fazaaazbpbWbKbZbMaMaNaqbnaubna1b1b`
15	$\begin{pmatrix} 0 & 1 & -14 \\ 0 & 0 & 1 \\ 1 & 0 & 15 \end{pmatrix}$	34	5366	`IvLLLPLzPMAAMQLzMLQAQzzPQPQQQcedgkfijkninmil kpporqrtsvvAxywywvzAByFCEDDFGCHGHGFHGHFaFaLa vbXa3a3aja1bjaFa1bCbmbcbmbXafaPaaa3aZb3aybyb vbIbmbLbXagbPbKbaa7acadblbFbKaKakafb2bDa2asb SaqbobRaHa`
15	$\begin{pmatrix} 0 & 5 & 12 \\ 0 & 2 & 5 \\ 1 & 0 & 13 \end{pmatrix}$	22	3710	`wvLLLPLPLQzAQzAQQQQcedgkjijkkmimirlpponursut svursttvvvFaFaLavbaa3avbaajaFajaqbjaWbmbmbFa LbOaaaEaRbobaavbobmbYbyb9a9abbJaOa`
16	$\begin{pmatrix} 0 & 1 & -15 \\ 0 & 0 & 1 \\ 1 & 0 & 16 \end{pmatrix}$	36	5676	`KvLLAvPzzQMAzMMMPMzMQLMPMPPQQQQdeghjfikljmqj npmqtqrprpyuwuvvuACyxzzFECDGDCJHIFHIGJIHJJOa OaZbIaabmbsb2aTbraXbIaCbJaGaPbhbZanbHabaRb9a aaFbJabbbbjaCbaaZa9ambpapaWb9aCabbSaQbCbaaOb ZasaHazbOarb7ajb6abb`
16	$\begin{pmatrix} 0 & 3 & 13 \\ 0 & 2 & 9 \\ 1 & 0 & 14 \end{pmatrix}$	26	4256	`AvLLLPLPPAMzQzAAAMMQQQkedgkfijlkmimiqkssonpq rtuvuxszzxywywyzxzyFaFaLavbXa3a3aaajaFajaqbj aWbcbaakbXaOaqaEaaaaaYbFaqb4acbaavb4a4aybxap bWbmapaaaFa`
16	$\begin{pmatrix} 0 & 9 & 13 \\ 0 & 2 & 3 \\ 1 & 0 & 14 \end{pmatrix}$	26	4410	`AvLvLAAMPLQwMMMMMLQQQQkeiggikjlkgnjmnjpspqrr stpvvyxzxywvxywwzzzVaPaebaaebPaRbvbPaKbVayb9 a9asaPaaavbaaLaRbvbKbebCbCbDbKb3bKbzaYa2azba ajabbTaja1b`
17	$\begin{pmatrix} 0 & 1 & -16 \\ 0 & 0 & 1 \\ 1 & 0 & 17 \end{pmatrix}$	38	6326	`MvLLLPLzPMAAQPLMMLMPAwQvQMMQzQQQkedgkfijknin milkpoprqrstsvvzxxAvyzBxADGDFEFGHDJHIILKLKLJ KLKFaFaLavbXa3a3aja1bjaFa1bCbmbcbmbVaXaPaaa3 aDbaa3aybybvbmbmbLaPbKbaaWbcaLaKaKbKaFakafbe bKbKaAblaKb3b-aybybybKajaqbka9a`
17	$\begin{pmatrix} 0 & 29 & 36 \\ 0 & 4 & 5 \\ 1 & 0 & 13 \end{pmatrix}$	26	4712	`AvLLLvvQAMQAAAALQPMQQQkcdeihmpkmnpimkponlrqq wswtxutuvyzzyxwyzyzyaUbCbDbWbaaaa2aFbqbkaYap bbbCaCaCbYbqaObOahbaaaa2awaUbOaKaYbxataPaQay aCahbdamaaa`
17	$\begin{pmatrix} 0 & 5 & 36 \\ 0 & 4 & 29 \\ 1 & 0 & 13 \end{pmatrix}$	26	4052	`AvLLLPLzPAMAMAALQAPQQQkedgkfijkmimirlkpponur sxsurvtyzxywzzyxzxyFaFaLavbXa3a3ajaFajaqbjaW bmbcbmbXafaOaaaEaMaQaMambYbFaMblanbVanbRaxax azbGalaXbUa`

18	$\begin{pmatrix} 0 & 1 & -17 \\ 0 & 0 & 1 \\ 1 & 0 & 18 \end{pmatrix}$	40	6874	OvLLLLMvPAMQQMzPMzMPwQPLMwQzAAQQQQcedgfjiqmi misoqpqoplqnsrutwvvvxuyAAzByCEDDFCGILIKGMJLIM KNKMLNNNFaFaLaXaPa3a1bFajaqbjaWbXaybYaYavaYa fb1bOaEaZaZbhambjajaybvaybrbWbZaRbBaZbmb2bja yb9aybrbaaEaRbcaMaPambYbFapb6ayaxbYaFa9a9a
18	$\begin{pmatrix} 0 & 17 & 28 \\ 0 & 3 & 5 \\ 1 & 0 & 15 \end{pmatrix}$	26	4842	AvLLLLwwQAMQPLAAMQLQQQkefgkfijjninirkmpsmupo qrsvwtvxzuyxyzyxyzzFaPbLa3acb3aebmbFajaqbjaW bXaIbYaRbCbaafaOaqaEaKbYbFaFbqbYa3aCbMaybMaO bxafbWbxaKb
19	$\begin{pmatrix} 0 & 1 & -18 \\ 0 & 0 & 1 \\ 1 & 0 & 19 \end{pmatrix}$	42	6636	QvLLLPLzPAAAMAPPPzAMwQMzAPzMQwMMQQQQedgkfijk miminlkpporurtssruyxxAvzyAxBCCDFIFGGKJFIHOKP NPLNMLPOONPOFaFaLavbXa3a3ajaFajaqbja1ambcbmb Xafa3aUaWbZbMaMaMb1bua9ambkbPbiaabRbOa7a1bmb 1aibea+adbObJbZbIbOafaHafbla9aMawabaRa+aiawb Abgaab3a
19	$\begin{pmatrix} 0 & 11 & 16 \\ 0 & 2 & 3 \\ 1 & 0 & 17 \end{pmatrix}$	28	4720	CvLLLzMzQQMvAwQzMMMMQQQQcedgkjiljkknimnisosq qvrvqustxxAzwBzBBAxyzABAFaFaLavbPa3avbPaPaja 1bjaqbFaCbvbtbPatatanbOaqbja1bUbga6atbhbPaba TaPaabvblaCaWbbbUbBa2a
19	$\begin{pmatrix} 0 & 13 & 30 \\ 0 & 3 & 7 \\ 1 & 0 & 16 \end{pmatrix}$	26	4150	AvLLLPLzPAMPMAPMMzQQQQkedgkfijkmimirkloosnrq ptsvuuwyzywxzzxwxyzFaFaLavbXa3a3ajaFajaqbjaW bcbNaKafaPaOaEaZaCbSbRbmbjajaCbRbob-aIbrarbW bQbQb9aGbyb
19	$\begin{pmatrix} 0 & 13 & 42 \\ 0 & 4 & 13 \\ 1 & 0 & 15 \end{pmatrix}$	28	4348	CvLLLMvPMzQQALPMMPLQPQQQcdfehjnimljinjlqqplr urvruttxtwxAzAzBBzyyBzABOaPboaUaaaabUaAbOaXb BbjaOalbUaDbaacbaaaaabaaabAbcbcbWbOa2aWbaaab ObabAbaaaaNbOaKalbXb2a
19	$\begin{pmatrix} 0 & 3 & 16 \\ 0 & 2 & 11 \\ 1 & 0 & 17 \end{pmatrix}$	28	4380	CLLAMPPzwMvQPLwvAwQQQQQQccdecdgfghihkkmoqomn tprvryuxzyAvwABBxzABzABzAbybXaXaFaaaaaZbXbXa FaaaAbqbRbEataCbbaaaLaYaDbYala2bobtaLahbebua ea8a1bYavaqbqb1aBa1bCa
19	$\begin{pmatrix} 0 & 7 & 30 \\ 0 & 3 & 13 \\ 1 & 0 & 16 \end{pmatrix}$	26	4054	AvLLLLwwQAMQPLAAMQzQQQkefgkfijjninirkmpsmtpo vrsvruwxxuyzwyzxyzzFaPbLa3acb3aebmbFajaqbjaW bXaIbYaRbCbabfaOaaaEaKbmbYbJa2bracbmbhb3atbE a8aTbrbEaXa

20	$\begin{pmatrix} 0 & 1 & -19 \\ 0 & 0 & 1 \\ 1 & 0 & 20 \end{pmatrix}$	44	6806	`SvLLLPLzPAMAMAALQMLAPwMAMPzQzAMPPAQQQkedgkfijkmimirlkpponqrswsuvutAwzCzxBACzGEEIDKGFIMHKLJMNPOONRRQRQPQQRFaFaLavbXa3a3ajaFajaqbjaWbmbcbmbXafaOaqaEaMazbMaYbFaqbNaHafaxaxaWbxbZbWbxbFaaaQbKaJbOaxazbyaPaZbXaqbFaca2bybLaxaaaubkbeaLaPaeboaraSaja`
20	$\begin{pmatrix} 0 & 5 & 17 \\ 0 & 2 & 7 \\ 1 & 0 & 18 \end{pmatrix}$	26	4064	`AvLLLPLPPAMzQzAAPLQQQQkedgkfijlkmimiqkssrnuqrsuqztyxxwzvwxzyyyzyFaFaLavbXa3a3aaajaFajaqbjaWbcbaakb3aOaaaEakb3ambYbaambUambFambdbOa6a6azbZadbdbda`
20	$\begin{pmatrix} 0 & 7 & 17 \\ 0 & 2 & 5 \\ 1 & 0 & 18 \end{pmatrix}$	26	4912	`AvLvLAAPzQPPzAPMwPQQQQkfghgkhkgjnpjpjrlnmssurpqxxzytyuwvzywxxzzOa-aUaaaUa-aUanbsbTbcbnaOaXbiagaQbXa3a3aKbvbXbaaXbXbKb-aQbnbBbUbXanb-aibfa2aaaCa`

Appendix A

Cappell-Shaneson sphere simplification algorithm

We list pseudocode illustrating the algorithm we used to simplify the Cappell-Shaneson sphere triangulations in Chapter 7. Some further discussion is also given in Section 7.1.1. Working Python code which is a slight variation of the following pseudocode is available from the author upon request[1].

Simplification Code A.1:

```
# Note this terminates only if it verifies triangulation tri
# is a triangulation of the standard 4-sphere. In practice we
# set a maximum time we allow the routine to run.
Define-Routine simplifyUntilS4(tri):
  # min_tri will be our local minimum smallest triangulation
  min_tri = tri.copy()
  loopCount = 0

  # Keep track of last loop in which we either found a smaller min_tri or expanded min_tri. If loopCount is large relative to this then we will expand min_tri a little.
  lastSimplificationLoopCount = 0

  # Number of times that tri was expanded and contracted to a triangulation with the same size as min_tri. If this is large then we'll greatly expand min_tri.
  achievedLocalMinimumCount = 0
  allow51 = True # Do we allow Pachner 5-1 moves?
  While (tri is not the two 4-simplex triangulation of the 4-sphere):
    loopCount += 1

    # Try to keep exactly 5 vertices
    If min_tri has <= 5 vertices:
      min_tri = do-1-5-moves-until-exactly-5-vertices(min_tri)
      tri = min_tri.copy()
      allow51 = False

    # Greedily simplify tri while randomly performing some random 3-3 moves.
    tri = greedySimplify(tri, allow51)
```

[1]Send an email to ahmadissa@gmail.com.

```

    If tri.numberOfPentachora() >= min_tri.numberOfPentachora():
      # Weren't able to simplify beyond the local minimum

      If tri.numberOfPentachora() == min_tri.numberOfPentachora():
        min_tri = tri.copy()

      # If unable to simplify tri to smaller triangulation than min_tri for many loops then expand min_tri a little bit.
      If loopCount - lastSimplificationLoopCount > 30:
        If tri.numberOfPentachora() == min_tri.numberOfPentachora():
          achievedLocalMinimumCount += 1
        # spikeHeighten is defined below.
        min_tri = spikeHeighten(min_tri, iterations=3, heat=3, allow51)
        lastSimplificationLoopCount = loopCount

      # If tri was expanded and contracted to the same size as min_tri 30 times, then expand tri significantly.
      If achievedLocalMinimumCount % 30 == 29:
        # If triangulation is small, don't expand too much.
        If min_tri.numberOfPentachora() < 20:
          Set iterations = 10, heat = 4
        Else:
          Set iterations = 60, heat = 60
        min_tri = spikeHeighten(min_tri, iterations, heat, allow51)
        achievedLocalMinimumCount = 0

      tri = min_tri.copy()
    Else If tri.numberOfPentachora()< min_tri.numberOfPentachora():
      # Smaller local minimum found
      min_tri = tri.copy()
      lastSimplificationLoopCount = loopCount

    If tri.numberOfPentachora() == min_tri.numberOfPentachora():
      # Perform n=2 random 2-4 moves, and six random 3-3 moves
      # then greedily simplify
      tri = heighten(tri, n=2, allow51) # Defined below

  return tri

# Simple routine which expands the triangulation
Define-Function heighten(tri, heat, allow51):
  i = 0
  While i < heat:
    If i == 0 and allow51 is True:
      tri = do-random-1-5-move(tri)
    Else:
      tri = do-random-2-4-move(tri)
    tri = do-three-random-3-3-moves(tri)
    tri = greedySimplify(tri, allow51)

# More sophisticated routine to expand the triangulation
Define-Function spikeHeighten(tri, iterations, heat, allow51):
  i = 0
  While i < iterations:
    tri = heighten(tri, heat, allow51)
```

```
    tri = perform-a-random-3-3-move(tri)
    i += 1

  j = 0
  While j < 100*iterations:
    tri = perform-a-random-3-3-move(tri)
    j += 1
```

Bibliography

[AK79] Selman Akbulut and Robion Kirby. An exotic involution of S^4. *Topology*, 18(1):75–81, 1979.

[AK85] Selman Akbulut and Robion Kirby. A potential smooth counterexample in dimension 4 to the Poincaré conjecture, the Schoenflies conjecture, and the Andrews-Curtis conjecture. *Topology*, 24(4):375–390, 1985.

[Akb88] Selman Akbulut. Constructing a fake 4-manifold by Gluck construction to a standard 4-manifold. *Topology*, 27(2):239–243, 1988.

[Akb10] Selman Akbulut. Cappell-Shaneson homotopy spheres are standard. *Ann. of Math. (2)*, 171(3):2171–2175, 2010.

[AR84] I. R. Aitchison and J. H. Rubinstein. Fibered knots and involutions on homotopy spheres. In *Four-manifold theory (Durham, N.H., 1982)*, volume 35 of *Contemp. Math.*, pages 1–74. Amer. Math. Soc., Providence, RI, 1984.

[BBH12] Ryan Budney, Benjamin A. Burton, and Jonathan Hillman. Triangulating a Cappell-Shaneson knot complement. *Math. Res. Lett.*, 19(5):1117–1126, 2012.

[BBP+14] Benjamin A. Burton, Ryan Budney, William Pettersson, et al. Regina: Software for 3-manifold topology and normal surface theory. `http://regina.sourceforge.net/`, 1999–2014.

[Bon09] Francis Bonahon. *Low-dimensional geometry*, volume 49 of *Student Mathematical Library*. American Mathematical Society, Providence, RI, 2009. From Euclidean surfaces to hyperbolic knots, IAS/Park City Mathematical Subseries.

[BS13] R. İnanç Baykur and Nathan Sunukjian. Round handles, logarithmic transforms and smooth 4-manifolds. *J. Topol.*, 6(1):49–63, 2013.

[Bur11] Benjamin A. Burton. The Pachner graph and the simplification of 3-sphere triangulations. In *Proceedings of the Twenty-seventh Annual Symposium on Computational Geometry*, SoCG '11, pages 153–162, New York, NY, USA, 2011. ACM.

[Can79] J. W. Cannon. Shrinking cell-like decompositions of manifolds. Codimension three. *Ann. of Math. (2)*, 110(1):83–112, 1979.

[CDGW] Marc Culler, Nathan M. Dunfield, Matthias Goerner, and Jeffrey R. Weeks. SnapPy, a computer program for studying the geometry and topology of 3-manifolds. Available at http://snappy.computop.org (05/07/2017).

[CR06] Charles W. Curtis and Irving Reiner. *Representation theory of finite groups and associative algebras*. AMS Chelsea Publishing, Providence, RI, 2006. Reprint of the 1962 original.

[CS76a] Sylvain E. Cappell and Julius L. Shaneson. Some new four-manifolds. *Ann. of Math. (2)*, 104(1):61–72, 1976.

[CS76b] Sylvain E. Cappell and Julius L. Shaneson. There exist inequivalent knots with the same complement. *Ann. of Math. (2)*, 103(2):349–353, 1976.

[Dev17] The Sage Developers. *SageMath, the Sage Mathematics Software System (Version 7.5.1)*, 2017. `http://www.sagemath.org`.

[Don83] S. K. Donaldson. An application of gauge theory to four-dimensional topology. *J. Differential Geom.*, 18(2):279–315, 1983.

[Edw06] Robert D. Edwards. Suspensions of homology spheres. arXiv:math/0610573v1 [math.GT], 2006.

[ES] Felix Effenberger and Jonathan Spreer. simpcomp: a gap package for working with simplicial complexes. `http://www.gap-system.org/Packages/simpcomp.html`.

[FH82] W. Floyd and A. Hatcher. Incompressible surfaces in punctured-torus bundles. *Topology Appl.*, 13(3):263–282, 1982.

[FQ90] Michael H. Freedman and Frank Quinn. *Topology of 4-manifolds*, volume 39 of *Princeton Mathematical Series*. Princeton University Press, Princeton, NJ, 1990.

[Fra87] George K. Francis. *A topological picturebook*. Springer-Verlag, New York, 1987.

[Fre82] Michael Hartley Freedman. The topology of four-dimensional manifolds. *J. Differential Geom.*, 17(3):357–453, 1982.

[GL89] C. McA. Gordon and J. Luecke. Knots are determined by their complements. *Bull. Amer. Math. Soc. (N.S.)*, 20(1):83–87, 1989.

[Glu62] Herman Gluck. The embedding of two-spheres in the four-sphere. *Trans. Amer. Math. Soc.*, 104:308–333, 1962.

[Gom86] Robert E. Gompf. Smooth concordance of topologically slice knots. *Topology*, 25(3):353–373, 1986.

[Gom91] Robert E. Gompf. Killing the Akbulut-Kirby 4-sphere, with relevance to the Andrews-Curtis and Schoenflies problems. *Topology*, 30(1):97–115, 1991.

[Gom10] Robert E. Gompf. More Cappell-Shaneson spheres are standard. *Algebr. Geom. Topol.*, 10(3):1665–1681, 2010.

[Gor76] C. McA. Gordon. Knots in the 4-sphere. *Comment. Math. Helv.*, 51(4):585–596, 1976.

[GS78] David E. Galewski and Ronald J. Stern. Simplicial triangulations of topological manifolds. In *Algebraic and geometric topology (Proc. Sympos. Pure Math., Stanford Univ., Stanford, Calif., 1976), Part 2*, Proc. Sympos. Pure Math., XXXII, pages 7–12. Amer. Math. Soc., Providence, R.I., 1978.

[GS80] David E. Galewski and Ronald J. Stern. Classification of simplicial triangulations of topological manifolds. *Ann. of Math. (2)*, 111(1):1–34, 1980.

[GS99] Robert E. Gompf and András I. Stipsicz. 4*-manifolds and Kirby calculus*, volume 20 of *Graduate Studies in Mathematics*. American Mathematical Society, Providence, RI, 1999.

[Gué06] François Guéritaud. On canonical triangulations of once-punctured torus bundles and two-bridge link complements. *Geom. Topol.*, 10:1239–1284, 2006. With an appendix by David Futer.

[Hat02] A. Hatcher. *Algebraic Topology*. Algebraic Topology. Cambridge University Press, 2002.

[HM74] Morris W. Hirsch and Barry Mazur. *Smoothings of piecewise linear manifolds*. Princeton University Press, Princeton, N. J.; University of Tokyo Press, Tokyo, 1974. Annals of Mathematics Studies, No. 80.

[Iss12] Ahmad Issa. Construction of non-geometric veering triangulations of fibered hyperbolic 3-manifolds. MSc thesis, University of Melbourne, 2012.

[JLT14] Michael Joswig, Frank H. Lutz, and Mimi Tsuruga. *Heuristics for Sphere Recognition*, pages 152–159. Springer Berlin Heidelberg, Berlin, Heidelberg, 2014.

[JR14] William Jaco and J. Hyam Rubinstein. Inflations of ideal triangulations. *Adv. Math.*, 267:176–224, 2014.

[Ker60] Michel A. Kervaire. A manifold which does not admit any differentiable structure. *Commentarii Mathematici Helvetici*, 34(1):257–270, 1960.

[KM63] Michel A. Kervaire and John W. Milnor. Groups of homotopy spheres. I. *Ann. of Math. (2)*, 77:504–537, 1963.

[KS77] Robion C. Kirby and Laurence C. Siebenmann. *Foundational essays on topological manifolds, smoothings, and triangulations*. Princeton University Press, Princeton, N.J.; University of Tokyo Press, Tokyo, 1977. With notes by John Milnor and Michael Atiyah, Annals of Mathematics Studies, No. 88.

[KY17] Min Hoon Kim and Shohei Yamada. Ideal classes and Cappell-Shaneson homotopy 4-spheres, 2017.

[Lac03] Marc Lackenby. The canonical decomposition of once-punctured torus bundles. *Comment. Math. Helv.*, 78(2):363–384, 2003.

[Lar15] Kyle Larson. Surgery on tori in the 4-sphere. arXiv:1502.06834v1 [math.GT], 2015.

[Lic99] W. B. R. Lickorish. Simplicial moves on complexes and manifolds. In *Proceedings of the Kirbyfest (Berkeley, CA, 1998)*, volume 2 of *Geom. Topol. Monogr.*, pages 299–320 (electronic). Geom. Topol. Publ., Coventry, 1999.

[LN16] Boris Lishak and Alexander Nabutovsky. Sizes of spaces of triangulations of 4-manifolds and balanced presentations of the trivial group, 2016.

[Lur09] Jacob Lurie. Topics in geometric topology (lecture notes). `http://www.math.harvard.edu/~lurie/937.html`, 2009.

[Man16] Ciprian Manolescu. Pin(2)-equivariant Seiberg-Witten Floer homology and the triangulation conjecture. *J. Amer. Math. Soc.*, 29(1):147–176, 2016.

[Mat78] Takao Matumoto. Triangulation of manifolds. In *Algebraic and geometric topology (Proc. Sympos. Pure Math., Stanford Univ., Stanford, Calif., 1976), Part 2*, Proc. Sympos. Pure Math., XXXII, pages 3–6. Amer. Math. Soc., Providence, R.I., 1978.

[Mel77] Paul Michael Melvin. *Blowing up and down in 4-manifolds*. ProQuest LLC, Ann Arbor, MI, 1977. Thesis (Ph.D.)–University of California, Berkeley.

[Mil56] John Milnor. On manifolds homeomorphic to the 7-sphere. *Ann. of Math. (2)*, 64:399–405, 1956.

[Moi52] Edwin E. Moise. Affine structures in 3-manifolds. V. The triangulation theorem and Hauptvermutung. *Ann. of Math. (2)*, 56:96–114, 1952.

[Mon76] José M. Montesinos. Three-manifolds as 3-fold branched covers of S^3. *Quart. J. Math. Oxford Ser. (2)*, 27(105):85–94, 1976.

[Nab96] A. Nabutovsky. Geometry of the space of triangulations of a compact manifold. *Comm. Math. Phys.*, 181(2):303–330, 1996.

[New72] Morris Newman. *Integral matrices*. Academic Press, New York-London, 1972. Pure and Applied Mathematics, Vol. 45.

[NS12] Daniel Nash and András I. Stipsicz. Gluck twist on a certain family of 2-knots. *Michigan Math. J.*, 61(4):703–713, 2012.

[OSS15] Peter S. Ozsváth, András I. Stipsicz, and Zoltán Szabó. *Grid homology for knots and links*, volume 208 of *Mathematical Surveys and Monographs*. American Mathematical Society, Providence, RI, 2015.

[Pac91] Udo Pachner. P.l. homeomorphic manifolds are equivalent by elementary shellings. *European Journal of Combinatorics*, 12(2):129 – 145, 1991.

[Rad25] T. Radó. Über den Begriff der Riemannschen Fläche. *Acta Sci. Math. Szeged.*, 2:101–121, 1925.

[Rub95] Joachim H. Rubinstein. An algorithm to recognize the 3-sphere. In *Proceedings of the International Congress of Mathematicians, Vol. 1, 2 (Zürich, 1994)*, pages 601–611. Birkhäuser, Basel, 1995.

[Rud98] Yuli B. Rudyak. *On Thom spectra, orientability, and cobordism*. Springer Monographs in Mathematics. Springer-Verlag, Berlin, 1998. With a foreword by Haynes Miller.

[Sco05] Alexandru Scorpan. *The wild world of 4-manifolds*. American Mathematical Society, Providence, RI, 2005.

[Ser85a] Caroline Series. The geometry of Markoff numbers. *Math. Intelligencer*, 7(3):20–29, 1985.

[Ser85b] Caroline Series. The modular surface and continued fractions. *J. London Math. Soc. (2)*, 31(1):69–80, 1985.

[Sma59] Stephen Smale. Diffeomorphisms of the 2-sphere. *Proc. Amer. Math. Soc.*, 10:621–626, 1959.

[Ste08] Peter Stevenhagen. The arithmetic of number rings. In *Algorithmic number theory: lattices, number fields, curves and cryptography*, volume 44 of *Math. Sci. Res. Inst. Publ.*, pages 209–266. Cambridge Univ. Press, Cambridge, 2008.

[Sun15] Nathan S. Sunukjian. Surfaces in 4-manifolds: concordance, isotopy, and surgery. *Int. Math. Res. Not. IMRN*, (17):7950–7978, 2015.

[Tau87] Clifford Henry Taubes. Gauge theory on asymptotically periodic 4-manifolds. *J. Differential Geom.*, 25(3):363–430, 1987.

[Tho94] Abigail Thompson. Thin position and the recognition problem for S^3. *Math. Res. Lett.*, 1(5):613–630, 1994.

[Thu97] William P. Thurston. *Three-dimensional geometry and topology. Vol. 1*, volume 35 of *Princeton Mathematical Series*. Princeton University Press, Princeton, NJ, 1997. Edited by Silvio Levy.

[TL13] Mimi Tsuruga and Frank H. Lutz. Constructing complicated spheres. arXiv:1302.6856, 2013.

[Tsu15] Mimi Tsuruga. *Constructing complicated spheres*. 2015. Thesis (Ph.D.)–Technische Universität Berlin.

[VKF74] I A Volodin, V E Kuznetsov, and A T Fomenko. The problem of discriminating algorithmically the standard three-dimensional sphere. *Russian Mathematical Surveys*, 29(5):71, 1974.

[Wee05] Jeff Weeks. Computation of hyperbolic structures in knot theory. In *Handbook of knot theory*, pages 461–480. Elsevier B. V., Amsterdam, 2005.

[Whi40] J. H. C. Whitehead. On C^1-complexes. *Annals of Mathematics*, 41(4):809–824, 1940.

[Yos94] Katsuyuki Yoshikawa. An enumeration of surfaces in four-space. *Osaka J. Math.*, 31(3):497–522, 1994.